Cancer stem cell niche: the place to be

Borovski, T.

Publication date
2012
Document Version
Final published version

Cancer Stem Cell Niche: The Place to Be

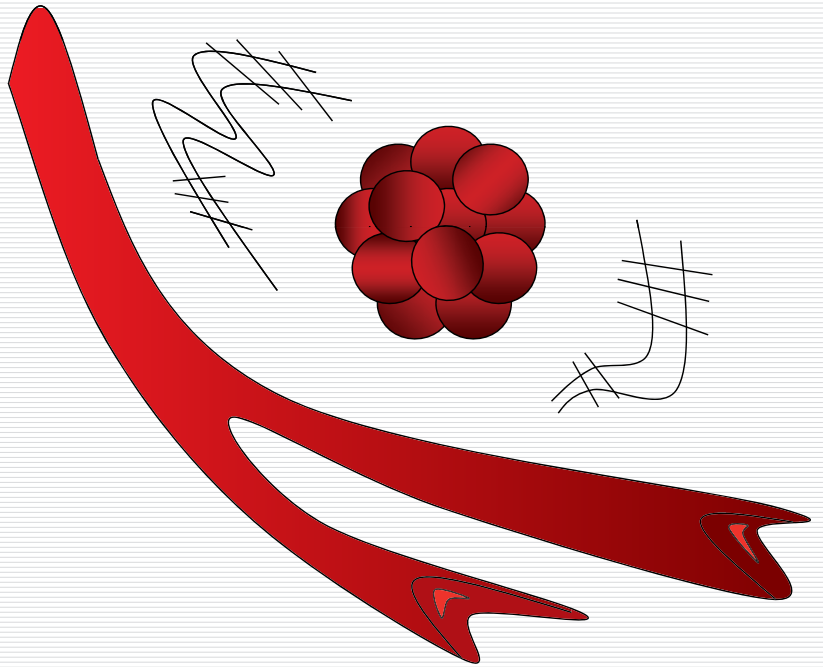

TIJANA BOROVSKI

Cancer Stem Cell Niche: The Place to Be

Tijana Borovski

Cancer Stem Cell Niche:
The Place to Be

The research described in this thesis was performed at the Center of Experimental and Molecular Medicine of the Academic Medical Center (AMC) in Amsterdam, The Netherlands.

The printing of this thesis was financially supported by University of Amsterdam, Greiner Bio-One and BD Biosciences.

Cancer Stem Cell Niche: The Place to Be

ACADEMISCH PROEFSCHRIFT

ter verkrijging van de graad van doctor aan de Universiteit van Amsterdam op gezag van de Rector Magnificus prof. dr. D.C. van den Boom ten overstaan van een door het college voor promoties ingestelde commissie, in het openbaar te verdedigen in de Agnietenkapel op

donderdag 24 mei 2012, te 14:00 uur

door

Tijana Borovski

geboren te Belgrado, Servië

Promotiecommissie

Promotor: prof. dr. J.P. Medema

Co-promotores: dr. M.R. Sprick
dr. N.A.P. Franken

Overige leden: prof. dr. D.J. Richel
prof. dr. C.C.E. Koning
prof. dr. C.J.F. van Noorden
dr. L.J.A. Stalpers
prof. dr. M. van Lohuizen
dr. T. Würdinger

Faculteit der Geneeskunde

CONTENTS

Thesis outline

GBM is a devastating disease, with poor prognosis and better understanding of the main factors enabling this malignancy is critical to combat this disease. GBM CSCs have been proposed to play the key role in growth, invasiveness and therapy resistance of GBM. Thus, we focused on this fraction of cells with the aim to learn more about the biology of CSCs and the factors critical for their maintenance. In Chapter 2 we review the literature on the CSC niche. In Chapter 3 we show that, opposite to what is commonly believed in the field, the CSC fraction is a complex, heterogeneous population of different clones, rather then a uniform one. Furthermore, the invasive morphology of tumors is driven by the CSCs and there is a direct correlation between the level of hierarchy and the degree of invasiveness of tumors (Chapter 4). Moreover, we discuss the critical role of tumor microvasculature in CSC maintenance, but also in extensive therapy resistance of GBM and plasticity of tumor cells (Chapters 2, 5, 6, 7). Notably, there is still limited knowledge on fundamental changes of chromatin following anti-cancer treatments, important for GBM but also the entire field of cancer. Thus, last but not least, we investigate the DNA damage response of the cells following treatments with DSB-inducing agents (Chapter 8).

1 General Introduction

Introduction

Glioblastoma Multiforme: General Features and Current Treatments

Glioblastoma multiforme (GBM) (WHO grade IV) is the most prevalent and the most devastating type of primary brain tumor. It mainly affects adults and is composed of a heterogeneous mixture of poorly differentiated neoplastic astrocytes. On the histo-pathological level, main hallmarks of GBM are pseudopalisading necrotic areas in the core of the tumor surrounded by the rim of abundant microvascular proliferation (Figure 1).

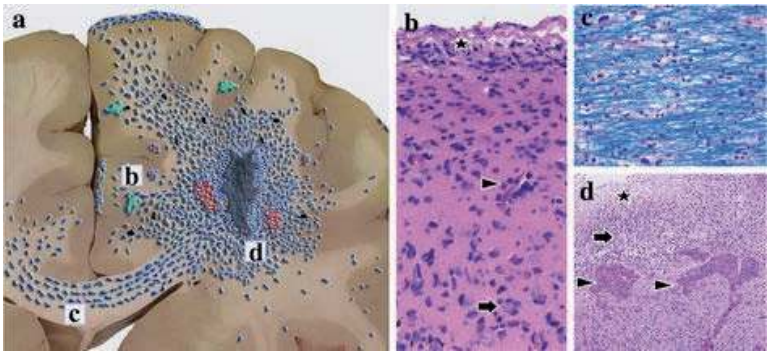

Figure 1. Main hallmarks of GBM (a) Schematic illustration of the GBM growth pattern: tumor cells in *blue*, blood vessels in *red*, neurons in *green*; Perineuronal satellitosis (*b*); Migratory, infiltrative tumor cells (c); Accumulation of tumor cells in the perivascular area (*d*); Necrotic core (*dark grey area*) is surrounded by pseudopalisading tumor cells and florid/glomeruloid neovascularisation. (b) Main histological features: *asterisk* indicates subpial growth, *arrowhead* perivascular accumulation of tumor cells and *arrow* perineuronal satellitosis. (c) Increased cellularity of corpus callosum due to diffuse infiltration of tumor cells in the myelinated tracts. (d) *asterisk* indicates necrotic area, *arrow* peri-necrotic pseudopalisading tumor cells and *arrowheads* glomeruloid microvascular proliferation; (b, d: H&E staining; c: combined Luxol Fast Blue and H&E staining); Claes *et al.* Acta Neuropathol. 2007

For the patients diagnosed with GBM, there are hardly any biomarkers of favorable prognosis and no treatments that can significantly influence the outcome of disease. Patients have median survival of less then a year, despite multimodality treatment consisting of surgical resection followed by concurrent (or sequential) radiotherapy and temozolomide (TMZ) chemotherapy (1). GBM cells are highly invasive and infiltrate into the surrounding healthy brain tissue along the blood vessels and white matter (2). This creates a big challenge for the treatment of the disease. Only the nodular component of the tumor can be controlled surgically. The infiltrative part, however, undergoes non-specific, cytotoxic irradiation and chemotherapy which are able to restrain tumor progression only for a limited period of time. Nevertheless, these tumors will eventually almost certainly recur.

Surgery is the first line treatment for GBM, with the aim to remove as much of the tumor tissue as possible. Recent improvements of imaging techniques such as MRI-guided neuro-navigation, intra-operative MRI, functional MRI and fluorescence-guided surgery further advanced the

surgical procedure. Ionizing radiation following surgery is the most effective treatment for this disease (3, 4). Standard irradiation schedule for GBM is 30 fractions of 2Gy during 6 weeks (1, 5). Furthermore, TMZ is currently used as standard adjuvant chemotherapy for GBM. Concurrent radiotherapy and TMZ treatment, followed by 6 months of TMZ monotherapy, extended median overall survival of GBM patients for three months as compared to surgery and radiotherapy alone (1). However, TMZ treatment was effective only in a selected group of patients. The potential explanation of this outcome might reside in a different methylation status of the *MGMT* promoter. The absence of this enzyme due to gene silencing has been reported to underlie the sensitivity of GBM to TMZ treatment, making it a promising prognostic factor (6). Furthermore, in an attempt to improve the treatment of GBM patients, novel therapeutics are being developed. As GBMs are characterized by massive neovascularization, with vascular endothelial growth factor (VEGF) as the main mediator of the process, newly formed tumor blood vessels have become the target of new drugs. Avastin (bevacizumab) is an anti-VEGF neutralizing antibody, already in a large, randomize phase III trial for GBM (7). Initial results suggest normalization of tumor vasculature and subsequent increase of chemotherapy efficiency (8). However, long-term effects of this treatment are still elusive and recent reports even suggested an increase in metastatic incidence upon this treatment (9). Thus, further information on bevacizumab treatment is yet to be obtained.

Primary and Secondary GBM

Two types of grade IV gliomas can be distinguished, so-called primary and secondary GBM (10). GBMs usually manifest as *de novo* malignancies, without any previous history of the disease. Accordingly, they are termed primary GBM. These tumors mainly occur in elderly patients (mean age 62 years) and are characterized by the rapid progression of the disease. On the other hand, secondary GBMs gradually develop from low-grade lesions. Patients with secondary GBM show higher overall survival and tend to be younger at presentation (mean age 45). These two subtypes of GBM are considered to constitute distinct disease entities as they evolve through different genetic pathways and as a consequence slightly differ in prognosis and response to treatments. Primary GBM, the prevailing type, typically bears *EGFR* and *PTEN* mutations and *p16* deletions. Secondary GBM, on the other hand, mainly presents *TP53* mutation as the earliest detectable alteration. However, the main morphological and biological hallmarks of GBM, namely abundant neovascularisation, necrosis and infiltration of tumor cells, can be detected in both subtypes.

Different Subtypes of GBM

Based on the different gene expression profiles and signalling-pathway alterations that underlie GBM pathogenesis, four GBM subtypes have recently been identified (11). The Classical type is mainly characterized by *EGFR* amplification which seems to be mutually exclusive with *TP53* mutation. Neural stem cell markers such as *NES*, Notch (*NOTCH3*, *JAG1* and *LFNG*) and Sonic

hedgehog (*SMO*, *GAS1* and *GLI2*) genes were also highly expressed in the Classical subtype. The Mesenchymal subclass predominantly carries co-mutations of *NF1* and *PTEN,* both intersecting with the AKT pathway. This group is characterized by higher overall fraction of necrosis and prominent inflammatory infiltration as compared to other types. The Proneural subclass has high occurrence of alterations in *PDGFRA* and *IDH1* genes encoding for platelet-derived growth factor receptor and isocitrate dehydrogenase-1 respectively. *TP53* mutations and loss of heterozygosity were also frequent events in this subtype which is further characterized by expression of neural developmental genes (*SOX2*, *ASCL1*, *TCF4*). Secondary GBMs were primarily found in the Proneural class. The Neural subtype displays high expression of neural markers (*NEFL*, *GABRA1*, *SYT1*, and *SLC12A5*). These are more differentiated tumors compared to the others types, with the expression pattern similar to healthy brain tissue. Proneural and Neural classes show the tendency toward better prognosis and longer overall survival, as compared to Mesenchymal and Classic subtypes. In terms of therapy response, aggressive treatments did not alter survival in the Proneural subclass, however they did significantly reduced mortality in Classical and Mesenchymal subtypes, and efficacy was suggested in Neural type. GBM classification based on this kind of high-throughput genomic and genetic analysis should establish the groundwork for better understanding of GBM pathogenesis. As a final goal, this kind of research should ultimately result in more effective, personalized therapeutic strategies for each, specific group of patients with GBM.

Cancer Stem Cell Hypothesis

One of the biggest challenges in managing GBMs is the nearly universal propensity of these tumors to contain cells that survive all applied therapies and subsequently form recurrent lesions resistant to further treatment. Recently a new explanation of tumor recurrence emerged, identifying cancer stem cells (CSCs) and their therapy resistance as the main cause of this event. CSC hypothesis postulates that malignancy can be viewed as an abnormal organ composed of heterogeneous population of cells with the CSC compartment on top of the hierarchy, orchestrating its structure. They were termed CSCs due to their similarities with normal stem cells, namely their ability to self renew and give rise to various, differentiated lineages (multilineage differentiation potential) (12). Most importantly, these cells are considered to be the only fraction of tumor cells with the tumorigenic capacity and the ability to propagate tumors upon serial xenotransplatation into immuno-compromised mice (12). Strickingly, a single CSC is sufficient to regenerate an entire parental malignancy (13). From the clinical point of view, the main difficulty with CSCs is their therapy resistance (14, 15). Namely, unlike differentiated tumor cells that comprise the majority of the tumor, the CSCs were proposed to be the therapy resistant fraction of tumor cells (Figure 2). This is a result of their highly efficient DNA-damage repair mechanisms, active cell-cycle check points and anti-apoptotic pathways, and numerous drug-transporters on

their membrane (14, 15). Thus, they are believed to be the main cause of tumor recurrence and are an emerging therapeutic target. Interestingly, in the previously mentioned genetic screen of GBMs, tumors with poor prognosis were primarily associated with neural stem cell and/or transient-amplifying cell markers. *Vice versa* proneural and neural subclasses that had better outcome, mainly expressed markers of developing or mature neurons, and thus were shifted towards more differentiated phenotype (11, 16) .

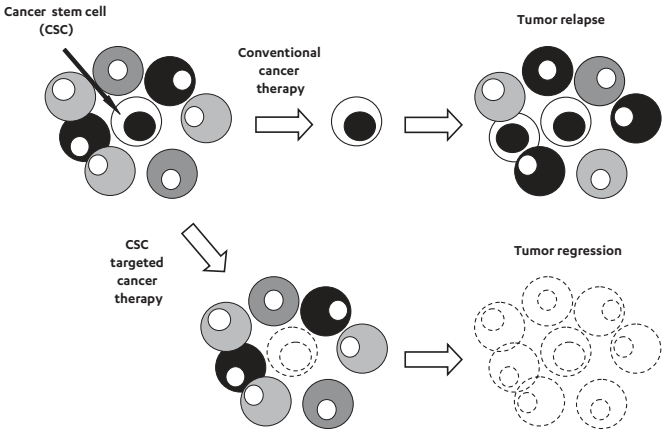

Figure 2. CSC therapy resistance and CSC targeted therapy

Recently, an additional layer of complexity has been added to CSC biology demonstrating that the CSC phenotype is not necessarily a uniform fraction of cells in terms of their genetic background and differentiation potential (17-19)(Chapter 3). It can be speculated that, as a tumor progresses, diverse selective pressures within different parts of tumor could result in a heterogeneous CSC pool with some clones being better adapted to survive, proliferate and invade compared to other clones, and potentially with different responses to treatments. Furthermore, it should be noted that in hierarchically organized tumors, CSCs are the driving force of tumor infiltration and invasiveness, due to their mobility and proliferative capacity (Chapter 4). The numerous clinical implications of these findings thus urge for defining factors that sustain CSCs, the most resistant and invasive clones in particular.

One of the crucial factors responsible for maintaining CSCs is the tumor vasculature. It forms the CSC niche and is implicated in therapy resistance, strongly suggesting a role for the vasculature in supporting the dominant CSC clones (20). This cross-talk has been confirmed by numerous studies of the interaction of CSCs with tumor microvascular endothelial cells (tMVECs), obtained

from *in vitro* as well as *in vivo* models, and further supported by genetic analysis (16, 20, 21) (Chapter 5). Accordingly, the study of different GBM subtypes demonstrated that more aggressive tumors are typified by the expression of both angiogenesis and neural stem cell genes. Furthermore upon recurrence these tumors tend to shift towards a mesenchymal GBM subtype that displays over-expression of these proteins, namely angiogenic and neural stem cell genes, implicating these genes to be the key drivers of tumor progression (16). Detailed overview of the current knowledge on the interaction of GBM CSCs and their microvascular niche and furthermore the consequences of this cross-talk for the treatment can be found in the review "CSC niche: the place to be", Chapter 2.

In an attempt to define the cause of tumor resistance, current research is mainly focused on analyzing tumor cells themselves, while neglecting the role of tumor microenvironment in this process. Subsequently, there is a lack of knowledge on how therapy affects the GBM niche and their interaction with CSCs. Therefore, we studied the effects of chemotherapy and radiation treatments on tumor vasculature, being the pivotal component of the CSC niche, and furthermore the consequences of these therapies on the cross-talk between tumor and micovasculature (Chapter 6). Our results demonstrate that this communication remains largely preserved despite the treatments due to extensive resistance of tMVECs. Upon radiation treatment these cells undergo permanent cell cycle arrest called senescence and subsequently continue to support CSCs. Strikingly, the tumor cells themselves are capable of differentiating into cells that phenocopy tMVECs in terms of their radiation response as well as their role of a CSC niche. Moreover, tMVECs are not only sustaining the CSCs but in addition are able to revert the more differentiated GBM cells back into the CSC phenotype, further repopulating this fraction of cells (Chapter 7). In conclusion, these results create an extremely complex scenario of the CSC-tMVECs interaction and predict a lot of challenges for the development of novel treatments to fight this disease.

Anti-Cancer Treatments and DNA-Damage

Even though numerous DNA-damaging anti-cancer therapies efficiently target tumors via different approaches, the fundamental changes in chromatin upon these treatments are still elusive. DNA is tightly packed within the nucleus in a highly organized yet dynamic fashion. DNA organization, while providing protection from various damaging factors, is still flexible enough to allow vital processes such as replication and transcription to occur. These contradictory requirements are enabled by the highly complex machinery that maintains DNA organization. The nucleosome is the basic unit of chromatin organization, composed of the DNA wrapped around a histone octamer (a pair of histones H2A, H2B, H3 and H4 per octamer), and connected by the linker-histone H1. The array of nucleosomes forms the so-called 'beads on the string" filament that folds into 30nm fiber and further coils into poorly understood higher order chromatin

structures (22). Even though DNA is a highly protected molecule, as its maintenance is an imperative for the cell, DNA double strand breaks (DSBs) still occur frequently in the genome either during replication or induced by various DNA-damaging agents. The cell deals with this situation by engaging complex mechanisms involved in cell cycle arrest, DNA repair and programmed cell death.

DSB, the most hazardous type of DNA damage, is initially being recognized by the Mre11-Rad50-NBS1 (MRN) complex, the DNA-dependant protein kinase (DNA-PK) and ataxia telangiectasia-mutated (ATM) protein (23-25). Activated ATM further phosphorylates histone H2AX that binds early-response proteins such as MDC1 and 53BP1 (26-28). Accumulation of these proteins on DSB occurs within minutes after the damage induction and signals to downstream targets, leading to checkpoint activation or apoptosis, mainly via Chk2 and p53 (29-32). Once a cell is arrested, the DSB repair machinery intervenes. Two distinct DSB repair pathways have been described: homologuous recombination (HR) and non-homologuous end joining (NHEJ) (Figure 3) (33). In HR, the undamaged sister chromatid serves as a repair template rendering this process essentially error-free but active only during S and G_2 phase of the cell cycle. HR starts with the replication protein A which binds to single-stranded DNA (ssDNA) ends and protects them from degradation. It is then replaced by BRCA2 and RAD51 recombinase that mediate binding of the ssDNA to homologous sequence. This is followed by RAD51 disassembly and chromatin remodeling promoted by RAD54. In the final steps of HR, the missing DNA is synthesized by DNA polymerases, mainly Pol δ and Pol η. NHEJ, on the other hand, operates irrespective of the cell cycle, directly re-ligating broken DNA ends without verification of homology and it is therefore regarded as error-prone, potentially able to link the DNA ends originating from different DSBs. The repair process starts with the KU70/80 heterodimer that accumulates at the damaged site and keeps the broken DNA ends in close proximity during repair. Binding of this protein to DNA attracts DNA-PKcs, associated with the juxtaposition of DNA ends, and facilitation of access of other proteins required for the repair. In the final steps of NHEJ, DNA ends are ligated by the DNA ligase IV/XRCC4 complex.

Although DSBs, induced upon anti-cancer treatments, are efficient in killing tumor cells and mainly succeed in doing so, they also can as a side-product create chromosomal rearrangements (CRs). This occurs in surviving tumor cells as well as in their surrounding healthy tissue that inevitably gets exposed to treatment. As a consequence of errors produced by the repair machinery, wrong DNA ends can be rejoined creating heritable mutations. These events may eventually lead to new, therapy-induced tumors (34, 35). Etoposide is one example of a frequently used anti-cancer drug known to promote the formation of CRs that can lead to specific types of

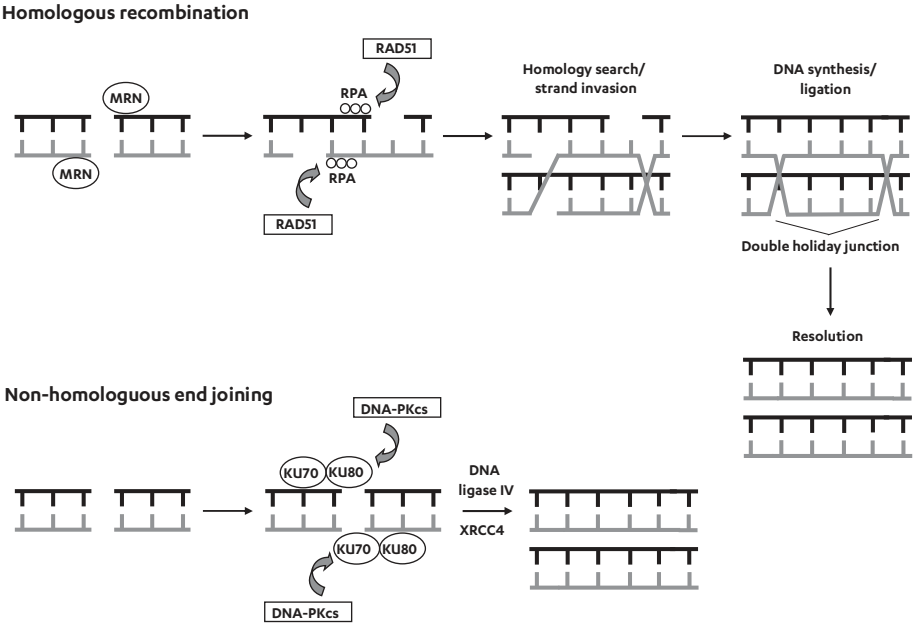

Figure 3. Schematic representation of two major DSB repair pathways: homologous recombination and non-homologous end joining

leukemia (36). In order to preserve the integrity of DNA in normal cells during anti-tumor therapies, it is essential to understand the fundamental chromatin changes and its behavior upon DNA damage induction. However, the exact mechanisms that control CR formation are still a subject of ongoing debate. Two hypotheses have been put forward trying to explain this process: the 'contact-first' theory postulates that the interactions between two ssDNA ends can only take place if the ends are colocalizing at the time of the DNA damage induction (37). The 'breakage-first' model, on the other hand, proposes that breaks formed at distant locations within the nucleus can come together to form a translocation (38). The main difference between these two models is, thus, their prediction regarding the dynamic behavior of chromatin and the extent to which the DNA ends can roam within the nucleus. Whether it is a large-scale or limited, local motion is yet to be determined as there are many contradictions among the available data (38-40).

As movement of DSB-containing chromatin domains is one of the factors that surely could facilitate the interactions of broken DNA ends and promote the formation of CRs, we examined the mobility of damaged DNA in living cells. Indeed, DSBs induced by DNA-damaging agents such

as gamma-irradiation or etoposide show higher mobility compared to intact chromatin. Importantly, this movement can be manipulated and decreased upon treatment with different chromatin remodeling agents, creating the opportunity for reducing side-affects of hazardous anti-cancer treatments. Detailed study of chromatin mobility can be viewed in Chapter 8.

Reference List

(1) Stupp R, Hegi ME, Mason WP, van den Bent MJ, Taphoorn MJB, Janzer RC, et al. Effects of radiotherapy with concomitant and adjuvant temozolomide versus radiotherapy alone on survival in glioblastoma in a randomised phase III study: 5-year analysis of the EORTC-NCIC trial. Lancet Oncology 2009;10:459-66.

(2) Giese A, Bjerkvig R, Berens ME, Westphal M. Cost of migration: Invasion of malignant gliomas and implications for treatment. Journal of Clinical Oncology 2003;21:1624-36.

(3) Stummer W, Pichlmeier U, Meinel T, Wiestler OD, Zanella F, Hans-Jurgen R. Fluorescence-guided surgery with 5-aminolevulinic acid for resection of malignant glioma: a randomised controlled multicentre phase III trial. Lancet Oncology 2006;7:392-401.

(4) Asthagiri AR, Pouratian N, Sherman J, Ahmed G, Shaffrey ME. Advances in brain tumor surgery. Neurologic Clinics 2007;25:975-+.

(5) Walker MD, Green SB, Byar DP, Alexander E, Batzdorf U, Brooks WH, et al. Randomized Comparisons of Radiotherapy and Nitrosoureas for the Treatment of Malignant Glioma After Surgery. New England Journal of Medicine 1980;303:1323-9.

(6) Hegi ME, Diserens A, Gorlia T, Hamou M, de Tribolet N, Weller M, et al. MGMT gene silencing and benefit from temozolomide in glioblastoma. New England Journal of Medicine 2005;352:997-1003.

(7) Chinot OL, Rouge TD, Moore N, Zeaiter A, Das A, Phillips H, et al. AVAglio: Phase 3 Trial of Bevacizumab Plus Temozolomide and Radiotherapy in Newly Diagnosed Glioblastoma Multiforme. Advances in Therapy 2011;28:334-40.

(8) Dickson PV, Hamner JB, Sims TL, Fraga CH, Ng CYC, Rajasekeran S, et al. Revacizumab-induced transient remodeling of the vasculature in neuroblastoma xenografts results in improved delivery and efficacy of systemically administered chemotherapy. Clinical Cancer Research 2007;13:3942-50.

(9) Paez-Ribes M, Allen E, Hudock J, Takeda T, Okuyama H, Vinals F, et al. Antiangiogenic Therapy Elicits Malignant Progression of Tumors to Increased Local Invasion and Distant Metastasis. Cancer Cell 2009;15:220-31.

(10) Ohgaki H, Kleihues P. Genetic pathways to primary and secondary glioblastoma. American Journal of Pathology 2007;170:1445-53.

(11) Verhaak RGW, Hoadley KA, Purdom E, Wang V, Qi Y, Wilkerson MD, et al. Integrated Genomic Analysis Identifies Clinically Relevant Subtypes of Glioblastoma Characterized by Abnormalities in PDGFRA, IDH1, EGFR, and NF1. Cancer Cell 2010;17:98-110.

(12) Clarke MF, Dick JE, Dirks PB, Eaves CJ, Jamieson CH, Jones DL, et al. Cancer stem cells--perspectives on current status and future directions: AACR Workshop on cancer stem cells. Cancer Res 2006;66:9339-44.

(13) Vermeulen L, Melo FDSE, van der Heijden M, Cameron K, de Jong JH, Borovski T, et al. Wnt activity defines colon cancer stem cells and is regulated by the microenvironment. Nature Cell Biology 2010;12:468-U121.

(14) Bao SD, Wu QL, McLendon RE, Hao YL, Shi Q, Hjelmeland AB, et al. Glioma stem cells promote radioresistance by preferential activation of the DNA damage response. Nature 2006;444:756-60.

(15) Bleau AM, Hambardzumyan D, Ozawa T, Fomchenko EI, Huse JT, Brennan CW, et al. PTEN/PI3K/Akt Pathway Regulates the Side Population Phenotype and ABCG2 Activity in Glioma Tumor Stem-like Cells. Cell Stem Cell 2009;4:226-35.

(16) Phillips HS, Kharbanda S, Chen RH, Forrest WF, Soriano RH, Wu TD, et al. Molecular subclasses of high-grade glioma predict prognosis, delineate a pattern of disease progression, and resemble stages in neurogenesis. Cancer Cell 2006;9:157-73.

(17) Odoux C, Fohrer H, Hoppo T, Guzik L, Stolz DB, Lewis DW, et al. A stochastic model for cancer stem cell origin in metastatic colon cancer. Cancer Research 2008;68:6932-41.

(18) Borovski T, Vermeulen L, Sprick MR, Medema JP. One renegade cancer stem cell? Cell Cycle 2009;8:803-8.

(19) Sottoriva A, Verhoeff JJC, Borovski T, McWeeney SK, Naumov L, Medema JP, et al. Cancer Stem Cell Tumor Model Reveals Invasive Morphology and Increased Phenotypical Heterogeneity. Cancer Research 2010;70:46-56.

(20) Calabrese C, Poppleton H, Kocak M, Hogg TL, Fuller C, Hamner B, et al. A perivascular niche for brain tumor stem cells. Cancer Cell 2007;11:69-82.

(21) Hovinga KE, Shimizu F, Wang R, Panagiotakos G, van der Heijden M, Moayedpardazi H, et al. Inhibition of Notch Signaling in Glioblastoma Targets Cancer Stem Cells via an Endothelial Cell Intermediate. Stem Cells 2010;28:1019-29.

(22) Woodcock CL, Dimitrov S. Higher-order structure of chromatin and chromosomes. Current Opinion in Genetics & Development 2001;11:130-5.

(23) Bakkenist CJ, Kastan MB. DNA damage activates ATM through intermolecular autophosphorylation and dimer dissociation. Nature 2003;421:499-506.

(24) Lavin MF. ATM and the Mre11 complex combine to recognize and signal DNA double-strand breaks. Oncogene 2007;26:7749-58.

(25) Uematsu N, Weterings E, Yano K, Morotomi-Yano K, Jakob B, Taucher-Scholz G, et al. Autophosphorylation of DNA-PKCS regulates its dynamics at DNA double-strand breaks. Journal of Cell Biology 2007;177:219-29.

(26) Rogakou EP, Boon C, Redon C, Bonner WM. Megabase chromatin domains involved in DNA double-strand breaks in vivo. J Cell Biol 1999;146:905-16.

(27) Schultz LB, Chehab NH, Malikzay A, Halazonetis TD. p53 Binding protein 1 (53BP1) is an early participant in the cellular response to DNA double-strand breaks. Journal of Cell Biology 2000;151:1381-90.

(28) Stucki M, Clapperton JA, Mohammad D, Yaffe MB, Smerdon SJ, Jackson SP. MDC1 directly binds phosphorylated histone H2AX to regulate cellular responses to DNA double-strand breaks. Cell 2005;123:1213-26.

(29) Banin S, Moyal L, Shieh SY, Taya Y, Anderson CW, Chessa L, et al. Enhanced phosphorylation of p53 by ATN in response to DNA damage. Science 1998;281:1674-7.

(30) Canman CE, Lim DS, Cimprich KA, Taya Y, Tamai K, Sakaguchi K, et al. Activation of the ATM kinase by ionizing radiation and phosphorylation of p53. Science 1998;281:1677-9.

(31) Chehab NH, Malikzay A, Appel M, Halazonetis TD. Chk2/hCds1 functions as a DNA damage checkpoint in G(1) by stabilizing p53. Genes & Development 2000;14:278-88.

(32) Hirao A, Kong YY, Matsuoka S, Wakeham A, Ruland J, Yoshida H, et al. DNA damage-induced activation of p53 by the checkpoint kinase Chk2. Science 2000;287:1824-7.

(33) Wyman C, Kanaar R. DNA double-strand break repair: All's well that ends well. Annual Review of Genetics 2006;40:363-83.

(34) Allan JM, Lois BT. Mechanisms of therapy-related carcinogenesis. Nature Reviews Cancer 2005;5:943-55.

(35) Stephens PJ, Greenman CD, Fu BY, Yang FT, Bignell GR, Mudie LJ, et al. Massive Genomic Rearrangement Acquired in a Single Catastrophic Event during Cancer Development. Cell 2011;144:27-40.

(36) Felix CA. Leukemias related to treatment with DNA topoisomerase II inhibitors. Medical and Pediatric Oncology 2001;36:525-35.

(37) Nikiforova MN, Stringer JR, Blough R, Medvedovic M, Fagin JA, Nikiforov YE. Proximity of chromosomal loci that participate in radiation-induced rearrangements in human cells. Science 2000;290:138-41.

(38) Aten JA, Stap J, Krawczyk PM, van Oven CH, Hoebe RA, Essers J, et al. Dynamics of DNA double-strand breaks revealed by clustering of damaged chromosome domains. Science 2004;303:92-5.

(39) Kruhlak MJ, Celeste A, Dellaire G, Fernandez-Capetillo O, Muller WG, McNally JG, et al. Changes in chromatin structure and mobility in living cells at sites of DNA double-strand breaks. Journal of Cell Biology 2006;172:823-34.

(40) Nelms BE, Maser RS, Mackay JF, Lagally MG, Petrini JHJ. In situ visualization of DNA double-strand break repair in human fibroblasts. Science 1998;280:590-2.

2

Cancer Stem Cell Niche: The Place to Be

Tijana Borovski, Felipe De Sousa E Melo, Louis Vermeulen and Jan Paul Medema

Authors' Affiliations: Laboratory for Experimental Oncology and Radiobiology (LEXOR), Center for Experimental Molecular Medicine (CEMM), Academic Medical Center (AMC), University of Amsterdam, Amsterdam, the Netherlands

Cancer Research 2011; 71:634-639

Abstract

Tumors are being increasingly perceived as abnormal organs that, in many respects, recapitulate the outgrowth and differentiation patterns of normal tissues. In line with this idea is the observation that only a small fraction of tumor cells is capable of initiating a new tumor. Because of the features that these cells share with somatic stem cells, they have been termed cancer stem cells (CSC). Normal stem cells reside in a "stem cell niche" that maintains them in a stem-like state. Recent data suggest that CSCs also rely on a similar niche, dubbed the "CSC niche," which controls their self-renewal and differentiation. Moreover, CSCs can be generated by the microenvironment through induction of CSC features in more differentiated tumor cells. In addition to a role in CSC maintenance, the microenvironment is hypothesized to be involved in metastasis by induction of the epithelial-mesenchymal transition, leading to dissemination and invasion of tumor cells. The localization of secondary tumors also seems to be orchestrated by the microenvironment, which is suggested to form a premetastatic niche. Thus, the microenvironment seems to be of crucial importance for primary tumor growth as well as metastasis formation. Combined with its role in the protection of CSCs against genotoxic insults, these data strongly put forward the niche as an important target for novel therapies.

Introduction

It is becoming increasingly clear that tumors are hierarchically organized heterogeneous populations of cells with the cancer stem cell (CSC) compartment on top. This fraction of tumor cells shares many similarities with normal stem cells, such as self-renewing capacity and multilineage differentiation properties (1). In addition, CSCs are highly tumorigenic and can generate a serially transplantable phenocopy of the primary human malignancy in immunocompromised mice (1). From a clinical point of view, the main concern with CSCs is their resistance to conventional treatments, a feature suggested to be the underlying cause of tumor recurrence (2, 3). Thus, it is necessary to define the factors that sustain CSCs in order to develop more efficient therapeutics. Normal stem cells reside in the distinct environment called the "stem cell niche." The niche regulates stemness, proliferation, and apoptosis resistance of stem cells. It has a complex architecture and is composed of diverse stromal cells, such as mesenchymal and immune cells, a vascular network, soluble factors, and extracellular matrix components. Analogously, tumorigenicity not only involves the biology of tumor cells themselves but also results from a rather complex interplay between tumor cells and the nonmalignant cells that make up the tumor environment. Like normal stem cells, CSCs seem to depend on a similar, permissive environment, the CSC niche, to retain their exclusive abilities to self-renew and give rise to more differentiated progenitor cells, while staying in an undifferentiated state themselves (5). Moreover, the CSC niche also has a protective role. By sheltering CSCs from diverse genotoxic insults, the niche contributes to their enhanced therapy resistance (6, 7). Here, we discuss the concept of the stem cell niche in a tumor setting, with special emphasis on brain and colon cancer as examples of malignancies in which CSCs seem to rely on a specialized microenvironment. Furthermore, we review the role of the tumor microenvironment in the progression of primary tumors, focusing on dedifferentiation of non-CSCs and epithelial-mesenchymal transition (EMT) induction by the niche and, finally, the involvement of a premetastatic niche in the formation of metastasis (Fig. 1).

The Perivascular Niche in Glioblastoma Multiforme

In the adult mammalian brain, neural stem cells reside in the hippocampus and subventricular zone, close to the blood vessels. During embryogenesis and early brain development, ventricular neuroectoderm secretes high levels of vascular endothelial growth factor (VEGF), which attracts and stimulates vessel growth in this region of the brain (8). Thus, vascular endothelial cells and neural stem cells come together during early development and stay in close proximity throughout life. Protein ligands found within the neural stem cell niche, such as pigment epithelium–derived factor and stem cell factor, have been implicated in both stem cell self-renewal and regulation of

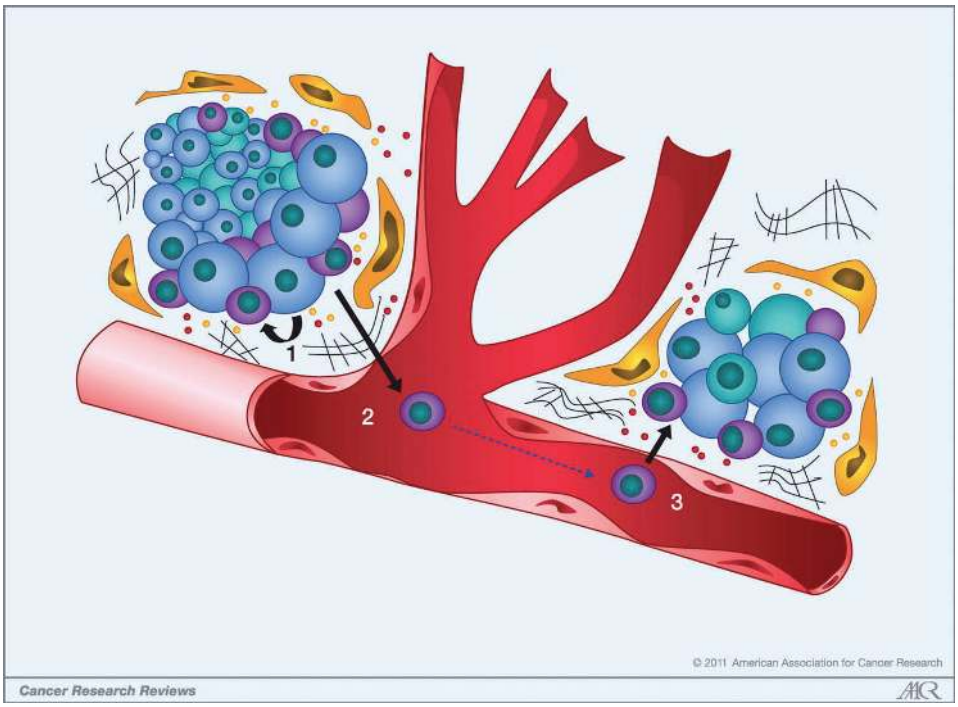

Figure 1. The CSC niche in tumor growth and metastasis. The CSC niche is composed of blood vessels (red), stromal cells such as myofibroblasts (orange), and extracellular matrix components. Tumors are organized in such a way that CSCs (purple) reside close to their niche. In addition to maintaining CSCs in a stemlike state, (1), the niche has the ability to dedifferentiate nontumorigenic cells (blue) into tumorigenic CSCs (purple) and, (2), to induce the EMT, leading to dissemination of tumor cells from the primary tumor and, (3), seeding at the metastatic place. Furthermore, tumor cell engraftment in different organs is suggested to be facilitated by the formation of a premetastatic niche that potentially enables the initiation and outgrowth of secondary tumors.

angiogenesis, also suggesting that these two processes are tightly linked (9–12). More direct evidence for the role of endothelial cells in neural stem cell biology comes from the observation that these cells regulate asymmetrical division of the stem cells in the subventricular zone (13). Furthermore, they maintain neural stem cell self-renewal, in part via Notch signaling, and simultaneously inhibit stem cell differentiation (4).

Glioblastoma multiforme (GBM) is the most aggressive type of primary brain tumor in humans, with high morbidity and median survival of less then a year. Recently, a CSC fraction was identified in these tumors. These glioma-initiating cells seem to have a higher DNA repair rate and resistance to treatment than more differentiated glioma cells, making them the main suspects for tumor regrowth after therapy (2). GBM is a highly vascularized tumor, which led to the speculation that GBM CSCs might depend on a similar niche as neural stem cells. Indeed, recent publications have shown the validity of this concept. Calabrese and colleagues showed the existence of a close relationship between brain CSCs and blood vessels and, furthermore, that the vascular endothelial cells are able to maintain patient-derived brain tumor cells in a stemlike state and promote their

tumorigenicity when coinjected in immunocompromised mice (5). A soluble factor mediating this interaction and promoting CSC self-renewal seems to be nitric oxide produced by endothelial cells, which activates the Notch pathway in glioma CSCs (14). However, the interaction between CSCs and tumor vasculature is likely a more complex and bidirectional process. Brain tumor CSCs are able to promote recruitment and formation of blood vessels by secreting VEGF (15). Furthermore, inhibition of angiogenesis and depletion of blood vessels by the VEGF-neutralizing antibody bevacizumab reduced the CSC pool and, subsequently, inhibited tumor growth (5). Moreover, tumor cells protect their niche and, *vice versa*, the vascular microenvironment contributes to enhanced therapy resistance of GBM CSCs. Accordingly, glioma cells induce upregulation of different survival genes in endothelial cells, protecting them from hypoxia or irradiation-induced apoptosis (16, 17). Reciprocally, inhibition of Notch signaling in an explant system of surgical GBM specimens leads to detachment of CSCs from their vascular niche and increased efficacy of radiotherapy on CSCs (6). Similarly, application of antiangiogenic therapy to gliomas and eradication of tumor vasculature results in a higher susceptibility of CSCs to cytotoxic agents (7). Although these data sound promising, they should be viewed with caution as the long-term effect of antiangiogenic therapy on tumor growth and the final outcome of the treatment is still not fully known. A recent publication even suggested that anti-VEGF treatment eventually leads to increased invasiveness and metastasis of the tumor (18). One of the undesired consequences of anti-VEGF treatment could be an increase in hypoxic areas, which are described to be refractory to therapy. Being located far from blood vessels, hypoxic tumor cells are usually exposed to relatively low concentrations of chemotherapeutics. Furthermore, cytotoxic drugs mainly target proliferating cells and, therefore, do not harm hypoxic tumor cells that are usually quiescent due to a lack of oxygen and nutrients (19). In addition, hypoxia also creates problems for radiotherapy, as it reduces the formation of oxygen free radicals that, as a byproduct of radiotherapy, would normally induce DNA damage in tumor cells (20). Hypoxia also has more direct cellular effects, as it has been linked to regulating cell survival, enhanced motility and invasiveness of tumor cells, and tumor angiogenesis. Moreover, hypoxic regions are related to the areas of pseudopallisading necrosis, another hallmark of GBM, and have been proposed to also form a GBM CSC niche, in addition to tumor vasculature (21). GBM CSCs are frequently found to be located at the edges of necrotic regions. Indeed, similar to normal neural stem cells, it has also been shown that hypoxia regulates GBM CSC maintenance (21, 22). The effects of hypoxia are mainly mediated by hypoxia-inducible factors (HIF), of which HIF2α is of particular importance for the GBM CSC pool, increasing their self-renewal and tumorigenic capacity (21). Not surprisingly, HIF2α expression correlates with the poor survival of GBM patients. Combined, these data clearly put forward the role of brain tumor vasculature and hypoxia in the maintenance of CSCs, as well as their therapy resistance; however, further investigations are needed to successfully apply this knowledge in treating GBM patients.

The Stem Cell Niche in Colorectal Cancer

Another example of an extensively studied stem cell niche exists in the intestine. The intestinal crypt is the functional unit of the intestinal tract, including colon and small intestine. Stem cells reside in the bottom region of the crypt, within a stem cell niche composed of epithelial cells and mesenchymal cells of the myofibroblast lineage that line the crypt. Moving upwards, progenitor cells start to differentiate and once they reach the top, they are shed into the lumen of intestine and die. Current data show that the Wnt signaling cascade is a prominent force controlling cell proliferation, differentiation, and apoptosis along the crypt–villus axis and in maintaining stem cell fate (23). The absence of Wnt signaling activity in *Tcf4*$^{-/-}$ mice or its inhibition by transgenic Dickkopf-1 expression leads to complete loss of crypts in adult mice (23). BMP signaling has opposite effects and drives the cells toward differentiation (24). A fine-tuned balance between these and other signaling pathways maintains the intestinal homeostasis and this is partially directed by the intestinal stem cell niche. Myofibroblasts that line the crypt produce Wnt ligands, together with BMP antagonists such as gremlin 1/2, which, in combination, are involved in preservation of the stem cell pool (25, 26).

A similar model has been suggested to delineate the colon CSC interaction with their microenvironment. Studies of heritable juvenile polyposis syndrome highlighted the importance of tumor stroma for the development of colorectal cancer. One of the features of the gastrointestinal polyps seen in *Apc-Smad4* mutant heterozygous mice is increased proliferation of stromal cells. It is also one of the characteristics of juvenile polyps seen in humans and predisposes for development of carcinomas that arise from epithelial cells. In addition, a connection between inflammatory processes and colon cancer is well established. For example, it has been described in models of colitis-associated cancer, as well as in other forms of colorectal cancer, that interleukin 6 secreted mainly by the infiltrating immune cells stimulates proliferation of tumor-initiating intestinal cells (27). Analogously to the normal intestinal stem cell niche, myofibroblasts and mesenchymal stem cells are shown to be components of the colon cancer stroma. Mesenchymal stem cells have the ability to enhance growth and metastasis of colon cancer and have been, furthermore, proposed to give rise to fibroblasts that further promote tumorigenesis (28, 29). Mutations in the *APC* gene, an inhibitor of Wnt signaling, are early events in the transition of healthy colon mucosa toward colon carcinoma, resulting in stabilization of β-catenin and subsequent translocation to the nucleus. In the nucleus, β-catenin binds to T-cell factor/lymphoid enhancer factor (TCF/LEF) family members and acts as a transcriptional regulator of many genes that control proliferation and differentiation. However, despite the same genetic background, cells within the tumors display differential Wnt activity, judging by the localization of β-catenin, which is referred to as the so-called β-catenin paradox (30, 31). It indicates that, besides *APC*

mutations, additional regulatory mechanisms of Wnt activity are at play in these tumors. One possible explanation could be additional *KRAS* mutations. According to Phelps and colleagues, *APC* mutations primarily play a role in stabilizing the levels of β-catenin in the cytoplasm, whereas additional mutations in KRAS are necessary for translocation of β-catenin to the nucleus (32). In addition to these cell-intrinsic events, the Wnt pathway also seems to be regulated by the tumor microenvironment. Accordingly, cells harboring nuclear β-catenin are mainly clustered at the invasive front of the tumor in regions highly populated with myofibroblasts (30, 31). How does this finding relate to colon CSCs? Tumor-associated myofibroblasts (TAF) are a major cellular component of colon cancer stroma. They have higher proliferation rates than normal fibroblasts and are the primary source of type I collagen, shown to promote a stem cell–like phenotype in colorectal carcinoma cell lines (33). The importance of TAFs in tumorigenesis is supported by data showing that depletion of TAFs through CD8+ T-cell–mediated killing significantly reduced tumor growth and metastasis in, among others, colon cancer (34). In addition, efficacy of chemotherapy was improved, implying that TAFs are also involved in tumor chemoresistance. Recently, we reported that high Wnt activity levels mark the colon CSC population and are orchestrated by myofibroblasts residing in the tumor microenvironment (35). More precisely, we found that hepatocyte growth factor (HGF) produced by myofibroblasts is capable of enhancing Wnt signaling activity in colon CSCs, suggesting a strong link between the microenvironment and CSC features in colorectal cancer as well.

Cancer Stem Cells, Dedifferentiation and the Epithelial-Mesenchymal Transition

Intriguingly, the effects of the microenvironment on CSCs are beyond just preservation and protection of this compartment. We observed that HGF-producing myofibroblasts were able to dedifferentiate nontumorigenic tumor cells into more immature cells by reactivating the Wnt pathway. These dedifferentiated cancer cells displayed all characteristics of CSCs, including expression of stem cell–associated genes, such as *LGR5*, and high tumorigenic potential (35). Our experiments imply that the tumor microenvironment, more specifically the CSC niche, is capable of inducing a CSC phenotype in differentiated tumor cells.

What would be the consequences of an ongoing process of dedifferentiation in malignancies? Cancer cells possess a certain level of plasticity that allows them to change their phenotype and acquire different functions and properties under the influence of the environment. Processes that reflect their plasticity are the EMT and its reverse, the mesenchymal- epithelial transition, highly conserved programs that are involved in embryonic development but also in carcinogenesis (36). EMT is one of the crucial, early steps in the invasion–metastasis cascade and has been associated

with poor clinical outcome of patients in many types of tumors. Epithelial tumor cells that undergo EMT lose cell–cell adhesion properties and polarity and acquire a more mesenchymal-like phenotype, including motility, invasiveness, and increased resistance to apoptosis. Importantly, tumor cells undergoing EMT acquire CSC-like features as can be concluded from experiments in which induction of EMT in immortalized human mammary epithelial cells led to the expression of CSC markers, increased self-renewal capacity, and enhanced tumor formation (37). EMT, thus, provides disseminated tumor cells with self-renewing properties and increased proliferative capacity, enhancing their chances to seed at a distant site and grow metastases. Considering the fact that the EMT promotes the generation of a CSC phenotype, it is crucial to know how this process is controlled and regulated. A variety of signals that can induce the EMT, such as hypoxia, are being received from the tumor microenvironment. Hypoxia was shown to regulate the plasticity of GBM cells as well. Heddleston and colleagues found hypoxia to promote the self-renewal capability and stem cell phenotype in the non–stem cell population, increasing their neurosphere-forming capacity and upregulating important stem cell factors, such as OCT4, NANOG, and c-MYC (38). Furthermore, expression of HIF2α in the non–stem cell population enhanced their tumorigenic potential. It should be noted, though, that, in addition to regulating cell plasticity, hypoxia, and other EMT-inducing factors from the microenvironment, such as TGF-β, are also known to stimulate proliferation and expansion of the preexisting CSC pool, thereby further increasing the chances for metastatic spread (37, 39, 40). One of the mechanisms of hypoxia-induced invasiveness is the activation of the Wnt signaling pathway via inhibition of glycogen synthase kinase 3β, which leads to the induction of the key EMT-inducing transcription factor Snail (41). Expression of SNAIL protein was detected at the tumor–stroma interface in diverse human cancers including colon cancer (42). Correspondingly, it was mentioned previously that colorectal cancer cells with nuclear β-catenin, a marker of colon CSCs on one hand and an inducer of EMT on the other, mostly reside at the host–tumor interface (30). Intriguingly, HGF, which we have described as being able to induce CSC properties in differentiated colon cancer cells, was used to induce cell scattering of MDCK cells in the initial studies on EMT (43). The ability of reacquiring stem cell features in the more differentiated cells by HGF-producing myofibroblasts puts these cells at the crucial position in the EMT-CSC framework.

The Premetastatic Niche

We have described how TAFs are involved in maintenance of CSCs and the induction of CSC features in more differentiated tumor cells, potentially via mechanisms related to EMT. Moreover, we have put forward how this model provides an elegant explanation for the intimate connection between CSC features, the EMT, and tumor cell invasion. However, the microenvironment might also be implicated in the final steps of the metastatic cascade. It is known that metastases

selectively occur in certain organs such as lungs, liver, brain, and bones. This observation led to the so-called seed and soil hypothesis. According to this hypothesis, the local microenvironment of these organs seems to be more receptive to disseminated tumor cells from particular malignancies than other organs. Thus, occurrence of metastasis does not happen randomly, but disseminated tumor cells need to meet a hospitable microenvironment in order to initiate a secondary tumor. Furthermore, in recent years, evidence suggested that the primary tumor itself is actively involved in adapting these so-called premetastatic niches for tumor cells to come, by secreting systemic factors and directing bone marrow–derived cells and macrophages to certain tissues, thereby priming certain tissues for tumor cell engraftment (44, 45). Accordingly, VEGFR1-positive bone marrow–derived hematopoietic progenitor cells (HPC) were shown to localize to premetastatic sites and form clusters before the arrival of tumor cells (44). Eradication of these cells from the bone marrow prevents the formation of premetastatic clusters and, subsequently, tumor metastasis. In addition to homing of HPCs, preexisting fibroblasts are noted to increase fibronectin deposition on these sites, which most likely binds to VLA4, a fibronectin receptor expressed on HPCs, and facilitates accumulation of these cells. Furthermore, activated fibroblasts were shown to induce remodeling of stroma required for liver metastasis in a murine melanoma model (46). Thus, in addition to their contribution to the CSC niche at the primary tumor site, fibroblasts are suggested to have a critical role in premetastasis niche formation as well.

Conclusions

In conclusion, the reviewed data point out a central role of the CSC niche in virtually every step of the tumorigenic cascade (Fig. 1). In primary tumors, the CSC niche is an important regulator of stemness. The importance of this interaction is supported by the fact that the loss of a niche environment mainly leads to the loss of CSCs. The reliance of CSCs on niche signals seems to be a general phenomenon and has been shown in a whole variety of different tumors. In addition to maintaining the CSC pool and supporting the growth of primary tumors, the niche plays a role in reverting nontumorigenic cells into CSCs by processes related to the EMT, leading to tumor invasion and dissemination. Finally, the putative premetastatic niche supposedly assures successful homing of cancer cells to distant organs and the development of metastasis. Whether premetastatic niches are also capable of installing a CSC phenotype in more differentiated cells or whether these particular environments are only capable of maintaining the function of metastasized CSCs is still a matter of speculation. Either way, the supporting role of the microenvironment in tumor growth and progression, including metastasis formation, clearly puts the CSC niche and, especially, the mediators of this interaction in the spotlight as future therapeutic targets. Emerging therapies are already targeting this strategy. For example, we previously highlighted the importance of HGF production by the microenvironment in colorectal cancer. HGF acts via the tyrosine kinase receptor MET on cancer cells and triggers its downstream

targets. Recently, it has been shown that anti-MET antibodies prevent HGF binding to MET and, subsequently, inhibit colon cancer tumor growth (47). This example is only one of the extensive studies that explore the modulation of the interaction between cancer cells and niche cells as a therapeutic strategy that could lead to major advances in cancer treatment in the years to come.

Disclosure of Potential Conflicts of Interest : No potential conflicts of interest were disclosed.

Grant Support : J.P. Medema is supported by a VICI grant from the Dutch Science Organization and through a grant from the Dutch Cancer Society (UvA2009–4416).

Acknowledgments : The authors would like to thank the members of the group for useful discussions.

Received September 2, 2010.
Revision received November 8, 2010.
Accepted November 11, 2010.

References

1. Clarke MF, Dick JE, Dirks PB, Eaves CJ, Jamieson CH, Jones DL, et al. Cancer stem cells–perspectives on current status and future directions: AACR Workshop on cancer stem cells. Cancer Res 2006;66:9339–44.

2. Bao S, Wu Q, McLendon RE, Hao Y, Shi Q, Hjelmeland AB, et al. Glioma stem cells promote radioresistance by preferential activation of the DNA damage response. Nature 2006;444:756–60.

3. Todaro M, Alea MP, Di Stefano AB, Cammareri P, Vermeulen L, Lovino F, et al. Colon cancer stem cells dictate tumor growth and resist cell death by production of interleukin-4. Cell Stem Cell 2007;1:389–402.

4. Shen Q, Goderie SK, Jin L, Karanth N, Sun Y, Abramova N, et al. Endothelial cells stimulate self-renewal and expand neurogenesis of neural stem cells. Science 2004;304:1338–40.

5. Calabrese C, Poppleton H, Kocak M, Hogg TL, Fuller C, Hamner B, et al. A perivascular niche for brain tumor stem cells. Cancer Cell 2007;11:69–82.

6. Hovinga KE, Shimizu F, Wang R, Panagiotakos G, Van Der Heijden M, Moayedpardazi H, et al. Inhibition of Notch signaling in glioblastoma targets cancer stem cells via an endothelial cell intermediate. Stem Cells 2010;28:1019–29.

7. Folkins C, Man S, Xu P, Shaked Y, Hicklin DJ, Kerbel RS. Anticancer therapies combining antiangiogenic and tumor cell cytotoxic effects reduce the tumor stem-like cell fraction in glioma xenograft tumors. Cancer Res 2007;67:3560–4.

8. Breier G, Albrecht U, Sterrer S, Risau W. Expression of vascular endothelial growth-factor during embryonic angiogenesis and endothelial cell differentiation. Development 1992;114:521–32.

9. Sun L, Hui AM, Su Q, Vortmeyer A, Kotliarov Y, Pastorino S, et al. Neuronal and glioma-derived stem cell factor induces angiogenesis within the brain. Cancer Cell 2006;9:287–300.

10. Jin K, Mao XO, Sun YJ, Xie L, Greenberg DA. Stem cell factor stimulates neurogenesis in vitro and in vivo. J Clin Invest 2002;110:311–9.

11. Ramirez-Castillejo C, Sanchez-Sanchez F, Andreu-Agullo C, Ferron SR, Aroca-Aguilar JD, Sanchez P, et al. Pigment epithelium-derived factor is a niche signal for neural stem cell renewal. Nat Neurosci 2006;9:331–9.

12. Dawson DW, Volpert OV, Gillis P, Crawford SE, Xu HJ, Benedict W, et al. Pigment epithelium-derived factor: A potent inhibitor of angiogenesis. Science 1999;285:245–8.

13. Knoblich JA. Mechanisms of asymmetric stem cell division. Cell 2008;132:583–97.

14. Charles N, Ozawa T, Squatrito M, Bleau AM, Brennan CW, Hambardzumyan D, et al. Perivascular nitric oxide activates notch signaling and promotes stem-like character in PDGF-induced glioma cells. Cell Stem Cell 2010;6:141–52.

15. Bao S, Wu Q, Sathornsumetee S, Hao YL, Li ZZ, Hjelmeland AB, et al. Stem cell-like glioma cells promote tumor angiogenesis through vascular endothelial growth factor. Cancer Res 2006;66: 7843–8.

16. Ezhilarasan R, Mohanam I, Govindarajan K, Mohanam S. Glioma cells suppress hypoxia-induced endothelial cell apoptosis and promote the angiogenic process. Int J Oncol 2007;30:701–7.

17. Brown CK, Khodarev NN, Yu JQ, Moo-Young T, Labay E, Darga TE, et al. Glioblastoma cells block radiation-induced programmed cell death of endothelial cells. FEBS Lett 2004;565:167–70.

18. Paez-Ribes M, Allen E, Hudock J, Takeda T, Okuyama H, Vinals F, et al. Antiangiogenic therapy elicits malignant progression of tumors to increased local invasion and distant metastasis. Cancer Cell 2009;15:220–31.

19. Minchinton AI, Tannock IF. Drug penetration in solid tumours. Nat Rev Cancer 2006;6:583–92.

20. Hockel M, Vaupel P. Tumor hypoxia: definitions and current clinical, biologic, and molecular aspects. J Natl Cancer Inst 2001;93:266–76.

21. Li Z, Bao S, Wu Q, Wang H, Eyler C, Sathornsumetee S, et al. Hypoxiainducible factors regulate tumorigenic capacity of glioma stem cells. Cancer Cell 2009;15:501–13.

22. Clarke L, Van Der Kooy D. Low oxygen enhances primitive and definitive neural stem cell colony formation by inhibiting distinct cell death pathways. Stem Cells 2009;27:1879–86.

23. Clevers H. Wnt/beta-catenin signaling in development and disease. Cell 2006;127:469–80.

24. He XC, Zhang JW, Tong WG, Tawfik O, Ross J, Scoville DH, et al. BMP signaling inhibits intestinal stem cell self-renewal through suppression of Wnt-beta-catenin signaling. Nat Genet 2004;36: 1117–21.

25. Kosinski C, Li VSW, Chan ASY, Zhang J, Ho C, Tsui WY, et al. Gene expression patterns of human colon tops and basal crypts and BMP antagonists as intestinal stem cell niche factors. Proc Natl Acad Sci U S A 2007;104:15418–23.

26. Gregorieff A, Pinto D, Begthel H, Destree O, Kielman M, Clevers H. Expression pattern of Wnt signaling components in the adult intestine. Gastroenterology 2005;129:626–38.

27. Grivennikov S, Karin E, Terzic J, Mucida D, Yu GY, Vallabhapurapu S, et al. IL-6 and Stat3 are required for survival of intestinal epithelial cells and development of colitis-associated cancer. Cancer Cell 2009;15: 103–13.

28. Shinagawa K, Kitadai Y, Tanaka M, Sumida T, Kodama M, Higashi Y, et al. Mesenchymal stem cells enhance growth and metastasis of colon cancer. Int J Cancer 2010;127:2323–33.

29. Mishra PJ, Mishra PJ, Humeniuk R, Medina DJ, Alexe G, Mesirov JP, et al. Carcinoma-associated fibroblast-like differentiation of human mesenchymal stem cells. Cancer Res 2008;68:4331–9.

30. Brabletz T, Jung A, Reu S, Porzner M, Hlubek F, Kunz-Schughart LA, et al. Variable beta-catenin expression in colorectal cancers indicates tumor progression driven by the tumor environment. Proc Natl Acad Sci U S A 2001;98:10356–61.

31. Fodde R, Brabletz T. Wnt/beta-catenin signaling in cancer stemness and malignant behavior. Curr Opin Cell Biol 2007;19:150–8.

32. Phelps RA, Chidester S, Dehghanizadeh S, Phelps J, Sandoval IT, Rai K, et al. A two-step model for colon adenoma initiation and progression caused by APC loss. Cell 2009;137:623–34.

33. Kirkland SC. Type I collagen inhibits differentiation and promotes a stem cell-like phenotype in human colorectal carcinoma cells. Br J Cancer 2009;101:320–6.

34. Loeffler M, Kruger JA, Niethammer AG, Reisfeld RA. Targeting tumorassociated fibroblasts improves cancer chemotherapy by increasing intratumoral drug uptake. J Clin Invest 2006;116:1955–62.

35. Vermeulen L, De Sousa E Melo F, Van Der Heijden M, Cameron K, de Jong JH, Borovski T, et al. Wnt activity defines colon cancer stem cells and is regulated by the microenvironment. Nat Cell Biol 2010;12:468–
76.

36. Yang J, Weinberg RA. Epithelial-mesenchymal transition: At the crossroads of development and tumor metastasis. Dev Cell 2008;14:818–29.

37. Mani SA, Guo W, Liao MJ, Eaton EN, Ayyanan A, Zhou AY, et al. The epithelial-mesenchymal transition generates cells with properties of stem cells. Cell 2008;133:704–15.

38. Heddleston JM, Li ZZ, McLendon RE, Hjelmeland AB, Rich JN. The hypoxic microenvironment maintains glioblastoma stem cells and promotes reprogramming towards a cancer stem cell phenotype. Cell Cycle 2009;8:3274–84.

39. Blazek ER, Foutch JL, Maki G. Daoymedulloblastoma cells that express CD133 are radioresistant relative to CD133- cells, and the CD133þ sector is enlarged by hypoxia. Int J Radiat Oncol Biol Phys 2007;67:1–5.

40. Das B, Tsuchida R, Malkin D, Koren G, Baruchel S, Yeger H. Hypoxia enhances tumor stemness by increasing the invasive and tumorigenic side population fraction. Stem Cells 2008;26:1818–30.

41. Cannito S, Novo E, Compagnone A, Valfre di Bonzo L, Busletta C, Zamara E, et al. Redox mechanisms switch on hypoxia-dependent epithelial-mesenchymal transition in cancer cells. Carcinogenesis 2008;29:2267–78.

42. Franci C, Takkunen M, Dave N, Alameda F, Gomez S, Rodriguez R, et al. Expression of Snail protein in tumor-stroma interface. Oncogene 2006;25:5134–44.

43. Stoker M, Perryman M. An epithelial scatter factor released by embryo fibroblasts. J Cell Sci 1985;77:209–23.

44. Kaplan RN, Riba RD, Zacharoulis S, Bramley AH, Vincent L, Costa C, et al. VEGFR1-positive haematopoietic bone marrow progenitors initiate the pre-metastatic niche. Nature 2005;438:820–7.

45. Hiratsuka S, Watanabe A, Aburatani H, Maru Y. Tumour-mediated upregulation of chemoattractants and recruitment of myeloid cells predetermines lung metastasis. Nat Cell Biol 2006;8:1369–75.

46. Olaso E, Santisteban A, Bidaurrazaga J, Gressner AM, Rosenbaum J, Vidal-Vanaclocha F. Tumor-dependent activation of rodent hepatic stellate cells during experimental melanoma metastasis. Hepatology 1997;26:634–42.

47. van der Horst EH, Chinn L, Wang M, Velilla T, Tran H, Madrona Y, et al. Discovery of fully human anti-MET monoclonal antibodies with antitumor activity against colon cancer tumor models in vivo. Neoplasia 2009;11:355–64

3

One Renegade Cancer Stem Cell?

Tijana Borovski, Louis Vermeulen, Martin R. Sprick† and Jan Paul Medema†

Authors' Affiliations: Laboratory for Experimental Oncology and Radiobiology; Center for Experimental and Molecular Medicine; Academic Medical Center; University of Amsterdam; Amsterdam, The Netherlands

†These authors share senior authorship.

Cell Cycle 8:6, 803-808; 15 March 2009

Abstract

The CSC compartment represents the subpopulation of tumor cells with clonogenic potential and the ability to initiate new tumors. Besides self renewal, one of their main features is their ability to differentiate into the variety of cells within the tumor. The question remains whether this potential resides within the single CSC or whether many different CSCs are necessary to generate a heterogeneous population of tumor cells. There is an increasing amount of evidence showing that a single CSC indeed has the potential to reconstitute the complete tumor phenotype. This is likely to be a general phenomenon and it has been demonstrated in many tumors so far. Here we show that single GBM CSCs have multilineage potential, although not exclusively. Furthermore, our results show that CSCs originating from same tumor are not necessarily uniform in respect to their differentiation potential.

There are two opposing models to explain the initiation and development of tumors. One is the stochastic model which proposes that in principle all cells in the malignancy have the potential to drive tumor growth. In contrast, the hierarchical model suggests that only a small fraction of cells has tumor-initiating properties and can generate new tumors. The latter hypothesis is consistent with the cancer stem cell (CSC) theory. In this model, CSCs are defined as cells that have the property of self-renewal and are able to generate all more differentiated cell types in the tumor.1-3 In addition, they are able to initiate tumors that mirror the original malignancy after serial transplantation in a xenograft model.2 This means that, in analogy to normal stem cells, new CSCs with the same capacity to proliferate and differentiate as the parental cell can be generated after cell divisions. Simultaneously, progeny with the ability to differentiate is generated. It is believed that CSCs, like normal stem cells, accomplish this by asymmetric division, where one daughter cell retains a stem cell phenotype and one differentiates into the various cell types found in the tumor.4 It has been shown that CSCs are more resistant to genotoxic treatments when compared to more differentiated cell types within the tumor and therefore, it has been suggested that CSCs are responsible for tumor regrowth after treatment.5-8 Together, these features make CSCs a potential target for the development of novel therapies.

Convincing evidence that supports the CSC hypothesis was obtained first in acute myeloid leukemia.9 Since then the principle has been extended to solid malignancies as well, and CSCs have been described in brain, prostate, breast, colon, lung, pancreas and ovarian cancers.1 Markers that are normally associated with immature cells and normal stem cells have been successfully used to identify and isolate those CSCs. However, to date the 'gold standard' to confirm stem-cell properties of tumor cells is their ability to give rise to a new tumor that recapitulates the phenotype of the original one in immunocompromized mice and, in addition, can be serially transplanted.2 This indicates that newly generated tumors contain a population of functional stem cells and confirms their self-renewal properties.

Normal stem cells are required for tissue maintenance and repair. They can be found in nearly every major organ. In particular, they are required in tissues that undergo continuous and rapid cellular turnover, such as skin and gut epithelial cells or cellular components of blood. Therefore, there is a constant demand for stem cells to generate new mature cells through differentiation. Simultaneously, the stem cell pool needs to be kept constant and be replenished if necessary.10 There are several examples that illustrate the potential that resides within a single stem cell. One is the colon crypt, the main structural unit of the colon. Crypts are invaginations of the colon epithelial layer with the stem cells situated at the bottom wherefrom they simultaneously migrate upwards and start differentiating. There are three different lineages of colon epithelial cells and it is thought that the same stem cell can generate all these distinct intestinal cell types.11,12 This is

exemplified by the finding that crypts consist of clonal populations of cells. Firm evidence that this is indeed the case was obtained from a study of a *X0/XY* mosaic patient suffering from familiar adenomatous polyposis.13 Analysis of the patients' intestine revealed that the crypts were formed of *X0* or *XY* cells exclusively. Furthermore, it has been shown that certain mutations which are moderately common in colon stem cells were either present or completely absent per crypt.14-16 The existence of crypts in which all the lineages carry the same mutations indicates that the crypt most likely arose from the same mutated stem cell that had the potential to differentiate into all colon cell types. In addition, the newly identified stem cell marker Lgr5 was recently used to study the behavior and differentiation of intestinal stem cells.17 Cells which are Lgr5 positive could be marked irreversibly by induction of β-Gal expression. β-Gal positive cells were located at the bottom of the crypts and thought to mark stem cells. As expected, initially only a few cells at the base of the crypt were Lgr5 positive. At later time points β-Gal positive cells emanated from the crypts and were present along the sides of the villi. Importantly, all differentiated cell types of the intestine were identified among the daughter cells of the β-Gal positive cells. This demonstrates that Lgr-5 expressing cells are indeed stem cells that give rise to all diverse cell types of the intestinal epithelium.

There is an increasing number of examples that demonstrate the generation of a complete organ from a single stem cell. Among others, these kinds of studies were performed in the mammary gland. The mammary gland is comprised of two different groups of epithelial cells, luminal and myoepithelial cells that both branch out and form ducts and lobulo-alveolar units. It has been speculated that these two groups of cells originate from the same stem cell. Convincing proof of this idea has recently been obtained by Shackleton et al.18 A stem-cell enriched population was isolated from a mouse mammary gland based on cell-surface markers (Lin- CD29 hi CD24+) and a single cell was injected into cleared mammary fat pads of recipient female mice. This resulted in outgrowths of the ductal-alveolar network. Furthermore, histological analysis revealed that these mammary structures formed functional mammary glands that contained both types of epithelial cells. Similar experiments have been performed with prostate stem cells. A single adult prostate stem cell (Lin-, Sca-1+, CD133+, CD44+, CD117+) could generate functional prostate tissue after transplantation in vivo.19 Consistently, a single muscle stem cell transplanted into the muscle of mice is capable of self-renewal and production of more progenitors that contribute to the muscle fibres.20 To demonstrate the properties contained within a single hematopoietic stem cell (HSC), specific markers were used for purification and characterization of HSCs (CD34 lo/-, c-Kit+, Sca-1+, Lin-).21 One of those cells has been injected into lethally irradiated mice and this lead to the reconstitution of the lymphohematopoietic system in 21% of the mice. This illustrates the plasticity imposed on stem cells by their microenvironment and that indeed one single somatic stem cell is capable to regenerate a whole organ in vivo.

Malignancies can be seen as an abnormal growth of the organ from which they originate. It has long been hypothesized that cancers contain a population of stem cells which are at the heart of cancer growth, in analogy to the way normal tissues are generated from somatic stem cells.22 Recent advances have yielded evidence that this is indeed the case, at least for some cancers. CSCs are supposed to have similar properties as normal stem cells, with respect to self-renewal and multilineage differentiation potential.2 However, as a result of acquired mutations CSCs may have acquired unregulated self-renewal that results in the generation of cancers. The same principles that have been employed to demonstrate the identity of normal stem cells have been used to identify CSCs.

One type of tumor that contains a population of cells which per definition are CSCs is the teratoma. Teratomas are the result of abnormal development of totipotent embryonic stem cells. The main hallmark of teratomas is the diversity of the cell types found in the tumor tissue which can resemble normal derivatives of all three germ layers and sometimes reaches a complete structure of certain organs such as eyeballs, hair or teeth. First attempts to address the question of whether this potential resides within a single embryonic carcinoma cell were undertaken a few decades ago. In 1964 it has been shown that one single teratoma cell deposited intraperitoneally into mice can give rise to tumors in 11% of the cases.23 These tumors were true teratocarcinomas as they were comprised of a variety of differentiated tissues from each of the three germinal layers. Furthermore, it has been shown that teratoma cells, on one hand, can give rise to teratocarcinomas in mice when injected subcutaneously. On the other hand, the same cells injected into the cavity of the blastocyst gave rise to tumor-free mosaic offspring.24 Therefore, in addition to demonstrating the differentiation potential of teratoma cells, these two experiments indicate that most likely the combination of both, mutations and epigenetic changes, regulated by the tumor microenvironment, determines the tumorigenic potential of a cell.25

Colon cancer is one of the most studied and best understood malignancies, yet it remains the second leading cause of cancer-associated death.26 Recently, the hypothesis that CSCs drive tumorigenesis in colorectal cancer and that a single CSC has the potential to recapitulate the original tumor phenotype gained support by experiments conducted in our laboratory.27 We utilized a method to generate single-cell derived CSC cultures by single-cell sorting GFP transduced spheroid colon CSC cultures. Different numbers of CD133+ cells were deposited into varying numbers of CD133- cells from a GFP- subculture. In all the cases only GFP+ spheres were obtained, indicating that only CD133+ cells have clonogenic potential in vitro. Moreover, subcutaneous injection of single-cell derived GFP+ CSCs into NOD-SCID mice lead to the growth of adenocarcinomas. The morphology of these tumors resembled that of the original malignancy and importantly, all epithelial structures within the tumor were derived from GFP+ cells. Further,

all tumors showed heterogeneous cellular morphology, protein expression and differentiation along different intestinal cell lineages. Cells that expressed markers associated with enterocyte, goblet and neuroendocrine cells were present. These single-cell derived xenografts retained a CD133+ compartment that displayed CSC properties. Moreover, we were able to confirm these findings by direct ex vivo sorting of single colon CSCs from human colon carcinomas. Odoux et al. used a similar approach to investigate the properties of single-cell derived colon CSC.28 They found, in agreement with our results, that a single cell has the potential to generate the full spectrum of differentiated cells found in the original tumor. In addition, they performed a karyotype analysis to assess the presence of chromosomal instability. While the same aberrations observed in the parental cells were also seen in the clonally derived tumor cells, surprisingly, some clones also had aberrations unique to each culture. These results open the question whether differences seen among clones, derived from a common progenitor, were present in the original isolate.

The presence of a small, genetically identical population of CSCs in all tumors has been challenged recently also for a mouse model of lymphoma.29 Kelly et al. demonstrated that as many as one in ten tumor cells were able to propagate lymphomas, fulfilling the postulates of cancer stem cells. Additionally, it has been demonstrated that as many as one in four melanoma cells is able to propagate tumor growth in a highly immunodeficient model.30 While a syngeneic system was used in the first publication, the authors of the second paper demonstrated that the tumorigenicity in xenograft models depended on the grade of immunodeficiency of the host. Interestingly, in the latter model the xenografts obtained from one patient specimen were heterogeneous in nature. This raises the question whether some tumors can contain several genetically or epigenetically distinct populations of cells with cancer stem-cell like properties. In order to address this question, we choose to analyze the CSC populations in glioblastoma multiforme.

Gliomas are the most common type of primary brain tumors, amongst which glioblastoma multiforme (GBM) is the most frequent and aggressive one.31 Mainly because of their ability to infiltrate into the healthy surrounding tissue, so far all the attempts to develop effective treatments against this disease failed. Despite progress in the research of GBMs, patients still have a median survival of less than a year.32 Thus, a better understanding of initiation and formation of GBM is necessary for development of new, more effective therapeutic approaches.

It has already been demonstrated that GBM CSCs are more resistant to therapy than the bulk of the tumor cells.7,32 In addition, it has been reported that, based on the molecular signature of high grade gliomas, these tumors can be classified into three distinct subgroups where the most

aggressive forms are enriched for genes normally expressed in neural stem cells.33 In addition, upon recurrence tumors have a tendency to shift towards this more aggressive, less differentiated phenotype.

The presence of different cell types in gliomas, along with the shift of tumor phenotype during progression, poses a challenge for an overly simplified view of CSC. How is the presence of neuronal, as well as glial, markers in the same tumor explained? We decided to assess the differentiation potential of GBM CSCs cultures in order to address the question whether one single population of CSCs is indeed responsible for the tumor phenotype, or several competing clonescan co-exist in one tumor to produce the diversity of phenotypes observed.

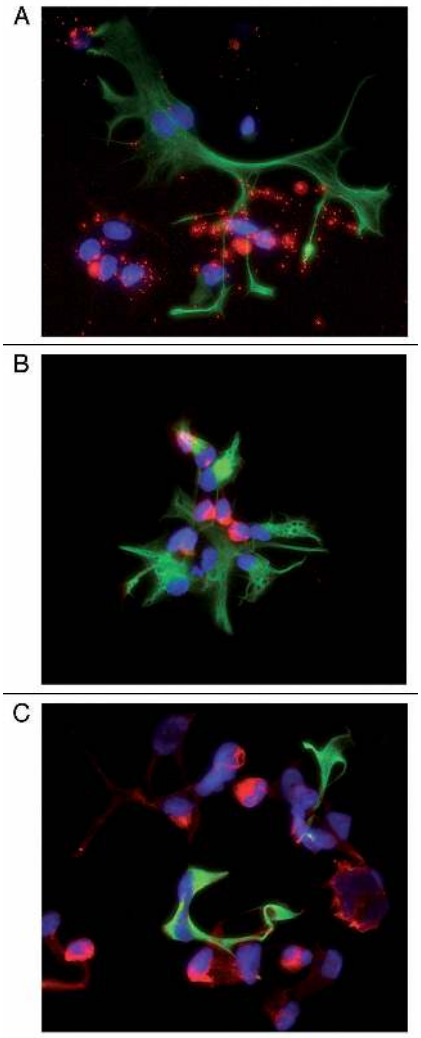

Glioma cancer stem cells are usually isolated and propagated from patient specimens under stem-cell conditions. This means non-adherent growth as spheres in serum-free medium supplemented with bFGF and EGF. Under these conditions the GBM CSCs retain the ability to induce phenocopies of the original human malignancy upon transplantation into immunocompromized mice.34 In addition, such GBM CSC cultures can differentiate among different cell lineages in vitro. Some examples of differentiated CSC cultures from our laboratory are shown in Figure 1. GBM073 cultures become positive for the early oligodendrocyte marker O4 and the astrocyte marker GFAP (Fig. 1A). In contrast, the GBM lines 408 (Fig. 1B) and 081 (Fig. 1C) show expression of the neural marker β3-Tubulin and GFAP. The CSC hypothesis postulates that a single, multipotent population of cells in those cultures should be capable to give rise to those differentiation patterns. If this would be universally true, single-cell cloning of GBM CSC cultures should yield clones that mirror the differentiation potential of the parental culture.

Figure 1. Marker expression of differentiated GBM CSCs cultures. (A) After 10 days of growth factor withdrawal, and addition of serum, the cells adhered and differentiated. Immunofluorescence staining was performed on differentiated GBM CSCs isolated from different tumor specimens. GBM073 were co-stained for the early oligodendrocyte marker O4 (red) and the astrocyte marker GFAP (green); (B) GBM408 and (C) GBM081 were co-stained for the neural marker β3-Tubulin (red) and GFAP (green); nuclei were stained with DAPI (blue).

We thus generated single-cell derived CSCs from one of our cultures by plating them at clonal density (Fig. 2). Upon differentiation, the parental line GBM006 showed mainly β3-Tubulin and GFAP expression with few cells being negative for both markers (Fig. 2A). However, the differentiation patterns of the single-cell derived spheroids showed an unexpected variety. Although the majority of the clones were positive for both β3-Tubulin and GFAP upon

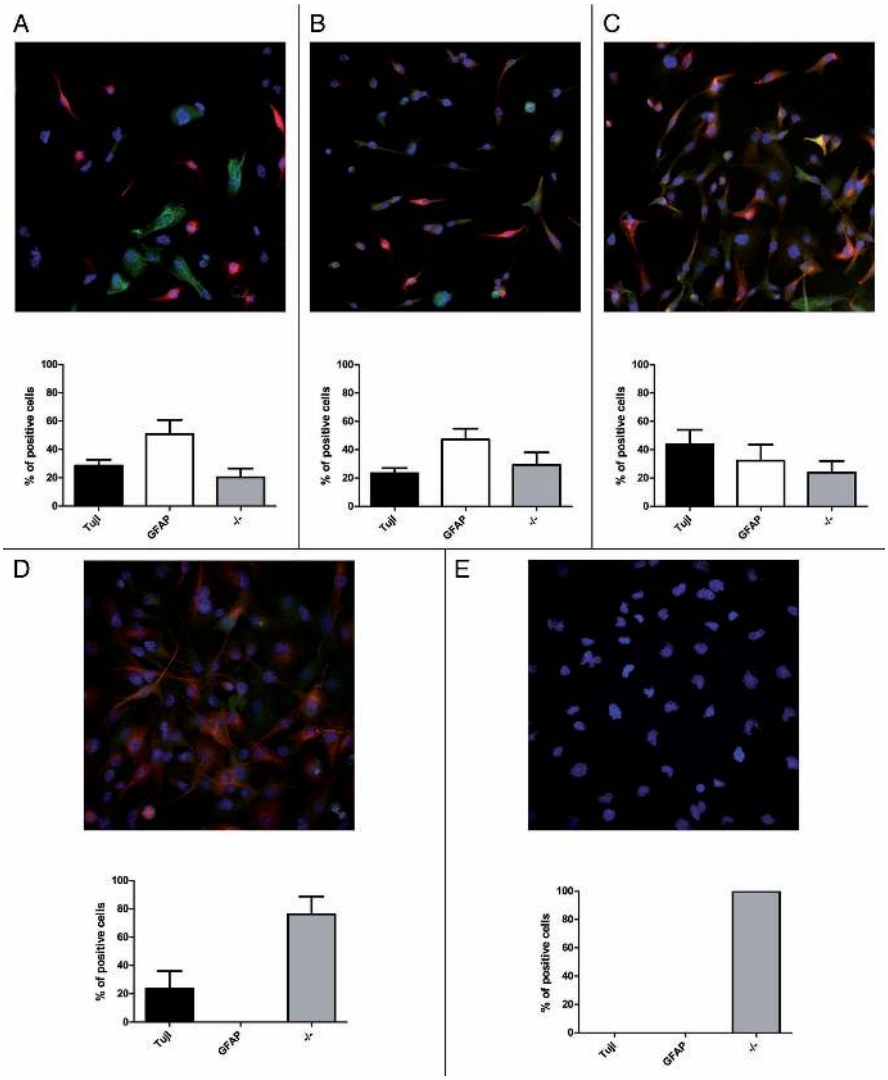

Figure 2. Marker expression of differentiated GBM006 parental cultures and single-cell derived clones (A) Immunofluorescence staining on parental GBM006 culture upon differentiation and quantification of marker expressing cells, as well as cells that do not express either of the markers: β3-Tubulin (red)/GFAP (green); Immunofluorescence staining of single-cell derived clones after differentiation for β3Tubulin (red)/GFAP (green) and quantification of differentiated cells per lineages. (B) clone 1; (C) clone 7; (D) clone 6; (E) clone 9.

differentiation, the ratio of the positive cells varied greatly. While in some cases the differentiation patterns of clones resembled the parental one (Fig. 2B), in others marker expression was shifted towards one of the two lineages (Fig. 2C). In addition, a few clones showed uni-lineage differentiation (Fig. 2D) and one clone did not express either of the two markers (Fig. 2E).

What do those results imply in the context of the CSC hypothesis?

If a single, genetically stable, CSC population is responsible for tumor growth then a change in the tumor-microenvironment could potentially be responsible for the observed change in tumor phenotype. However, in our experiment all clones were cultured and differentiated under the same conditions. Further, all clones we obtained appear to have a stable phenotype in our cultures. An alternative explanation for our observations would thus discard the strict requirement of a single population of CSCs and take into account a diversity of the CSC population with respect to differentiation programs. In that respect, our results would indicate that the original tumor contained several different clones and that CSCs isolated from the same tumor are not necessarily uniform in respect to their differentiation abilities. It is likely that all clones arose from one initial cell, but due to the diverse selective pressures in different areas of the tumor acquired different mutations.35 These mutations could influence their differentiation preferences, giving rise to several distinct daughter CSCs. Another explanation of the varied differentiation patterns of different clones could be different cells of origin. There are, for example, conflicting data regarding the cell of origin of GBM. It is proposed that gliomas arise from multipotent stem cells, partially differentiated unipotent progenitors or from mature glial cells that dedifferentiate.36 All three hypotheses are potential explanations for the diverging differentiation patterns of single-cell derived CSCs seen in our GBM clones and in other tumors. It remains to be determined if this diversity of CSCs is a common feature.37 In that respect, it's notable that the GBM CSCs mirror the diversity of the tumor phenotypes observed in vivo. Colon carcinomas, on the other hand, do not show this variety, which is consistent with the finding that even genetically different clones yield very similar in vivo differentiation patterns.28

What are the implications for the development of a CSCs-targeted therapy?

It has been shown in colon cancer already that inhibitors of the Notch pathway can drive colon cancers into differentiation.38 This kind of manipulation could be used for driving cells into differentiation or redirecting overall differentiation towards the cell type most sensitive to therapy. The presence of different CSC populations in the tumor would complicate this endeavor, as one can expect that the different CSC populations react differently to this treatment. Thus targeting one type of CSCs alone might not be enough for efficient tumor treatment.

References

1. Vermeulen L, Sprick MR, Kemper K, Stassi G, Medema JP. Cancer stem cells—Old concepts, new insights. Cell Death Differ 2008; 15:947-58.

2. Clarke MF, Dick JE, Dirks PB, Eaves CJ, Jamieson CH, Jones DL, et al. Cancer stem cells—perspectives on current status and future directions: AACR Workshop on cancer stem cells. Cancer Res 2006; 66:9339-44.

3. Dalerba P, Cho RW, Clarke MF. Cancer stem cells: models and concepts. Annu Rev Med 2007; 58:267-84.

4. Morrison SJ, Kimble J. Asymmetric and symmetric stem-cell divisions in development and cancer. Nature 2006; 441:1068-74.

5. Todaro M, Perez Alea M, Scopelliti A, Medema JP, Stassi G. IL-4-mediated drug resistance in colon cancer stem cells. Cell Cycle 2008; 7:309-13.

6. Dean M, Fojo T, Bates S. Tumour stem cells and drug resistance. Nat Rev Cancer 2005; 5:275-84.

7. Bao S, Wu Q, McLendon RE, Hao Y, Shi Q, Hjelmeland AB, et al. Glioma stem cells promote radioresistance by preferential activation of the DNA damage response. Nature 2006; 444:756-60.

8. Todaro M, Alea MP, Di Stefano AB, Cammareri P, Vermeulen L, Iovino F, et al. Colon cancer stem cells dictate tumor growth and resist cell death by production of interleukin-4. Cell Stem Cell 2007; 1:389-402.

9. Lapidot T, Sirard C, Vormoor J, Murdoch B, Hoang T, Caceres-Cortes J, et al. A cell initiating human acute myeloid leukaemia after transplantation into SCID mice. Nature 1994; 367:645-8.

10. Blanpain C, Horsley V, Fuchs E. Epithelial stem cells: turning over new leaves. Cell 2007; 128:445-58.

11. Cheng H, Leblond CP. Origin, differentiation and renewal of the four main epithelial cell types in the mouse small intestine V. Unitarian Theory of the origin of the four epithelial cell types. Am J Anat 1974; 141:537-61.

12. Ponder BA, Schmidt GH, Wilkinson MM, Wood MJ, Monk M, Reid A. Derivation of mouse intestinal crypts from single progenitor cells. Nature 1985; 313:689-91.

13. Novelli MR, Williamson JA, Tomlinson IP, Elia G, Hodgson SV, Talbot IC, et al. Polyclonal origin of colonic adenomas in an XO/XY patient with FAP. Science 1996; 272:1187-90.

14. Novelli M, Cossu A, Oukrif D, Quaglia A, Lakhani S, Poulsom R, et al. X-inactivation patch size in human female tissue confounds the assessment of tumor clonality. Proc Natl Acad Sci USA 2003; 100:3311-4.

15. Campbell F, Williams GT, Appleton MA, Dixon MF, Harris M, Williams ED. Post-irradiation somatic mutation and clonal stabilisation time in the human colon. Gut 1996; 39:569-73.

16. Taylor RW, Barron MJ, Borthwick GM, Gospel A, Chinnery PF, Samuels DC, et al. Mitochondrial DNA mutations in human colonic crypt stem cells. J Clin Invest 2003; 112:1351-60.

17. Barker N, van Es JH, Kuipers J, Kujala P, van den Born M, Cozijnsen M, et al. Identification of stem cells in small intestine and colon by marker gene Lgr5. Nature 2007; 449:1003-7.

18. Shackleton M, Vaillant F, Simpson KJ, Stingl J, Smyth GK, Asselin-Labat ML, et al. Generation of a functional mammary gland from a single stem cell. Nature 2006; 439:84-8.

19. Leong KG, Wang BE, Johnson L, Gao WQ. Generation of a prostate from a single adult stem cell. Nature 2008; 456:804-8.

20. Sacco A, Doyonnas R, Kraft P, Vitorovic S, Blau HM. Self-renewal and expansion of single transplanted muscle stem cells. Nature 2008; 456:502-6.

21. Osawa M, Hanada K, Hamada H, Nakauchi H. Long-term lymphohematopoietic reconstitution by a single CD34-low/negative hematopoietic stem cell. Science 1996; 273:242-5.

22. Cho RW, Clarke MF. Recent advances in cancer stem cells. Curr Opin Genet Dev 2008; 18:48-53.

23. Kleinsmith LJ, Pierce GB Jr. Multipotentiality of single embryonal carcinoma cells. Cancer Res 1964; 24:1544-51.

24. Mintz B, Illmensee K. Normal genetically mosaic mice produced from malignant teratocarcinoma cells. Proc Natl Acad Sci USA 1975; 72:3585-9.

25. Bissell MJ, Labarge MA. Context, tissue plasticity and cancer: Are tumor stem cells also regulated by the microenvironment? Cancer Cell 2005; 7:17-23.

26. Weitz J, Koch M, Debus J, Hohler T, Galle PR, Buchler MW. Colorectal cancer. Lancet 2005; 365:153-65.

27. Vermeulen L, Todaro M, de Sousa Mello F, Sprick MR, Kemper K, Perez Alea M, et al. Single-cell cloning of colon cancer stem cells reveals a multi-lineage differentiation capacity. Proc Natl Acad Sci USA 2008; 105:13427-32.

28. Odoux C, Fohrer H, Hoppo T, Guzik L, Stolz DB, Lewis DW, et al. A stochastic model for cancer stem cell origin in metastatic colon cancer. Cancer Res 2008; 68:6932-41.

29. Kelly PN, Dakic A, Adams JM, Nutt SL, Strasser A. Tumor growth need not be driven by rare cancer stem cells. Science 2007; 317:337.

30. Quintana E, Shackleton M, Sabel MS, Fullen DR, Johnson TM, Morrison SJ. Efficient tumour formation by single human melanoma cells. Nature 2008; 456:593-8.

31. Stupp R, van den Bent MJ, Hegi ME. Optimal role of temozolomide in the treatment of malignant gliomas. Curr Neurol Neurosci Rep 2005; 5:198-206.

32. Stupp R, Hegi ME. Targeting brain-tumor stem cells. Nat Biotechnol 2007; 25:193-4.

33. Phillips HS, Kharbanda S, Chen R, Forrest WF, Soriano RH, Wu TD, et al. Molecular subclasses of high-grade glioma predict prognosis, delineate a pattern of disease progression and resemble stages in neurogenesis. Cancer Cell 2006; 9:157-73.

34. Lee J, Kotliarova S, Kotliarov Y, Li A, Su Q, Donin NM, et al. Tumor stem cells derived from glioblastomas cultured in bFGF and EGF more closely mirror the phenotype and genotype of primary tumors than do serum-cultured cell lines. Cancer Cell 2006; 9:391-403.

35. Rapp UR, Ceteci F, Schreck R. Oncogene-induced plasticity and cancer stem cells. Cell Cycle 2008; 7:45-51.

36. Stiles CD, Rowitch DH. Glioma stem cells: A midterm exam. Neuron 2008; 58:832-46.

37. Campbell LL, Polyak K. Breast tumor heterogeneity: Cancer stem cells or clonal evolution? Cell Cycle 2007; 6:2332-8.

38. van Es JH, van Gijn ME, Riccio O, van den Born M, Vooijs M, Begthel H, et al. Notch/gamma-secretase inhibition turns proliferative cells in intestinal crypts and adenomas into goblet cells. Nature 2005; 435:959-63.

4

Cancer Stem Cell Driven Tumor Growth Promotes Invasive Morphology

Tijana Borovski[1], Andrea Sottoriva[2,†], Peter M.A. Sloot[2,], Jan Paul Medema[1] and Louis Vermeulen[1].

1Laboratory for Experimental Oncology and Radiobiology (LEXOR), Center for Experimental Molecular Medicine, Academical Medical Center, Amsterdam, The Netherlands, 2Computational Science, Faculty of Science, University of Amsterdam, Amsterdam, The Netherlands, †Current Address: Department of Oncology, University of Cambridge, CRUK Cambridge Research Institute, Li Ka Shing Centre, Cambridge, UK.

Adapted from: Cancer stem cell tumor model reveals invasive morphology and increased phenotypical heterogeneity (*Andrea Sottoriva, Joost J.C. Verhoeff, Tijana Borovski, Shannon K. McWeeney,Lev Naumov, Jan Paul Medema, Peter M.A. Sloot, and Louis Vermeulen)*; Cancer Res. 2010 Jan 1;70(1):46-56.

Abstract

Glioblastoma multiforme is a highly lethal malignancy mainly due to the invasive growth of tumor cells. Therefore, understanding infiltrative behavior of cancer cells is of vital importance in the development of new treatments. Tumor growth and invasion are complex processes that depend on both cell intrinsic parameters and microenvironmental factors. The recently developed concept of Cancer Stem Cells (CSCs) sheds new light on these processes. Herein we describe the results of a mathematical model, revealing that the CSC model of malignancies has great implications for the invasive behavior of tumors. Furthermore, tumor growth directed by the CSC niche results in the same invasive phenotype. This indicates that the hierarchical organization of malignant clones, supported by microenvironment, is of pivotal importance when investigating tumor cell invasion.

Introduction

Glioblastoma multiforme (GBM) is the most common primary brain tumor with significant morbidity and mortality. It consists of a main core mass and a rim of invasive tumor cells that widely disseminate into surrounding, normal brain tissue, decreasing in numbers towards the periphery and being detectable even several centimeters away from the main tumor lesion. This prevents curative surgery. Thus it is not surprising that GBM remained one of the greatest clinical challenges for decades largely due to its invasive phenotype. In most cases, tumor recurrence manifests within 2-3 centimeters of the resection cavity, although lesions adjacent to the resection line or distant satellite tumor masses, located several centimeters away from the site of initial tumor presentation are also frequently found (1, 2). Tumor cells can migrate to such an extent that these nodular lesions can sometimes even be found in the contralateral hemisphere (3). The diffuse nature of this malignancy was already recognized several decades ago by neurosurgeons that performed extremely radical resection, hemispherectomy, and even this procedure failed to eradicate these tumors (4, 5).

The invasion of GBM cells into the surrounding healthy tissue has been associated with distinct anatomical structures that enable it, namely blood vessels, myelinated axons and the subependyma (6). Small anaplastic cells were identified as the predominant invasive cell type (7). These cells exhibit an undifferentiated phenotype, have the motility to invade surrounding healthy tissue and the ability to proliferate into a clinically significant mass, indicative of their clonogenicity. According to ^{3}H-thymidine uptake *in vivo*, these small cells display the highest labeling index and thus effectively contribute to tumor growth (8, 9). Furthermore, in transplantation models the number of these small cells increased with time or passage number suggesting their survival advantage compared to other tumor cell types (10-12). The predominance of these small cells has been reported in recurrent gliomas and has been attributed to selection of these clones by chemo and radio therapy. This is in line with the recently established cancer stem cell (CSC) hypothesis that proposes a hierarchical organization of tumor cells, in analogy to healthy tissues. CSCs, similar to normal stem cells, have the ability to self-renew and generate various differentiated tumor lineages (multilineage differentiation capacity). Importantly, they are the only fraction of tumor cells with the tumorigenic potential and the ability to generate tumors that mirror original malignancy in serial transplant assays (13, 14). Notably, GBMs often recur in nodular-like fashion suggesting that these have a clonal origin. Within the tumor, the GBM CSC fraction is primarily located adjacent to tumor vasculature that forms its niche and maintains the CSC pool (15). Moreover, CSCs have been seriously implicated in therapy resistance of GBM and its recurrence, as shown *in vitro* and *in vivo* (16). This correlates with the clinical data. Namely, radiation therapy is commonly used treatment for GBM and demonstrates significantly prolonged survival of patients over surgical treatment alone. Nevertheless, tumors

frequently recur regardless of the radiotherapy due to survival of small fraction of tumor cells. Considering current knowledge of cancer biology, these are potentially CSCs.

In various tumors CSCs are found on the invasive edges of the tumor and show tendency to migrate (17-19). Even though a similar assumption was made for GBM, the real contribution of CSCs to tumor infiltration is still speculative and detailed experimental examination of this matter is posing a lot of challenges. In addition, it remains a matter of debate to what extend CSC functions are cell intrinsically regulated or subject to (micro-) environmental control (20, 21). Although the dynamics of cancers, including GBM, is being studied intensely, a lot of attempts to learn more about it fail due to its complexity. Therefore, there is an increasing tendency recently to use the mathematical models for this kind of research in order to study various aspects of tumor biology difficult to perform in commonly used experimental models.

Here we apply computational modeling techniques to investigate the consequences of hierarchically organized cancer cell populations on solid tumor growth dynamics. Furthermore, we investigate the role of the vascular CSC niche on tumor growth characteristics. The classical view of tumor growth considers all cancer cells to contribute equally to tumor growth and explains heterogeneity of cancer cells with the continuous acquisition of additional genetic lesions due to competition for resources. In this paper we refer to this view of malignancies as the *Classical* model. Although this model greatly contributes to our understanding of malignancies, recent experimental evidence suggests an additional layer of complexity. As previously introduced, the heterogeneity present in tumors could, in part, be the result of the diversity in differentiation grade of genetically identical cells (22, 23). In GBM, cells with an immature phenotype expressing the cell surface marker AC133 are the cells that fuel tumor growth, have the exclusive capacities to self-renew, differentiate and transplant the malignancy into SCID mice, and are defined as CSCs (13). We describe that, strikingly, implementing the concept of CSCs in a mathematical tumor growth model directly results in a more invasive morphology. Furthermore, we find that highly invasive growth in tumors dependent on a small subset of cells is not restricted to CSC-driven tumors, but is also observed in tumors where the CSC capacity of tumor cells is completely defined by the microenvironment.

Materials and Methods

Stem Cellular Automaton (SCA) Model

We developed a hybrid tumor growth model based on cellular automata (24) and partial differential equations. We refer to this model as the Stem Cellular Automaton (SCA) model. In the SCA model the individual cancer cell is the fundamental unit of the tumor, we simulate its proliferation, metabolism, migration, stemness and differentiation.

Implementing the CSC model of malignancies means to simulate cancer cells with different replicative potential within the tumor. For simplicity, we assume that in our model there are only two types of cells: cancer stem cells (CSCs) and differentiated cancer cells (DCCs). CSCs possess unlimited replicative potential and can either generate new CSCs (with a probability P_S) or DCCs. DCCs can divide for a maximum of *H* generations before stopping to proliferate irreversibly. This method yields a hierarchy with CSCs at the top and DCCs at the bottom. We simulate the classical model of malignancies, in which all cells possess tumor growth-promoting capacities, by simply setting P_S=1. In such situation all cells possess stem cell characteristics. With this method we have an intuitive way to compare the flat, classical tumor model with the hierarchically organized CSC model. Furthermore, in the SCA model CSC niche component is implemented as an interaction with the symmetrical division parameter P_S. CSCs that do not reside close to niche structures/locations have a decreased P_S value. In addition to the effects on self-renewal we also model the chemoattractive properties of the niche. The exact mathematical approach and detailed description of the parameters are described elsewhere (25, 26).

Degree of Tumor Invasiveness

Tumor invasion is responsible of roughness of the tumor surface, large inhomogeneities and fingering tumor fronts. As a simple measure of invasiveness in 2D, we consider a non-invasive tumor, being spherical, to have the minimum ratio between the perimeter *P* and the surface *S*. As the irregularity of the tumor borders increases with its invasiveness, such ratio increases as well. By comparing the *P*/*S* ratio of a tumor mass with the minimum ratio (the one of a perfect disk), we can measure the level of invasiveness of a solid malignancy. Hence, the Invasion Measure (*IM*) reads:

$$IM = P \Big/ \sqrt{4 \pi S}$$

A non-invasive, spherical tumor would have *IM* close to 1 (the closest to a disk or, in 3D, to a sphere) while a tumor with a highly irregular border, made by fingers and cluster of invasive cells, would display a high value of *IM*. For quantification of *in vitro* invasion the same measure was applied.

In vitro experiments

Cells were cultured according to standard protocol in DMEM, IMDM or MEM medium (Gibco/Invitrogen) supplemented with 10% Fetal Calf Serum (BioWhittaker) and 5 mmol/L L-glutamine (Invitrogen) and were kept in 2%, 5% or 10% CO_2 conditions. Limiting dilution assay was performed by FACS deposition of 1, 2, 4, 8, 16, 32, 64, 128, 256 cells in a 96 well plate (Corning). Clonogenicity was calculated using the *limdil* function in the 'statmod' software package (http://bioinf.wehi.edu.au/software/limdil/). To determine the invasiveness cells were plated at

clonal density in Growth Factor Reduced Matrigel (BD Biosciences) and overlaid with medium. After 10 days, surface and perimeter of cellular structures were measured and an *IM* was calculated. Cell lines that did not form clear visible aggregates of cells but completely dispersed were excluded from analysis.

Results

Emergent Invasive Morphology

Computational modeling allows the exploration of highly complex systems, such as tumor growth. In this study we have employed a computational tumor growth model to test the consequences of hierarchically organized clones on different areas of tumor biology, such as invasion. For simplicity, our model is based on the assumption that there are only two types of tumor cells: CSCs and DCCs. CSCs divide symmetrically with probability P_S and asymmetrically with probability 1 - P_S. Two new CSCs result from the former, a DCC and a CSC from the latter. CSCs possess unlimited replicative potential and self-renewal whereas DCCs can divide up to *H* times. We fix *H*=5 and vary P_S to simulate different CSC frequencies. A CSC growth model has small P_S values whereas for P_S=1 we simulate the classical model of malignancies. As suggested experimentally for CSCs, we have restricted migration to this fraction of cells (17-19). The applied computational modeling technique allows us to get more insight into the underlying dynamics of this aspect of cancer growth and progression that would be rather challenging in a conventional experimental biological setting. The exact mathematical approach and conditions are described elsewhere (25). Here we will highlight the findings based on this model.

We first investigated how tumor growth dynamics change upon varying the CSC fraction within a modeled tumor. In the SCA model this corresponds to changing the parameter P_S, which represents the fraction of symmetric divisions and is thus determining the fraction of clonogenic cells. For high values of P_S, i.e. values close to 1, we expect to model the classical interpretation of tumors since all cell divisions are symmetric and all cells are therefore clonogenic. In contrast, low values of P_S would limit the clonogenic fraction to a smaller subset and therefore represent the CSC model. We simulated the growth of tumors with P_S=1, P_S=0.1 and P_S=0.03.

Figure 1A shows the fraction of CSCs on the total amount of tumor cells for different values for P_S. The selected P_S values correspond to CSCs populations comprising roughly 100%, 1% or 0.1% of the total tumor volume and therefore cover mainly the CSCs fractions observed in a variety of solid malignancies (27). In the CSC model (P_S=0.1 and P_S=0.03) small (early) lesions have relatively high fractions of CSCs while this number decreases and tends to stabilize when the tumor progresses (Figure 1A). This observation is supported by *in vivo* studies that find increased numbers of CSC marker bearing cells in micro-metastases compared to larger tumors (28). This

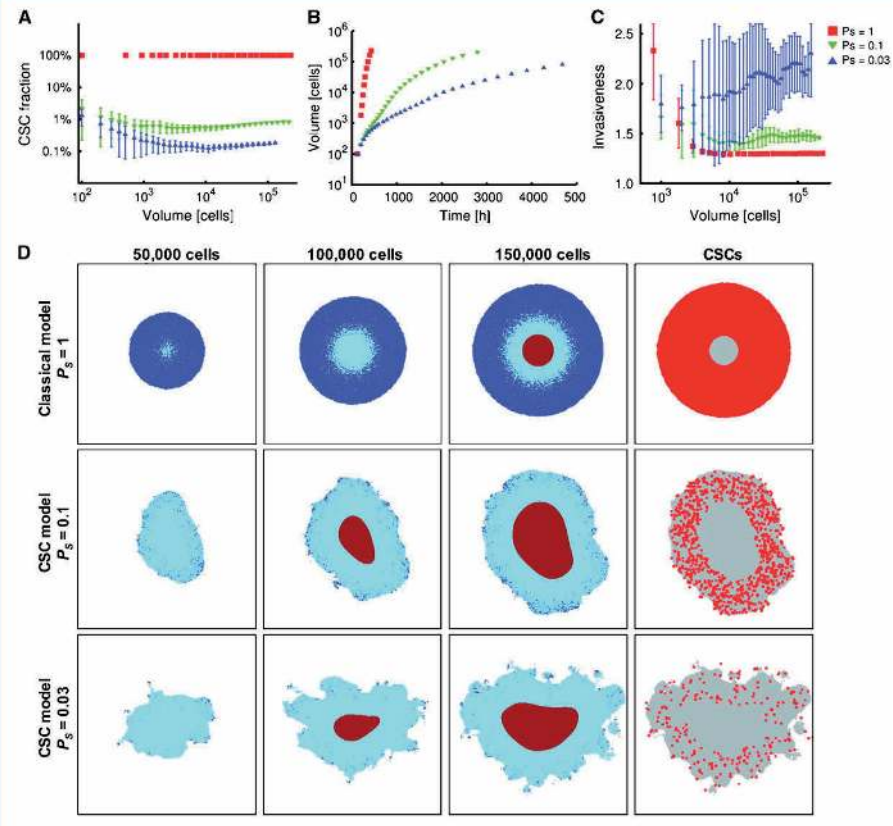

Figure 1. Emergent Invasive Behavior in the CSC Model
(A) Different P_S values result in different CSC fractions. (B) Growth curves for different P_S values. (C) Quantitative measure for invasiveness shows increasing invasive behavior with declining P_S. See methods for details. (A-C) Error bars represent standard deviation, n=16. (D) Hierarchical organization in the SCA model affects tumor morphology. Depicted are tumors for different values of self-renewal probability (P_S) and different volumes. Dark blue: cells which have divided within the last 48 hours (depicted larger); Light blue: non-dividing cells; Brown: necrotic center. The rightmost column shows localization of CSCs in the tumor mass. Grey: tumor mass; Red: CSCs (depicted larger). In all the figures 6×6 mm of tissue is represented.

indicates that even with fixed self-renewal rates (P_S) this phenomenon is intrinsic to lesions initiated by a single CSC although environmental factors influencing self-renewal frequencies are also likely to contribute. Tumor growth curves for various P_S values all display the classical Gompertzian-like growth kinetics. However, as expected with equal cell cycle durations the self-renewal rates of the stem cell fraction influences proliferation rate greatly, hence low self-renewal rates (small P_S) correspond to slow tumor growth (Figure 1B). Interestingly, the decrease in accumulation of tumor volume is accompanied by a stabilization of the fraction of CSCs suggesting an intimate relationship between these two processes.

Spatially, all experiments display a three layers structure consisting of an external proliferative area, an inner senescent layer, and a necrotic core. However, tumor morphologies for different P_S values are remarkably dissimilar (Figure 1D). For P_S=1, where there is no hierarchy, a symmetrical, sphere-like tumor morphology is generated that closely resembles previous mathematical tumor growth models (29, 30). In contrast, the shape of the tumors generated with low P_S values is highly irregular (especially P_S=0.03). CSC driven tumors yield highly invasive morphology with fingering fronts and clusters of cancer cells beyond the tumor margin, driven by the mobility and the exclusive proliferative properties of CSCs.

From Figure 1C it is evident how hierarchically organized tumors (P_S=0.03 and P_S=0.1) generate a higher degree of invasiveness, compared to tumors in the classical model (P_S=1). It is important to note that the intrinsic properties of the cells in the classical tumor and the stem cells in the CSC driven tumor are completely identical.

In Vivo and In Vitro Validation

Magnification of a tumor border in a CSC fueled tumor growth model (P_S=0.03), demonstrates how CSCs migrate beyond the margins of the tumor mass. CSCs colonize the surrounding tissue and expand locally forming small satellites that grow back into, and are engulfed by, the main tumor mass (Figure 2A). These results are paralleled by recent findings in a different model system were high migration levels in a small subset of cells give rise to small proliferating extra-tumoral lesions and therefore tumors are 'conglomerates of self-metastasis' as the authors propose (31).

In an endeavor to validate these observations from our computational model we investigated human tumor specimens. Close examination of the histology of different highly diverse human malignancies, including GBM, displayed a relatively confined large tumor mass with clearly detached tumor cells forming small lesions in the surrounding normal tissue (Figure 2B). This exemplifies that human tumor histology contains indications of a stepwise infiltration and colonization of the surrounding tissue as our model predicts would follow from a hierarchical organized malignancy. Next we attempted to determine the relationship between CSC fraction and invasive properties, as predicted by the model, using *in vitro* cell culture (Figures 2C, S1-S2). We first determined the clonogenicity of a set of cell lines derived from different tumor types (n=24) as a surrogate for their CSC fraction. Additionally, we quantified the invasive properties of clonally derived structures with our measure of irregular morphology (*IM*) both on adherent plates and in matrigel for all these lines. A significant inverse relationship between clonogenic fraction and the invasive properties of these lines exists (Figure 2C). This implicates that tumor structures driven by a small fraction of clonogenic cells tend to generate a more irregular and invasive morphology, a finding that corroborates the predictions of our model.

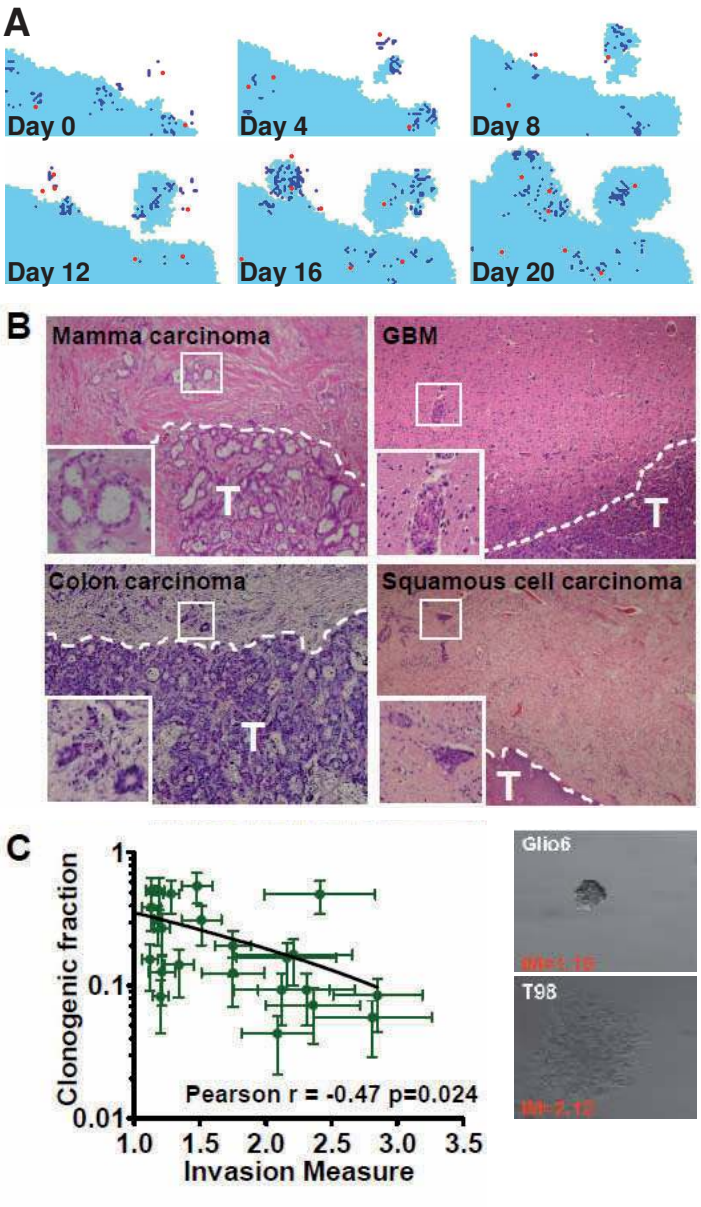

Figure 2. Invasive Behavior *in silico, in vivo and in vitro* (A) Close-up of tumor border showing invasive behavior for P_S=0.03. CSCs (red) infiltrate surrounding tissue and spin-off DCCs that proliferate (dark blue). Small satellites are formed in the surrounding normal tissue (white) and grow back to and are engulfed by the main tumor mass. Non-dividing cells are depicted in light blue. (B) Representative figures of various malignancies. All images reveal island like formation at the rim of the main tumor mass (*T*). These findings are in line with tumor expansion as predicted by the SCA model that implements a CSC hierarchy. (C) Cell lines (n=24) have been plated at clonal density in matrigel. Simultaneously the clonogenic fraction of the lines has been determined by limiting dilution analysis. A significant (p=0.02) inverse relationship exists between clonogenicity and invasion as quantified by the measure of invasiveness we defined. Two examples of GBM cell lines are shown and invasiveness (IM) and clonogenicity are indicated (right). See Figures S1-S2 for details.

Combined, we take this as evidence that the SCA model based on the CSC concept closely resembles tumor growth patterns and morphology.

CSC Niche Directed Tumor Growth

Using the CSC-driven modeling we have so far shown how hierarchically-organized malignancies, containing a small population of CSCs, display highly invasive behavior as compared to non-hierarchical organized, classical tumors. Within this model we assumed that the CSC phenotype is a completely cell intrinsic feature and purely dependent on stochastically regulated symmetrical divisions (Figure 1). However, important novel data indicates that the CSC phenotype is as well dependent on microenvironmental interactions (15, 32). This sparks the question whether the invasive growth dynamics we observe in the CSC model are unique for tumor growth driven by intrinsically regulated CSCs or whether it is a more universal phenomenon for tumors that are dependent on a rare subset of cells for tumor growth. Thus, we focus on the comparison between the niche model and the intrinsic model of CSC growth, where no niche is present. The exact mathematical approach and conditions are described elsewhere (26).

In order to model the self-renewal promoting properties of the niche, we assume that the self-renewal probability P_S of CSCs is proportional to the niche level present in the grid cell where they are located. Hence, CSCs that reside within locations with high CSC niche levels would more likely self-renew. The results of the experiment with a CSC niche are illustrated in Figure 3A, with P_S = 0.03. We observe an invasive morphology with the CSCs closely localized to areas with high niche values. The detailed analysis of modeling CSC niche directed tumor growth is described elsewhere (26).

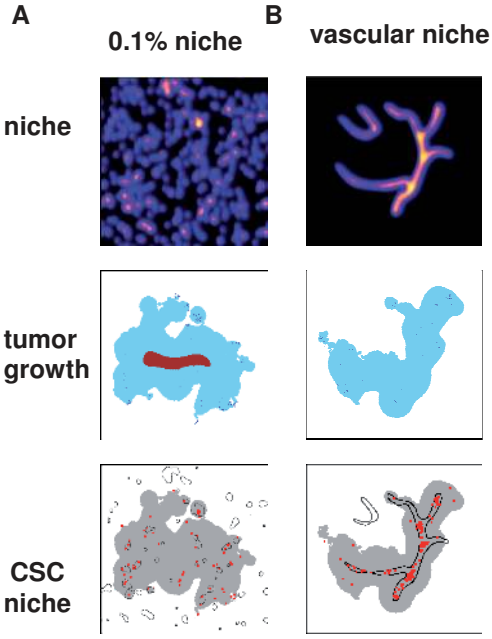

Figure 3. CSC Niche Driven Tumor Growth
(A) Top row depicts 0,1% niche distribution. Middle row shows tumor mass in light blue and proliferative cells in dark blue. Brown represents necrotic core. Bottom row shows outline of niche regions and reveals co-localization of CSCs with high niche values. Grey: tumor mass; Red: CSCs, lines represent niche outline (P_S=0.03). (B) Tumor growth simulated on top of a niche distribution that resembles a vascular structure clearly develops an invasive morphology that follows the underlying niche structure as observed in aggressive brain tumors. Parameters are equal to previous experiment.

From Figure 3A it is evident that the tumor shape is directed by the niche distribution as the tumor morphology tends to follow the underlying niche structure, with CSCs located in niche region. To further verify this in a more

realistic setting we initiated a modeling experiment in which we use a niche layout representing a small vascular system (Figure 3B). This experiment is of special interest for GBM as it was reported that vascular endothelial cells are implicated in CSC self-renewal and attraction of CSC (15, 33). In this scenario we assume the CSC symmetrical division rate to be coupled to the niche concentration and CSCs to migrate upwards to the niche concentration gradient as proposed for GBM (15). In this experiment we observe co-localization of the CSCs with the niche rich areas, and evidently the tumor shape follows the vasculature (Figure 3B). However, strikingly also in this niche-induced model the tumor shows an irregularly shaped morphology. Therefore, morphologically, the intrinsic and extrinsic CSC models yield similar results (Figure 3). Also the degree of invasiveness that we determined is relatively unaltered (data not shown). Note that in this analysis we did not take into account the metabolic effects the vasculature might have on tumor cell functions. Here we observe that those qualities are capable of orchestrating invasive patterns and therefore might provide an alternative explanation why *in vivo* GBM cells appear to infiltrate along vessel structures.

Discussion

CSC Driven Tumor Growth

Despite advances in GBM treatment, little progress has been made in improving the survival of the patients suffering from this disease. After surgical resection remaining infiltrating tumor cells considerably contribute to the tumor recurrence and mortality of the patients. Notably, even in the absence of massive tumor load, a number of GBM patients die due to neurological deterioration, suggesting that infiltrating portion of the tumor significantly contributes to the poor outcome of the patients (34). Thus, successful therapy would have to target infiltrative portion of the tumor, in addition to the main tumor mass and for this reason more knowledge has to be obtained about the infiltrative behavior of GBM. CSCs have been implicated in numerous aspects of tumor biology, including invasiveness. Here we use a mathematical model to investigate how a hierarchically organized cancer cells, with CSC fraction at the apex, affect the fundamental properties of solid malignancies, such as invasiveness and how a CSC niche influences the development of an invasive phenotype.

Crossing tissue boundaries is the first step in the process of tumor invasion and therefore of special interest. Here, we report how in the SCA model invasion directly emerges from the hierarchical organization of malignant clones, i.e. in a setting where not all cells are capable of unlimited replicative potential and migration. As we describe in this study the fraction of CSCs determines the extent of the invasive morphology of the tumor. The SCA model provides evidence for the notion that a heterogeneous proliferative potential of cells in a malignancy induces apparent invasive tumor growth. The microscopic invasion we observe in our model is clearly in line with histo-pathological findings, which show that the margin of most tumors,

including GBM, is not a defined border between normal and cancerous tissue, but much more a heterogeneous zone of invading cells that first form islands that grow out and then are incorporated back into the main tumor mass (Figure 2). Furthermore, we expand these initial results by demonstrating that these growth dynamics are not exclusive for an intrinsic hierarchical model, but also apparent in a setting were CSC functions are installed by a CSC niche. This again demonstrates that tumor growth is not the frontal marching up of tumor cells as it is often depicted and assumed in prior models, but develops from the continuous outgrowth of migrating clonogenic tumor cells in the surrounding tissue and is likely to be supported by a niche.

Experimental Validation and Future Directions

The model presented provides a range of predictions and implications regarding CSC-fuelled tumor growth that can be tested and exploited to investigate the properties of hierarchical organized malignancies. Here we report that clonogenicity of cell lines is connected with invasive properties of these lines *in vitro* as suggested by our model. In future research it would be interesting to expand this finding to human tumor specimens or in established CSC lines in which the CSC fraction can be manipulated.

The current version of the SCA model clearly demonstrates the dynamics of CSC-driven tumor growth and its consequences for tumor morphology. However, further research efforts will undoubtedly lead to increased insight into the nature of the hierarchical organization of tumor cells. If so, the SCA model can be easily adapted to implement potential new information and subsequently come to even more accurate description of tumor growth.

Importantly, from the current formulation of the SCA model we conclude that hierarchical organization of malignancies significantly contributes to invasive morphology of tumors and is therefore a crucial issue for better understanding tumor biology and to improve current anti-cancer treatments.

Reference List

(1) Burger PC, Dubois PJ, Schold SC, Smith KR, Odom GL, Crafts DC, et al. Computerized Tomographic and Pathologic-Studies of the Untreated, Quiescent, and Recurrent Glioblastoma-Multiforme. Journal of Neurosurgery 1983;58:159-69.

(2) Gaspar LE, Fisher BJ, Macdonald DR, Leber DV, Halperin EC, Schold SC, et al. Supratentorial Malignant Glioma - Patterns of Recurrence and Implications for External Beam Local Treatment. International Journal of Radiation Oncology Biology Physics 1992;24:55-7.

(3) Giese A, Westphal M. Treatment of malignant glioma: a problem beyond the margins of resection. Journal of Cancer Research and Clinical Oncology 2001;127:217-25.

(4) Gardner WJ. Removal of the right cerebral hemisphere for infiltrating glioma. Journal of the American Medical Association 1933;101:823-6.

(5) Bell E, Karnosh LJ. Cerebral Hemispherectomy. Journal of Neurosurgery 1949;6:285-93.

(6) Giese A, Bjerkvig R, Berens ME, Westphal M. Cost of migration: Invasion of malignant gliomas and implications for treatment. Journal of Clinical Oncology 2003;21:1624-36.

(7) Giangaspero F, Burger PC. Correlations Between Cytologic Composition and Biologic Behavior in the Glioblastoma-Multiforme - A Postmortem Study of 50 Cases. Cancer 1983;52:2320-33.

(8) Johnson HA, Haymaker WE, Rubini JR, Fliedner TM, Bond VP, Cronkite EP, et al. A radioautographic study of a human brain and glioblastoma multiforme after the in vivo uptake of tritiated thymidine. Cancer 1960;13:636-42.

(9) Hoshino T, Wilson CB, Ellis WG. Gemistocytic Astrocytes in Gliomas - Autoradiographic Study. Journal of Neuropathology and Experimental Neurology 1975;34:263-81.

(10) Gluszcz A, Alwasiak J, Papierz W, Lach B. Morphological observations of dysplastic gliomas heterotransplanted to experimental animals. Acta Neuropathologica 1975;31:21-8.

(11) Manuelidis EE. The fate of serial heterologously transplanted glioblastoma multiforme in the eye of the guinea pig. Am J Pathol 1966;48:65-89.

(12) Jones TR, Bigner SH, Schold SC, Eng LF, Bigner DD. Anaplastic Human Gliomas Grown in Athymic Mice - Morphology and Glial Fibrillary Acidic Protein Expression. American Journal of Pathology 1981;105:316-27.

(13) Singh SK, Hawkins C, Clarke ID, Squire JA, Bayani J, Hide T, et al. Identification of human brain tumour initiating cells. Nature 2004;432:396-401.

(14) Clarke MF, Dick JE, Dirks PB, Eaves CJ, Jamieson CH, Jones DL, et al. Cancer stem cells--perspectives on current status and future directions: AACR Workshop on cancer stem cells. Cancer Res 2006;66:9339-44.

(15) Calabrese C, Poppleton H, Kocak M, Hogg TL, Fuller C, Hamner B, et al. A perivascular niche for brain tumor stem cells. Cancer Cell 2007;11:69-82.

(16) Bao SD, Wu QL, McLendon RE, Hao YL, Shi Q, Hjelmeland AB, et al. Glioma stem cells promote radioresistance by preferential activation of the DNA damage response. Nature 2006;444:756-60.

(17) Brabletz T, Jung A, Spaderna S, Hlubek F, Kirchner T. Opinion - Migrating cancer stem cells - an integrated concept of malignant tumour progression. Nature Reviews Cancer 2005;5:744-9.

(18) Hermann PC, Huber SL, Herrler T, Aicher A, Ellwart JW, Guba M, et al. Distinct populations of cancer stem cells determine tumor growth and metastatic activity in human pancreatic cancer. Cell Stem Cell 2007;1:313-23.

(19) Sheridan C, Kishimoto H, Fuchs RK, Mehrotra S, Bhat-Nakshatri P, Turner CH, et al. CD44(+)/CD24(-) breast cancer cells exhibit enhanced invasive properties: an early step necessary for metastasis. Breast Cancer Research 2006;8.

(20) Ailles LE, Weissman IL. Cancer stem cells in solid tumors. Current Opinion in Biotechnology 2007;18:460-6.

(21) Fuchs E, Tumbar T, Guasch G. Socializing with the neighbors: Stem cells and their niche. Cell 2004;116:769-78.

(22) Reya T, Morrison SJ, Clarke MF, Weissman IL. Stem cells, cancer, and cancer stem cells. Nature 2001;414:105-11.

(23) Vermeulen L, Todaro M, Mello FD, Sprick MR, Kemper K, Alea MP, et al. Single-cell cloning of colon cancer stem cells reveals a multi-lineage differentiation capacity. Proceedings of the National Academy of Sciences of the United States of America 2008;105:13427-32.

(24) Sloot PMA, Hoekstra AG. Modeling dynamic systems with cellular automata. In: Fishwick PA, editor. Handbook of dynamic system modeling. Chapman & Hall/CRC; 2007. p. 1-20.

(25) Sottoriva A, Verhoeff JJC, Borovski T, McWeeney SK, Naumov L, Medema JP, et al. Cancer Stem Cell Tumor Model Reveals Invasive Morphology and Increased Phenotypical Heterogeneity. Cancer Research 2010;70:46-56.

(26) Sottoriva A, Sloot PMA, Medema JP, Vermeulen L. Exploring cancer stem cell niche directed tumor growth. Cell Cycle 2010;9:1472-9.

(27) Vermeulen L, Sprick MR, Kemper K, Stassi G, Medema JP. Cancer stem cells - old concepts, new insights. Cell Death and Differentiation 2008;15:947-58.

(28) Balic M, Lin H, Young L, Hawes D, Giuliano A, McNamara G, et al. Most early disseminated cancer cells detected in bone marrow of breast cancer patients have a putative breast cancer stem cell phenotype. Clinical Cancer Research 2006;12:5615-21.

(29) Dormann S, Deutsch A. Modeling of self-organized avascular tumor growth with a hybrid cellular automaton. In Silico Biol 2002;2:393-406.

(30) Jiang Y, Pjesivac-Grbovic J, Cantrell C, Freyer JP. A multiscale model for avascular tumor growth. Biophysical Journal 2005;89:3884-94.

(31) Enderling H, Hlatky L, Hahnfeldt P. Migration rules: tumours are conglomerates of self-metastases. British Journal of Cancer 2009;100:1917-25.

(32) Vermeulen L, Melo FDSE, van der Heijden M, Cameron K, de Jong JH, Borovski T, et al. Wnt activity defines colon cancer stem cells and is regulated by the microenvironment. Nature Cell Biology 2010;12:468-U121.

(33) Borovski T, Verhoeff JJC, ten Cate R, Cameron K, de Vries NA, van Tellingen O, et al. Tumor microvasculature supports proliferation and expansion of glioma-propagating cells. International Journal of Cancer 2009;125:1222-30.

(34) Silbergeld DL, Rostomily RC, Alvord EC. The Cause of Death in Patients with Glioblastoma Is Multifactorial - Clinical Factors and Autopsy Findings in 117 Cases of Supratentorial Glioblastoma in Adults. Journal of Neuro-Oncology 1991;10:179-85.

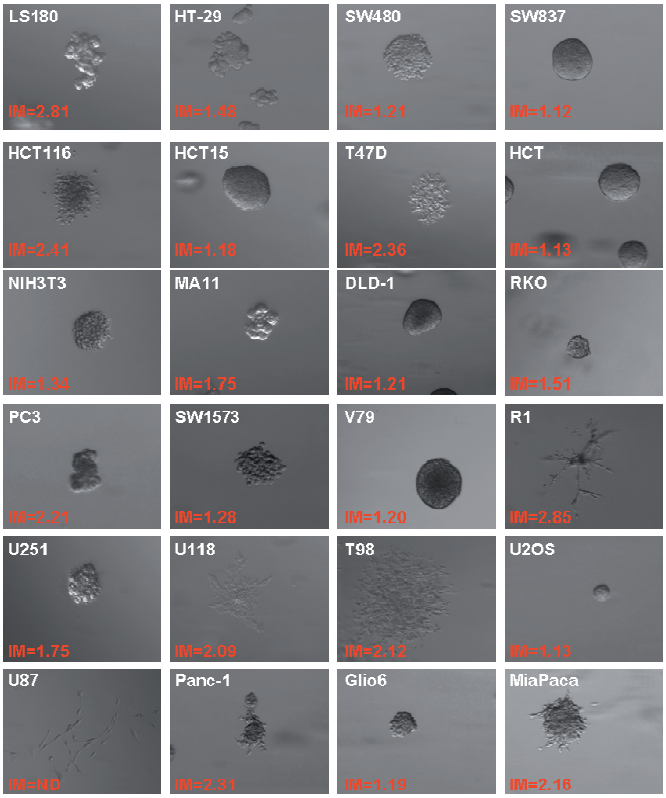

Figure S1. In vitro validation; matrigel cultures: Cells from various cell lines have been mixed with growth factor reduced matrigel at clonal density and overlaid with medium. At day 10 pictures have been taken and invasion/irregularity was quantified as described in material and method section.

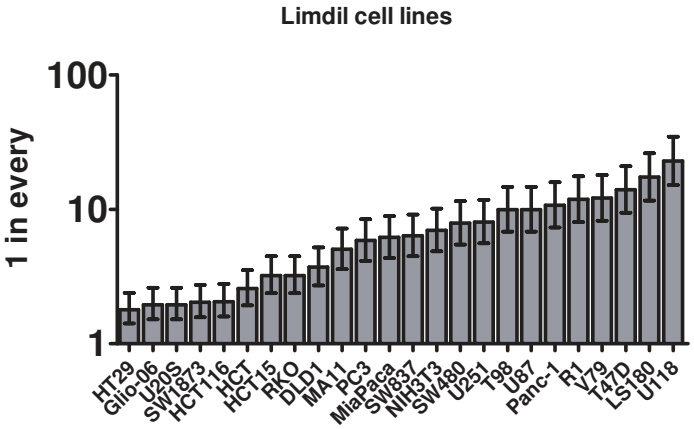

Figure S2. In vitro validation: limiting dilution assay : Cells from various cell lines have been deposited by FACS in a limiting dilution fashion. 1, 2, 4, 8, 16, 32, 64, 128, 256 cells have been sorted in a 96 well plate. Limiting dilution calculation has been performed using the *limdil* function of the 'statmod' software package (http://bioinf.wehi.edu.au/software/limdil/). Error bars represent 95% CI.

5 Tumor Microvasculature Supports Proliferation and Expansion of Glioma-Propagating Cells

Tijana Borovski[1], Joost J.C. Verhoeff[1,2], Rosemarie ten Cate[1], Kate Cameron[1], Nienke A. de Vries[3], Olaf van Tellingen[3], Dirk J. Richel[4], Wouter R. van Furth[5], Jan Paul Medema[1†] and Martin R. Sprick[1†]

1Laboratory for Experimental Oncology and Radiobiology, LEXOR, CEMM, 2Department of Radiotherapy, 4Department of Oncology, 5Department of Neurosurgery AMC, University of Amsterdam, 1105AZ Amsterdam, The Netherlands
3Department of Clinical Pharmacology, NKI, Plesmanlaan 121, 1066CX Amsterdam, The Netherlands

† Jan Paul Medema and Martin R. Sprick share senior authorship.

Int. J. Cancer: 125, 1222–1230 (2009)

Abstract

Glioblastoma multiforme (GBM) is the most common and aggressive primary brain tumor. The identification of ‘cancer stem cells (CSC) has shed new light on the potential mechanism of therapy resistance of these tumors. Because these cells appear to be more resistant to conventional treatments, they are thought to drive tumor regrowth after therapy. Therefore, novel therapeutic approaches that target these cells are needed. Tumor cells interact with their microenvironment. It has been reported that close contact between CSCs and tumor microvascular endothelium in GBM is important for CSCs to preserve their undifferentiated state and self-renewal ability. However, our understanding of this interaction is still rudimentary. This is in part due to a lack of suitable in vitro models that accurately represent the in vivo situation. Therefore, we set up a co-culture system consisting of primary brain tumor microvascular endothelial cells (tMVECs) and glioma propagating cells (GPCs) derived from biopsies of GBM patients. We found that tMVECs support the growth of GPCs resulting in higher proliferation rates comparing to GPCs cultured alone. This effect was dependent on direct contact between the 2 cell types. In contrast to GPCs, the FCS-cultured cell line U87 was stimulated by culturing on tMVEC-derived ECM alone suggesting that both cell types interact different with their microenvironment. Together, these results demonstrate the feasibility and utility of our system to model the interaction of GPCs with their microenvironment. Identification of molecules that mediate this interaction could provide novel targets for directed therapy for GBM.

Introduction

Glioblastoma multiforme (GBM) is a devastating disease with a dismal prognosis.[1] Although new treatment strategies improved survival slightly, GBM almost always recurs.[2] Novel therapeutic approaches are thus urgently needed. Recently, it has been demonstrated that only a small fraction of cells in various tumors is able to initiate new tumors in xenograft models (reviewed in Ref.[3]). These cells have been termed 'cancer stem cells' (CSCs) as they share certain features with somatic stem cells. In addition, it has been shown that CSCs are more resistant to genotoxic treatments when compared to more differentiated cell types within the tumor and therefore, could be responsible for tumor regrowth after treatment.[4] One of the major factors that plays an important role in tumor support and that contributes to its therapy resistance is the tumor microenvironment.[5] Thus, it has been speculated that the microenvironment plays a crucial role in sustaining CSCs in tumors.[6, 7]

A subpopulation of CSCs has also been identified in gliomas and transplanting as little as 100 $CD133^+$ cells into immune-deficient mice gave rise to tumors that mirrored the original patients' tumors.[8] Glioma cells have been successfully cultured under stem-cell like conditions, which means serum-free suspension culture with the addition of bFGF and EGF. It has been demonstrated that the gene expression pattern of these suspension cultures more closely mirror the primary tumor as compared to serum-cultured cell lines and that they can initiate tumors that show a better similarity to the original one in mice.[9]

It has been suggested that endothelial cells can support the growth and prevent the differentiation of brain-tumor cells.[6, 10] Recent studies further confirm this idea by demonstrating that $CD133^+$ CSCs are located in the perivascular niche and that the interaction with this niche promotes growth and therapy-resistance of brain tumor CSCs.[11, 12] Interfering with this interaction could thus be an attractive treatment strategy for the highly therapy resistant GBM. However, both our current *in vitro* as well as *in vivo* systems to study this interaction pose some problems. Current i*n vitro* model systems for the interaction of glioma cells with their microenvironment mainly utilize human umbilical vein endothelial cells (HUVECs) and long-term FCS cultured glioma cells. As it has been demonstrated that normal and tumor-derived endothelial cells differ vastly in their gene-expression pattern they might not accurately represent the situation *in vivo*.[13] Xenografts of human tumor cells in mice can model some aspects of human tumors. However, as the tumor microenvironment is recruited from the host there is a potential mismatch of cytokines and receptors that the tumor and its environment use to interact. We thus set out to develop an improved *in vitro* system to model this interaction. Our model-system consists of a co-culture of tumor-derived microvascular endothelial cells (tMVECs) and glioma-propagating cells (GPCs) which we co-isolate from GBM specimens. Using this system, we sought to find out the influence of the tumor microenvironment on proliferation of GPCs. Further, we

demonstrate that a direct interaction between tMVECs and GPCs is needed for those effects. To our knowledge this is the first description of an *in vitro* system which models the interaction of GPCs with tMVECs that consists exclusively of cells derived from GBM specimens and glioma cells cultured under stem-cell like conditions.

Materials and methods

Co-purification of tumor microvascular endothelial cells and glioblastoma-propagating cells

Glioblastoma-derived tumor microvascular endothelial cells (tMVECs) were purified essentially as described14 with some modifications. Initially, the glioblastoma specimens were digested in 1 mg/ml Liberase-1 (Roche) for 10 min at room-temperature. The cell suspension was passed through a cell strainer with 70-μm pore size (BD-Biosciences). The flow-through containing the glioblastoma cells was washed 3 times in GPC-medium and subsequently cultured as described below. The endothelial cells that were contained in the filter residue were further digested in 0.05 U/ml Collagenase/Dispase (Roche) for 60 min at 37°C under constant agitation. The resulting suspension was filtered through a cell-strainer with 40-μm pore-size (BD-Biosciences) to remove undigested tissue components. The flow-through containing the endothelial cells was washed 3 times in IMDM containing 10% FCS and subsequently cultured as described below. Occasionally, excess lipids were removed by centrifugation of the cell suspension through a layer of 20% Dextran in PBS. Patient specimens were obtained according to established and approved protocols.

Cell culture

Purified GPC spheroids were cultured in "GPC-medium." GPC medium consists of advanced DMEM/F12 medium (Invitrogen, 12634) supplemented with N2 supplement (Invitrogen, 17502-048), 2 mM glutamine, 0,3% glucose, 100 μM β-Mercaptoethanol, Trace-Elements B and C (VWR, 99-175-CL, 99-176-CL), 5 mM HEPES, 2 μg/ml heparin, lipid mixture (Sigma, L0288), 25 μg/ml insulin, 50 ng/ml h-bFGF and 20 ng/ml h-EGF (Peprotech, 500-P18, 100-15) in ultra low attachment flasks (Corning). Growth factors were supplemented twice weekly and spheroids were dissociated weekly by trituration or enzymatic digestion with Liberase 1 (Roche). tMVECs and HUVECs (Promocell, C-12200) were cultured in Endothelial Cell Medium MV 2 (Promocell, C-22221). GPCS were used at passages 10–20 (GPC 006 and 011) or 5–10 (GPC051). The tMVECs were used at passages 2–7.

Intracranial cell transplantation into NOD-SCID mice

Spheroids were dissociated and resuspended in PBS in 3 µl aliquotscontaining 2 × 10^5 cells. These aliquots were injected stereotactically into the frontal cortex of 5- to 8-week-old NOD-SCID mice following administration of general anaesthesia. All animal experiments were approved by the local animal welfare committee.

Mouse brain fixation and histopathology

Mice were killed and their brains were immediately removed and fixed in 4% freshly depolymerized formaldehyde in PBS, embedded in paraffin or frozen in liquid nitrogen and stored at −80°C. Brains were sectioned at 6-µm thickness and stained with Haematoxylin and Eosin stain.

Generation of GFP^+-GPCs

We used the lentiviral transfer vector pWPT-GFP (Addgene plasmid 12255) to generate lentiviral particles coding for GFP. Lentiviral particles were produced by using the packaging vector psPAX2 (Addgene plasmid 12260) and the envelope vector pMD2.G (Addgene plasmid 12259). The viral supernatants were concentrated and resuspended in PBS containing 2% BSA. For transduction, GPC006 were dissociated by trypsinization and lentiviral particles were added in the presence of 10 ug/ml polybrene for 12 hr.

Co-cultures, transwell experiments and ECM preparation

TMVEC and HUVECs were grown in 12-well culture dishes until confluence. Before plating GPCs, endothelial cells were kept in GPC medium without bFGF and EGF for 2 days. GPCs were mechanically dissociated into a single cell suspension and washed 3 times in PBS/1%BSA. Subsequently, 5,000 GPCs were added to each well containing fresh growth-factor free GPC medium. After 7 days the cells were incubated with BrdU or EdU and processed further.

For transwell experiments, endothelial cells were seeded in transwell inserts (0,4-µM pore size, Corning 3470). After the endothelial cells reached confluency the inserts were moved to fresh wells containing GPCs in the bottom compartment.

To prepare cell-free ECM, endothelial cells were grown to confluence and then removed by incubation with 10 mM EDTA in PBS for 20 min. The cells were then gently scraped off and the remaining matrix-deposits were washed extensively with PBS before seeding of GPCs.

Immunocytochemistry

Cells were fixed with 4% freshly depolymerized formaldehyde in PBS, permeabilized with 0,3% Triton X-100 in phosphate-buffered saline (PBS), blocked with 1% BSA (Sigma, A3424) in PBS. Immunostaining was performed with rabbit anti-GFAP (Sigma, G9269) and mouse anti-β-3-Tubulin (Clone TujI, R&D systems, MAB1195). After incubation with primary antibodies for 2 h at 37°C, the cells were washed 3 times with PBS and incubated with secondary antibodies for 30 min. Secondary antibodies were anti-rabbit Alexa-546 (Invitrogen, A11001) and goat anti-mouse Alexa-488 (Invitrogen, A11029). Cells were washed 3 times with PBS and incubated with 5 μg/ml DAPI in PBS before analysis by fluorescence microscopy.

Scoring of proliferation and absolute cell numbers

To detect proliferating cells, 5-bromo-2-deoxyuridine (BrdU) (or in some experiments EdU) incorporation was used. Cells were incubated for 90' with 10 μM of the respective nucleotide-analogs at 37°C. Staining was performed according to the manufacturers' recommendation with anti-BrdU Alexa Fluor 488 conjugate (Invitrogen, A21303). EdU staining was performed with the Click-iT EdU Alexa Fluor 488 Imaging Kit (Invitrogen, C35002) according to the manufacturers' instructions. Fluorescent images of random fields containing 1,000 cells in total were scored by 2 independent observers. Absolute cell numbers were determined by harvesting the cells by trypsinization. The wells were washed with PBS and the wash-fractions pooled with the first harvest. The cells were washed and resuspended in a 500 μl of FACS-buffer. Subsequently, the whole cell suspension was added to a Trucount tube (BD Biosciences #340334) and the cell numbers were then determined by FACS. The co-cultures were previously stained with the anti-CD105 antibody to separate glioma cells from endothelial cells.

Results

To obtain primary tMVECs for our studies, we utilized freshly resected material from GBM patients undergoing surgery. The isolated tMVECs show the typical cobblestone-like morphology as has been reported before15 (Fig. 1*a*). To verify the purity of the isolated tMVECs we stained them for the endothelial markers CD105 and CD31. The positive control, HUVECs stained strongly for both markers while the staining on tMVECs was weaker (Fig. 1*b*). Contamination with glioma cells and microglia was excluded by verifying the absence of β-3-Tubulin, GFAP and CD11b, respectively (Fig. 3*a*, lower panel and data not shown). However, later passages of the tMVECs lost the surface expression of CD31, a phenomenon that has been noted before and was dependent on the migratory state of the cells and the density of the culture.16, 17 In another publication it has been suggested, that intracellular retention of the molecule could also account for a downregulation of

surface-CD31.13, 18 Although the cells of the passages we used still showed the typical endothelial morphology, largely excluding overgrowth of the culture by contaminating cells, we determined the mRNA expression of a panel of markers. To that end, we subjected tMVECs of the latest passage used to RT-PCR for a panel of markers. As shown in (Fig. 1c), the tMVECs expressed the endothelial markers CD34, CD31, CD144, CD146 and CD141. Expression of desmin, a marker for pericytes, was hardly detectable. Interestingly, the tMVECs were negative for van Willebrand Factor (vWF), which is regarded as a classical endothelial marker. However, it has been reported that vWF expression differs between endothelial cells of large and small vessels with vWF expression being the strongest in endothelial cells derived from large vessels and being low or absent in microvascular endothelia.19 These results are thus in accordance with the reported phenotype of microvascular endothelial cells and largely exclude a significant contamination with other cells.

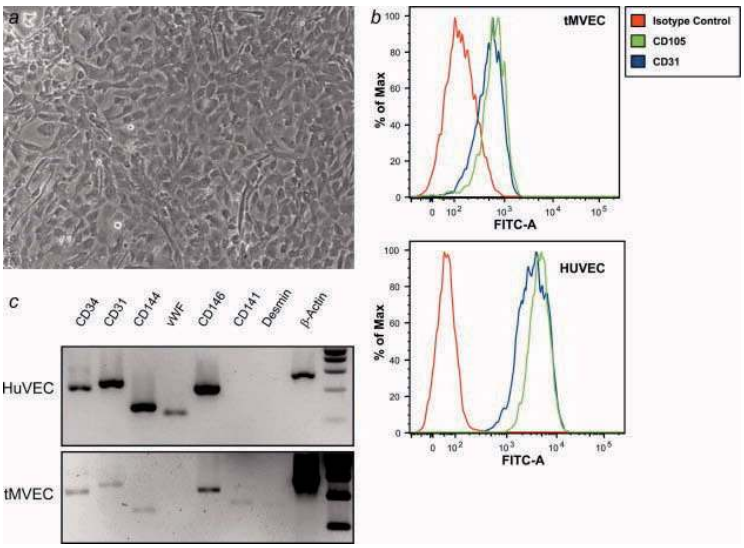

Figure 1. Characterization of tMVECs purified from GBM specimens. (*a*) Microscopic analysis of tMVECs showing spheroid growth (*b*) Expression of surface markers on tMVECs. tMVECs and HUVECs as a positive control were stained with anti CD105 (M3527, DAKO), anti CD31 (555444, BD Biosciences) or an isotype control, detected with anti mouse-IgG-FITC (F0261, DAKO) and analyzed by flow-cytometry. (*c*) Analysis of marker expression by RT-PCR.

We also established several cultures from glioma cells, which we purified from freshly resected material. All lines grew in suspension as spheroids, 1 example is shown in (Fig. 2*a*). As our cell cultures are defined by their ability to propagate gliomas in a xenograft model, we use the term glioma-propagating cells (GPCs) to denote the cultures. We initially chose 2 GPC lines for our further experiments, GPC006 and GPC011. To verify their self renewal capacity, we used the neurosphere assay. Cells were seeded at clonal density and after 7 days, the formation of neurospheres was assessed. The cells were then re-seeded under the same conditions for 2 additional rounds. In each case, we observed the outgrowth of spheres, indicating the presence of cells with self-renewal potential (Fig. 4c). Additionally, we stained the GPCs for CD133 and nestin, known markers for stem-cells and CSCs. Both, GPC006 and GPC011 were negative for CD133. This

has been reported for a subclass of GPCs before, indicating that our GPCs belong to that subclass. Nestin expression could be detected in all GPC006 cells, although at varying intensities (Fig. 2*d*, upper panel), while only a subset of GPC011 was positive for this marker (Fig. 2e, upper panel). While marker expression is useful to determine stem-cell populations, it has been reported that in some cases only a subset of stem-cell marker positive cells possess true self-renewing capacity. Therefore, we used limiting dilution, a more rigorous approach to determine the frequency of stem-like cells in our cultures (Fig. 2*d*, and 2e lower panels). The results show the frequency of self-renewing cells to be about 1 in 510 and 1 in 430 for GPC006 and GPC011, respectively. One has to bear in mind though, that this assay provides harsh conditions for the cells and that the self-renewal capacity is likely to be higher when supporting cells are present. Finally, we assessed the tumor-initiating potential of the GPCs by orthotopic transplantation into NOD-SCID mice. One example is shown in (Figs. 2*b*–2*d*). Injection of the cells resulted in tumor formation after 20–80

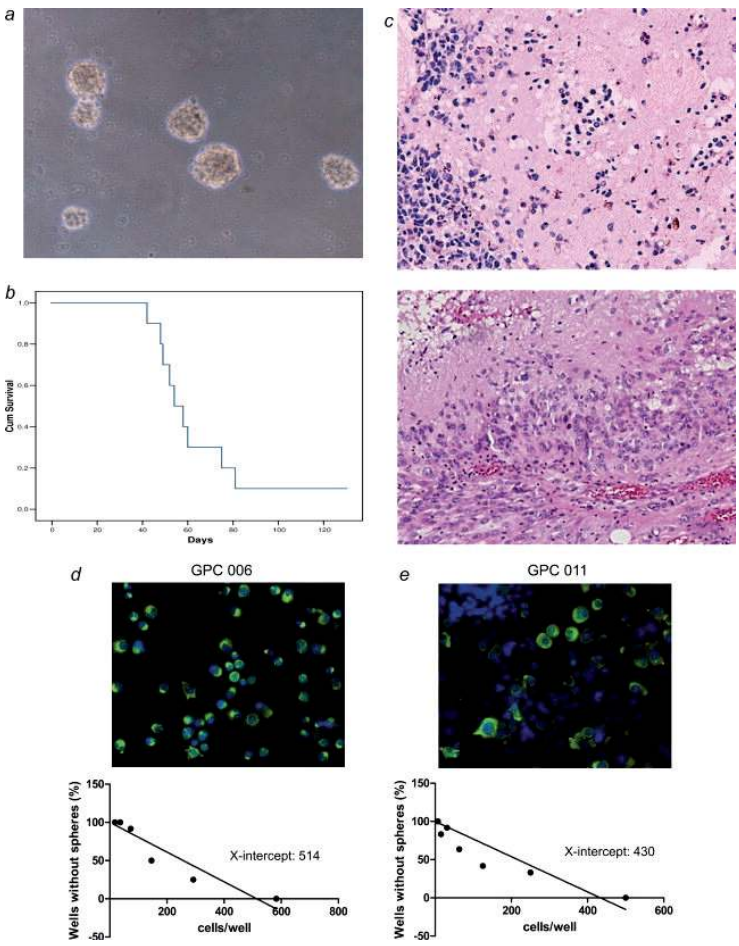

Figure 2. Glioblastoma cells retain their characteristic properties under stem-cell like culture conditions. (*a*) Microscopic analysis of GPC spheroids. (*b*) Tumor-initiating potential of GPCs. Aliquots of 2×10^5 cells were injected stereotactically into the frontal cortex of 5- to 8-week-old NOD-SCID mice. Mice were killed when they showed neurological signs. In (*c*), the morphology of Hematoxylin and Eosin stained tumors is demonstrated. The tumors obtained from the xenografts (upper panel) show a similar gross morphology as the original tumor (lower panels). Note especially the scattered invasive tumor cells which can be identified by their dark blue staining pattern. (*d*) Nesting staining (upper panels) and limiting dilution assay (lower panels) to determine the frequency of self-renewing cells. Different dilutions of GPCs were seeded into 96-well plates. After 14 days, the frequency of cells without detectable sphere-growth was determined and plotted against the number of cells plated per well. The x-intercept of the linear regression indicates the frequency of self-renewing cells.

days in almost all mice injected (Fig. 2*b*). Histological analysis of xenografts revealed that the GPCs gave rise to fast-growing and highly invasive tumors, recapitulating some of the distinctive features that were found in the original patient specimen, such as invasive growth and necrosis as well as GFAP positivity (Fig. 2*c* compare upper and lower panel and supporting Figure S1). However, the extent of vascularization and necrosis was much less pronounced in the xenografts than in the original specimens (Fig. S1). We hypothesize that this is due to the fast growing nature of the transplants or the small absolute diameter of the xenografts, which allows the tumor to acquire nutrients and oxygen by diffusion alone.

It has been described, that GBM CSCs are located in a perivascular niche and that this niche can support the growth of self-renewing cells.6, 10 We thus asked if our tMVECs, which would represent a major constituent of this perivascular niche, can influence the proliferation of GPCs. Therefore, we cultured the GPCs in medium devoid of bFGF and EGF either on an endothelial monolayer or on normal cell culture plastic. Both conditions promote adhesion of GPCs and expression of the glioma markers GFAP and β-3-tubulin (Fig. 3*a*). We next asked if the co-culture changes the amount of proliferating GPCs cells. For that reason, we used an EdU incorporation assay, shown in (Fig. 3*b*). To distinguish between tMVECs and GPCs in the co-culture, we stained for CD105 to label all tMVECs (Fig. S3). Interestingly, the GPCs continued to incorporate EdU even after 7 days of growth factor withdrawal (Fig. 3*b*). When we scored the number of EdU positive cells, we detected a significantly higher proliferation rate in the co-cultures as compared to the controls in both cell lines tested, indicating that indeed tMVECs can support the growth of GPCs *in vitro* (Fig. 3*b*).

EdU-incorporation could also be the result of ongoing repair activity or DNA-replication without cytokinesis. Moreover, the balance between proliferation and cell death ultimately decides whether a tumor expands. We therefore determined the absolute numbers of GPCs in the control and in the co-cultures (Fig. 3*c*). Both, GPC006 (Fig. 3*c*, upper panel) and GPC011 (Fig. 3*c*, lower panel) expand in the control cultures. However, the amount of GPCs in the co-cultures was more than double (500 *versus* 1,100% expansion for GPC006) or 1.7-fold (180 *versus* 310% for GPC011) compared to the control cultures. As both GPC lines had a high basal proliferation index, we were interested if tMVECs could also support GPCs with a much lower proliferation rate. For that reason, we used a third line, GPC051, which had a 20-fold lower EdU labelling index than GPC006. Analysis of co-cultures with tMVECs revealed that proliferation and expansion of GPC051 was also stimulated in the co-cultures (Fig. 3*d*). Together, our results show that tMVECs can stimulate the proliferation and expansion of GPCs *in vitro*.

To further confirm that the proliferation-enhancing effects we detected are not exclusive to one tMVEC preparation, we tested 2 additional independent tMVEC preparations. Both, tMVEC075 and

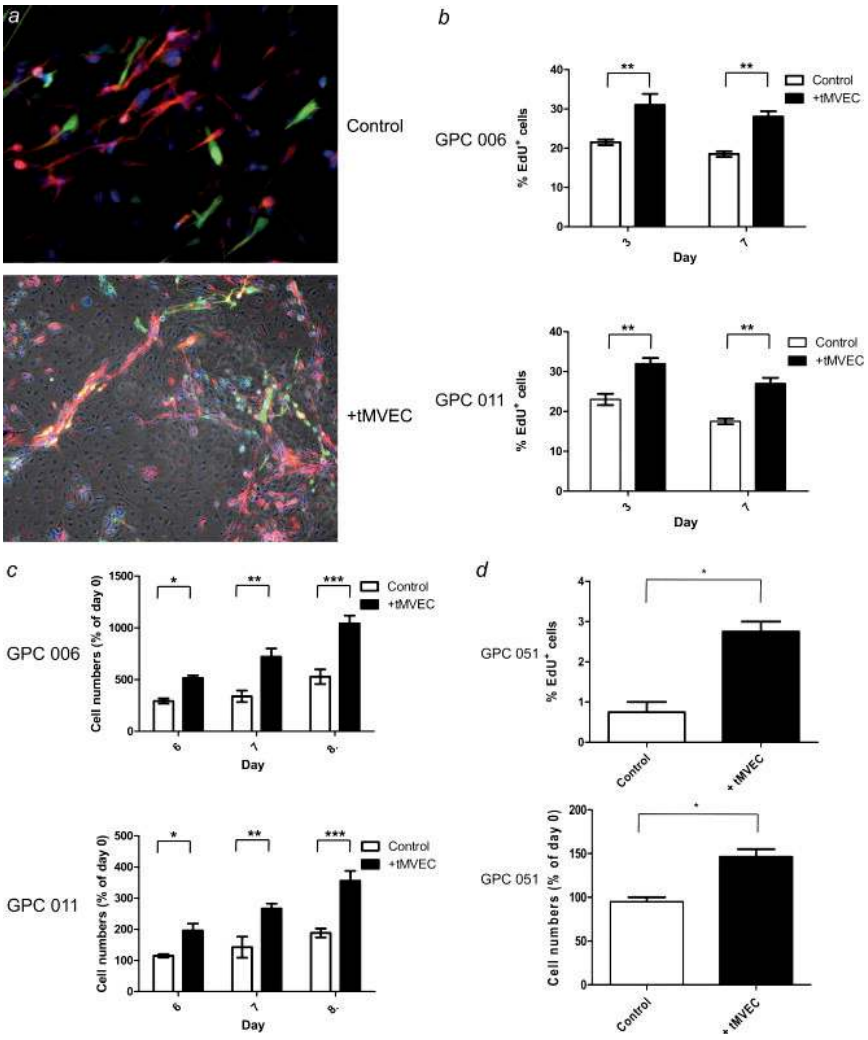

Figure 3. Co-culture of GPCs with tMVECs stimulates proliferation and expansion of GPCs. (*a*) Immunofluorescence of control cultures (upper panel) and co-cultures (lower panel) demonstrate GFAP (red) and β-3-Tubulin (green) positive cells which adhere to their substrate and undergo morphological differentiation. Note that the tMVECs in the lower panel are negative for either marker and can be further distinguished by their difference in morphology, appearing large and flat. (*b*) Co-culture of GPCs with tMVECs enhances the amount of EdU^+ GPCs compared to GPCs cultured alone. Proliferation of GPCs was scored by incorporation of the BrdU-analogue EdU and detected with Alexa647 inco-cultures of 2 different GPC lines. To distinguish between GPCs and tMVECs, the co-cultures were stained with CD105-FITC, which labels all tMVECs (See Fig. S2). Shown are the mean of EdU+ cells plus SD of a representative example of 5 experiments. (*c*) The co-culture increases expansion of GPCs. The absolute amount of cells was determined by FACS using counting beads. To distinguish tMVECs from GPCs in the co-cultures, we previously stained for CD105 as described for (Fig. S2). The control cultures were treated in the same manner to control for cell loss during the staining procedure. The amount of GPCs in the cultures was then determined by FACS. GPCs were identified by gating on the $CD105^-$ population. The cell numbers are expressed as % of initially plated GPCs. Shown is one representative example of 3 independent experiments. (*d*) tMVECs stimulate proliferation and expansion of a GPC line with a low proliferative index. Proliferation and expansion was determined as in (*b*) and (*c*). Significance levels for (*b*) and (*c*) were determined by two-way ANOVA with Bonferroni's post-test. For (*d*) the two-tailed student's *t*-test was used. Stars denote the *p*-values (*$p < 0.05$, **$p < 0.01$, ***$p < 0.001$) for clarity reasons only the comparisons yielding differences with $p < 0.05$ are shown.

tMVEC085 were able to significantly enhance the proliferation of GPC006, demonstrating that the stimulatory effect is of a more general nature (Fig. 4*a*).

It has also been described that HUVECs are able to increase the proliferation of medulloblastoma cells.10 To assess if the increase in proliferation we observed is specific for tMVECs, we co-incubated GPCs with HUVECs under the same conditions. In this case we did not observe a significant effect on the proliferation of GPCs, demonstrating that the stimulation is not a general endothelial cell activity (Fig. 4*b*). These results are in contrast to the findings by Calabrese *et al.* who showed that HUVECs can increase proliferation of CSCs in a transwell chamber.10 How could this difference be explained? It is known that microvascular endothelial cells in general and especially tumor derived microvascular endothelial cells contain a different array of secreted and cell bound factors compared to HUVECs.14 Additionally, Calabrese *et al.* used a medulloblastoma cell line in their experiments,10 which may differ in their requirements from GPCs and interact differentially with their microenvironment.

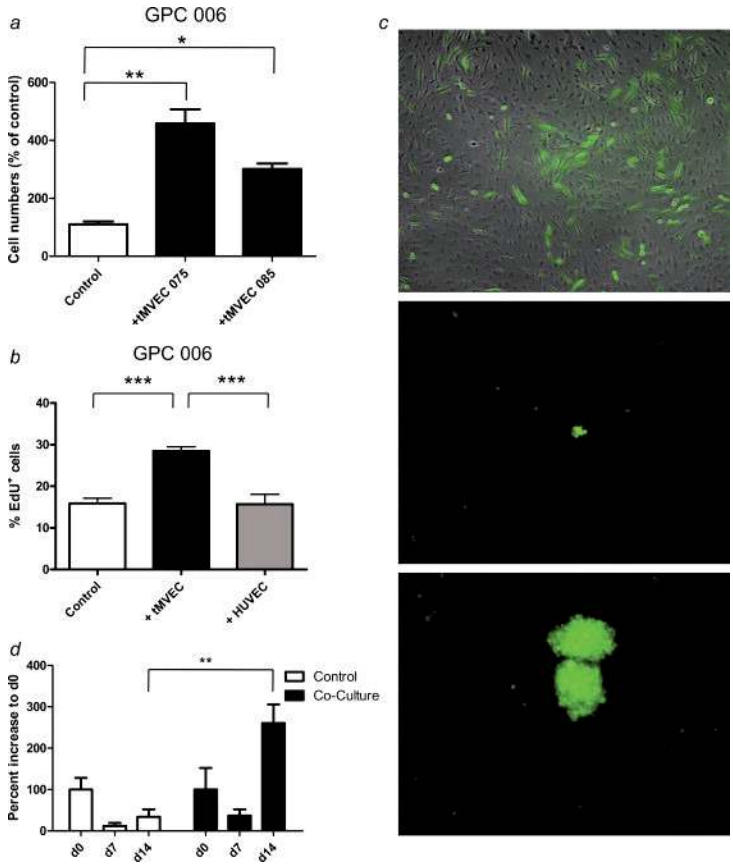

Figure 4. tMVECs, but not HUVECs, enhance the proliferation of GPCs and preserve the self-renewing potential of GPCs. (*a*) Two additional tMVEC preparations were co-cultured with GPC006 and EdU incorporation determined as described. (*b*) The proliferation-enhancing effect is specific for tMVECs but not for HUVECs. GPC006 were co-cultured on tMVECs or on HUVECs under identical conditions and EdU incorporation was determined as described. Statistical testing was done as described for (Fig. 3*b*). (*c*) Microscopical analysis of GPC006-GFP that were co-cultured on tMVECs for 14 days (upper panel), trypsinized and subjected to a neurosphere-forming assay; Some GPCs were able to form spheres after 7 days (middle panel), expanding further after 14 days (lower panel). (*d*) Live cell counts of spheroid cultures initiated from co-cultures of GPC006-GFP with tMVEC or from control-cultures were determined by FACS. To account for the differences in cell numbers between co-culture and control-cultures, the values were normalized to the amount of live cells at the day of replating, when spheroid cultures were initiated. Significance was determined one-way ANOVA with Tukey's post test. Significance levels are indicated as for Fig. 3.

It has been reported that the perivascular niche in tumors is able to support the stem-like phenotype of GPCs.6, 10 We thus asked, if the GPCs in our co-culture retain the potential for self-renewal even after prolonged co-culture. To that end, we co-cultured a GFP$^+$ derivative of GPC006 for 10 days with tMVECs in growth-factor free medium. Subsequently, all cells were trypsinized, plated under stem-cell like conditions and neurosphere outgrowth was assessed. The GFP marker allowed us to reliably distinguish between GPCs and tMVECs. While most of the GFP$^+$ cells stayed as single cells, we observed a small amount of GPCs that formed sphere-like structures after 7 days, which expanded into larger spheres after 14 days (Fig. 4c). To ascertain that the expanding cells were derived from the GPCs and not the tMVECs, we subjected the cultures to FACS analysis. The results show that all cells were GFP$^+$ and thus derived from the GPCs (Supporting Fig. S3). To determine if the co-culture with tMVECs supports the self-renewal capacity of GPCs better than the control cultures where GPCs are cultured alone, we determined the numbers of GFP+ cells at the day of replating, as well as a week and 2 weeks after. We normalized the numbers of cells to the amount of live cells present at the day of replating. Seven days after replating a drop in cell numbers is observed, which is probably due to the death of cells unable to survive in suspension (Fig. 4*d*). Importantly, after 14 days we see a strong increase in cell numbers in the cultures derived from the co-culture, while only a limited increase in cell numbers was observed in the cultures initiated from the controls (Fig. 4*d*). These results indicate that a significantly higher percentage of cells with self-renewing properties was present in the co-cultures, even after prolonged co-culturing without the addition of exogenous growth factors.

The interaction between normal neural stem cells with their niche is mediated by both, soluble factors such as VEGF, PDGF and PEDGF, and a contact-dependent interaction of the stem cell with their niche.20, 21 It is thus tempting to speculate that the same holds true for at least a subset of GPCs.7 Conversely, it has been suggested that soluble factors are sufficient to increase the proliferation of brain-tumor cells.10 To determine the effect of tMVECs secreted soluble factors on the proliferation of GPCs, we co-cultured tMVECs and GPCs in transwell chambers. This setup allows only soluble factors to be exchanged. In this assay however, we did not detect an increased proliferation and expansion of the GPCs, demonstrating that soluble factors are not sufficient for the effect (Fig. 5*a*,*b*). Extracellular matrix secreted by endothelial cells could also be responsible for the effects we observed, either by direct stimulation of ECM receptors, or by retention and local concentration of ECM-binding growth factors.. Thus, we tested the effect of tMVEC-derived matrix preparations on the proliferation and expansion of GPCs. While the ECM promoted the adhesion of GPCs (not shown), neither the proliferation nor the cell numbers were significantly increased (Fig. 5c). This suggests that tMVEC-derived ECM alone is not sufficient to mediate the proliferation-enhancing effects.

It has been shown before that HUVECs are able to stimulate the proliferation of U87, a traditionally derived glioma cell line. Therefore we were interested to see if the effects of our tMVECs are specific to GPCs or could also stimulate the proliferation and expansion of the FCS-cultured glioma line U87. Thus, we subjected U87 cells to the same co-culture, transwell and ECM assays as the GPCs and determined the amount of cell expansion. The results reveal that, like GPCs, the expansion of U87 is stimulated by the co-culture on tMVECs (Fig. 5c). However, we noted a difference in the transwell and ECM assays. While co-culture in the transwell setup showed no effect, we saw a significant increase in cell numbers by culturing U87 on tMVEC-derived ECM alone (Fig. 5c). We speculate that this difference reflects a different selective pressure U87 and GPCs underwent during their isolation and culture.

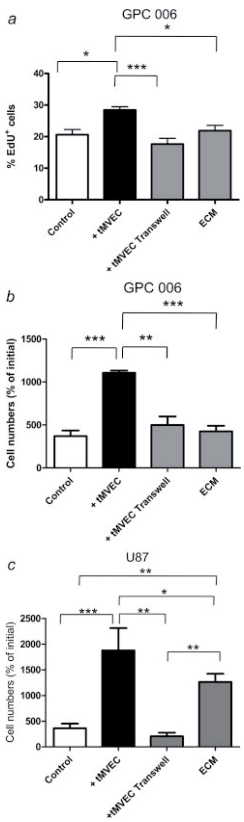

Taken together, our results demonstrate the utility and necessity of an improved *in vitro* model system for the tumor-microenvironment interaction. The method demonstrated has several advantages over the current model systems. First, we can study tumor cells and microvascular cells from the same species. It is also possible to co-isolate microvascular cells and GPCs from the same patient and thus evaluate the effects of a microenvironment that co-evolved with the tumor. Further, we utilize tumor microvasculature instead of the commonly used HUVECs. We and others have shown that these 2 cell types show significant differences with respect to their phenotype14 (Fig.4b). Further, our analysis of a traditional, FCS-cultured glioma line, U87, revealed a different requirement for interaction as compared to GPCs. While U87 were stimulated by tMVEC-derived ECM alone, GPCs required a direct contact to the tMVECs. How could that difference be explained? While the GPCs are adapted to grow in a serum free medium in suspension, U87 usually grow adherent to the culture dish in FCS-containing medium. As serum contains ECM-components, most notably fibronectin,22 one could imagine that U87 underwent a selection for cells which, at least partially, depend on ECM anchorage and the addition of FCS-derived growth factors. Adhesion to substrate, withdrawal of growth factors and the addition of FCS has been

Figure 5. GPCs and U87 differ in their mode of interaction with tMVECs. GPC006 were co-cultured with tMVECs in a transwell chamber, or grown on ECM which was secreted by tMVECs. EdU incorporation was determined as described on day 7. A direct interaction of GPCs with tMVECs is required for the proliferation-enhancing effect. tMVECs were cultured as described in Figure 3 with the exception that tMVECs were seeded in transwell inserts. After the endothelial cells reached confluency, the inserts were moved to fresh wells containing the GPCs in the bottom compartment. (*a*) After 7 days, proliferation was determined as in (Fig. 3*b*). (*b*) Cell numbers were determined as in (Fig. 3c). (*c*) U87 cells are stimulated by direct interaction with tMVECs or ECM. U87 cells were co-cultured with or tMVEC-derived ECM and cell numbers determined as described for (*b*). Statistical analysis was performed as described for Figure 4.

shown to induce the differentiation of GPCs. Thus there would be no selective pressure for this phenotype in GPC cultures.

What could be a potential mechanism by which the tMVECs stimulate the proliferation of GPCs? While our current studies do not reveal a detailed mechanism, we show that substrate-adhesion or the presence of soluble, tMVEC-derived factors alone is not sufficient. We hypothesize that factor(s) that require close proximity between these 2 cell types could mediate the effects we observed. Such factors could be, for example, short range acting members of the Sonic Hedgehog family or membrane-bound receptors and ligands of the notch-family, both of which have already been shown to stimulate the growth of brain-tumors.5, 23

The *in vitro* system presented here can complement *in vivo* systems by providing easy experimental access to many parameters of the interaction. Currently, we use our model system to further examine the intricate interactions between endothelial cells and glioma cells that promote growth and therapy resistance of this tumor. Identifying the molecules involved in this interaction can provide novel targets to fight this disease.

Acknowledgements The authors thank Mr. Louis Vermeulen and Dr. Lukas J.A. Stalpers for helpful discussions and critical reading of the manuscript and Mr. Hans Rodermond for excellent technical assistance. The authors appreciate Prof. D. Tronos' kind gift of lentiviral vectors. M.R.S. is recipient of an EMBO Long-Term Fellowship (ALTF 1063-2005). J.P.M. is supported by a KWF project grant (UvA 2007-3750) and by a NWO Vici grant.

References

1. Stupp R, Mason WP, van den Bent MJ, Weller M, Fisher B, Taphoorn MJ, Belanger K, Brandes AA, Marosi C, Bogdahn U, Curschmann J, Janzer RC, et al. Radiotherapy plus concomitant and adjuvant temozolomide for glioblastoma. N Engl J Med 2005;352:987–96.

2. Stupp R, Hegi ME. Targeting brain-tumor stem cells. Nat Biotechnol 2007;25:193–4.

3. Vermeulen L, Sprick MR, Kemper K, Stassi G, Medema JP. Cancer stem cells–old concepts, new insights. Cell Death Differ 2008; 15:947–58.

4. Bao S, Wu Q, McLendon RE, Hao Y, Shi Q, Hjelmeland AB, Dewhirst MW, Bigner DD, Rich JN. Glioma stem cells promote radioresistance by preferential activation of the DNA damage response. Nature 2006;444:756–60.

5. Becher OJ, Hambardzumyan D, Fomchenko EI, Momota H, Mainwaring L, Bleau AM, Katz AM, Edgar M, Kenney AM, Cordon-Cardo C, Blasberg RG, Holland EC. Gli activity correlates with tumor grade in platelet-derived growth factor-induced gliomas. Cancer Res 2008;68: 2241–9. GBM INTERACTION WITH ENDOTHELIA 1229

6. Gilbertson RJ, Rich JN. Making a tumour's bed: glioblastoma stem cells and the vascular niche. Nat Rev Cancer 2007;7:733–6.

7. Veeravagu A, Bababeygy SR, Kalani MS, Hou L, Tse V. The Cancer stem cell-vascular niche complex in brain tumor formation. Stem Cells Dev 2008;17:859–67.

8. Singh SK, Hawkins C, Clarke ID, Squire JA, Bayani J, Hide T, Henkelman RM, Cusimano MD, Dirks PB. Identification of human brain tumour initiating cells. Nature 2004;432:396–401.

9. Lee J, Kotliarova S, Kotliarov Y, Li A, Su Q, Donin NM, Pastorino S, Purow BW, Christopher N, Zhang W, Park JK, Fine HA. Tumor stem cells derived from glioblastomas cultured in bFGF and EGF more closely mirror the phenotype and genotype of primary tumors than do serum-cultured cell lines. Cancer Cell 2006;9:391–403.

10. Calabrese C, Poppleton H, Kocak M, Hogg TL, Fuller C, Hamner B, Oh EY, Gaber MW, Finklestein D, Allen M, Frank A, Bayazitov IT, et al. A perivascular niche for brain tumor stem cells. Cancer Cell 2007;11:69–82.

11. Hambardzumyan D, Becher OJ, Rosenblum MK, Pandolfi PP, Manova-Todorova K, Holland EC. PI3K pathway regulates survival of cancer stem cells residing in the perivascular niche following radiation in medulloblastoma in vivo. Genes Dev 2008;22:436–48.

12. Christensen K, Schroder HD, Kristensen BW. CD133 identifies perivascular niches in grade II-IV astrocytomas. J Neurooncol 2008;90: 157–70.

13. Charalambous C, Hofman FM, Chen TC. Functional and phenotypic differences between glioblastoma multiforme-derived and normal human brain endothelial cells. J Neurosurg 2005;102:699–705.

14. Charalambous C, Pen LB, Su YS, Milan J, Chen TC, Hofman FM. Interleukin-8 differentially regulates migration of tumor-associated and normal human brain endothelial cells. Cancer Res 2005;65: 10347–54.

15. Charalambous C, Virrey J, Kardosh A, Jabbour MN, Qazi-Abdullah L, Pen L, Zidovetzki R, Schonthal AH, Chen TC, Hofman FM. Glioma- associated endothelial cells show evidence of replicative senescence. Exp Cell Res 2007;313:1192–202.

16. Bastaki M, Nelli EE, Dell'Era P, Rusnati M, Molinari-Tosatti MP, Parolini S, Auerbach R, Ruco LP, Possati L, Presta M. Basic fibroblast growth factor-induced angiogenic phenotype in mouse endothelium. A study of aortic and microvascular endothelial cell lines. Arterioscler Thromb Vasc Biol 1997;17:454–64.

17. RayChaudhury A, Elkins M, Kozien D, Nakada MT. Regulation of PECAM-1 in endothelial cells during cell growth and migration. Exp Biol Med (Maywood) 2001;226:686–91.

18. Rupnick MA, Carey A, Williams SK. Phenotypic diversity in cultured cerebral microvascular endothelial cells. In Vitro Cell Dev Biol 1988; 24:435–44.

19. M€uller AM, Hermanns MI, Skrzynski C, Nesslinger M, M€uller K-M, Kirkpatrick CJ. Expression of the Endothelial Markers PECAM-1, vWf, and CD34 in Vivo and in Vitro. Exp Mol Pathol 2002;72:221–9.

20. Conti L, Cattaneo E. Controlling neural stem cell division within the adult subventricular zone: an APPealing job. Trends Neurosci 2005; 28:57–9.

21. Quinones-Hinojosa A, Sanai N, Gonzalez-Perez O, Garcia-Verdugo JM. The human brain subventricular zone: stem cells in this niche and its organization. Neurosurg Clin N Am 2007;18:15–20, vii.

22. Vuento M, Wrann M, Ruoslahti E. Similarity of fibronectins isolated from human plasma and spent fibroblast culture medium. FEBS Lett 1977;82:227–31.

23. Fan X, Matsui W, Khaki L, Stearns D, Chun J, Li YM, Eberhart CG. Notch pathway inhibition depletes stem-like cells and blocks engraftment in embryonal brain tumors. Cancer Res 2006;66:7445–52.

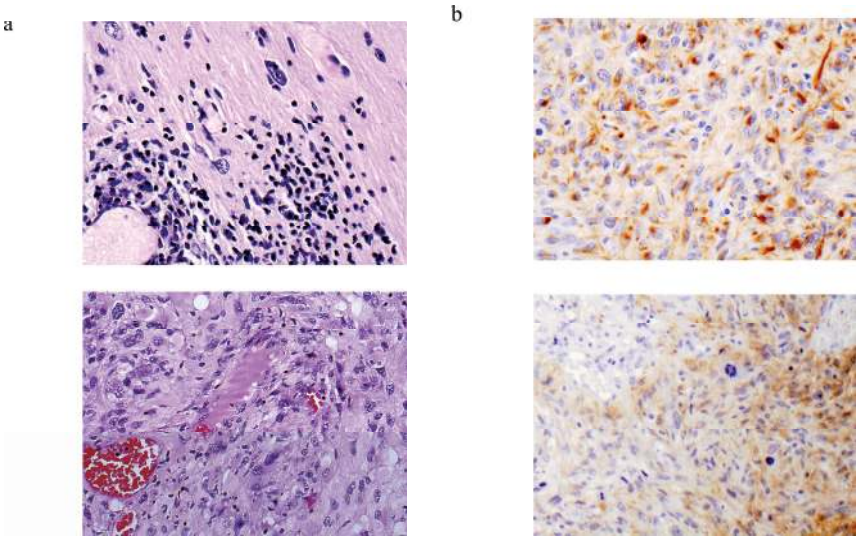

Supplemental Figure S1
Histological analysis of xenografts and the original patient specimen (a) Higher magnification analysis of HE-stained sections of mouse xenografts (upper panel) and the original patient specimen (lower panel) shows necrosis in both specimens, while vascularisation is preferentially present in the original specimen. (b) Comparison of GFAPstaining of the xenografts (upper panel) and the patient specimen (lower panel) reveals intermittent GFAP positive cells in both tumours

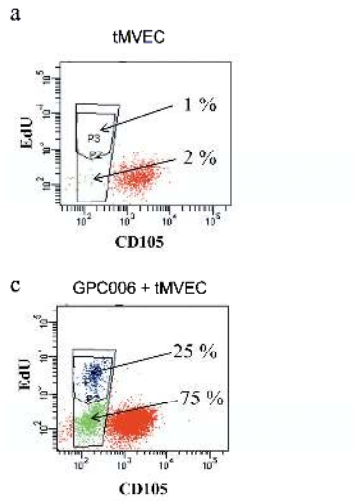

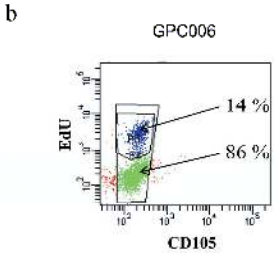

Supplemental Figure S2

Only GPCs are labelled with EdU in co-cultures. tMVECs or GPC006 were cultured as described for Fig. 1 or Fig.2, respectively. Co-cultures were performed as described for Fig.3. Subsequently, the cells were incubated with EdU for 3h, harvested and washed with ice-cold PBS. Subsequently, they were resuspended in FACS buffer consisting of PBS with 2% FCS and 0.02% (v/v) sodium azide and were stained for CD105 by incubation with 3 µg/ml anti CD105 for 20'. The cells were washed three times with FACS buffer and incubated with anti-mouse-IgG FITC (DAKO) for 20'. After washing the cells with PBS/1%BSA for three times they were fixed with 4% formaldehyde and EdU detection performed according to the manufacturers' recommendation. EdU was detected with Alexa 674. The cells were detected in a FACS Canto II flow cytometer and the amount of EdU positive cells determined by gating on the Alexa 647 positive fraction.

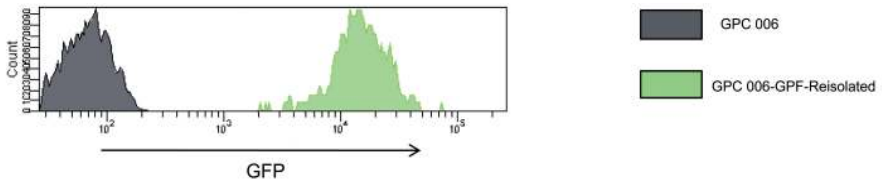

Supplemental Figure S3
Spheroid cultures re-isolated from co-cultures are derived from GPCs FACS-analysis of the spheroid cultures demonstrates selective outgrowth of GFP+ GPC. Spheroid cultures from the GPC006-tMVEC co-culture experiment were analysed by FACSscan in the presence of propidium-Iodide to exclude dead cells. As a control we included GFP-GPC006. Virtually all cells which were reisolated from the co-culture are GFP+.

6

Therapy Resistant Tumor Microvascular Endothelial Cells Contribute To Treatment Failure in Glioblastoma Multiforme

Tijana Borovski[1], Patrick Beke[1], Olaf van Tellingen[2], Hans M. Rodermond[1], Joost J. Verhoeff [3], Valeria Lascano[1], Joost B. Daalhuisen[1], Jan Paul Medema[1*] and Martin R. Sprick [4, 5*]

1. Laboratory for Experimental Oncology and Radiobiology (LEXOR), Center for Experimental Molecular Medicine (CEMM), 2. Department of Clinical Chemistry/Preclinical Pharmacology, The Netherlands Cancer Institute (Antoni van Leeuwenhoek Hospital), Amsterdam, The Netherlands. 3. Department of Radiation Oncology, Academic Medical Center (AMC), University of Amsterdam, Amsterdam, The Netherlands, 4. Deutsches Krebsforschungszentrum (DKFZ), Heidelberg, Germany,5. HI-STEM gGmbH, Heidelberg, Germany

* shared senior authorship

Oncogene, accepted for publication March 2012

Abstract

Glioblastoma multiforme (GBM) is a devastating disease with high mortality and poor prognosis. Cancer stem cells (CSCs) have recently been defined as a fraction of tumor cells highly resistant to therapy and subsequently considered to be responsible for tumor recurrence. These cells have been characterized in GBM and suggested to reside in and be supported by the tumor microvascular niche. Here we evaluated the response of tumor microvascular endothelial cells (tMVECs) to radio- and chemotherapy and analyzed how this effects their interaction with CSCs. Our data demonstrate that tMVECs exhibit extreme resistance to both therapies, with the main response to irradiation being senescence. Importantly, senescent tMVECs can be detected in human GBM samples as well as in mice upon irradiation. Even though permanently arrested, they are still viable and able to support CSC growth with the same efficacy as non-senescent tMVECs. Intriguingly, GBM CSCs themselves are capable of differentiating into cells with similar features as tMVECs that subsequently undergo senescence when exposed to radiation. This indicates that endothelial-like cells are therapy resistant and more importantly, support expansion of GBM cells.

Introduction

Glioblastoma multiforme (GBM) is the most common primary brain tumor, characterized by diffuse infiltration into surrounding healthy brain tissue (1). Patients with a malignant glioma have poor prognosis due to local recurrence, with a 5 year survival of only 9.8%, despite surgery, radiotherapy and temozolomide (TMZ) chemotherapy (2). These facts stress the need for more effective novel therapeutic strategies.

There is growing evidence showing that tumors are driven by a rare fraction of tumor cells named cancer stem cells (CSCs) (3). This population of cells has been identified in different solid malignancies, including GBM (4). In analogy to normal stem cells, CSCs are also capable of self-renewal and multipotency (5). In addition to these hallmarks of stemness, CSCs are suggested to further possess active anti-apoptotic pathways, efficient DNA damage repair and the expression of multidrug transporters on the plasma membrane, making them highly resistant to conventional therapies (6;7). It is thus believed that they are the cause of tumor recurrence. Therefore, it is important to identify the factors responsible for sustaining this population of cells.

Induction of angiogenesis is an essential prerequisite for tumor growth and progression. Once tumors reach a certain size (≈1mm^3), simple diffusion of oxygen and nutrients is not sufficient to supply all tumor cells with necessary factors. This result in hypoxic areas, which trigger the formation of tumor vasculature, termed the angiogenic switch. This way the tumor establishes its own independent blood supply, which consequently facilitates its further expansion. GBMs are one of the most vascularized human cancers, and the formation of tumor-associated vessels occurs early during tumor progression. In fact, endothelial proliferation is one of the pathological criteria for grading a glioma as high grade, indicative of a poor prognosis (8). Since development of tumor vasculature is an essential component of tumor progression, tumor blood vessels have been a target of novel therapeutics. The neutralizing anti-VEGF antibody Bevacizumab is currently in a phase III non-randomize trial for recurrent GBM. Initial results show that this treatment slightly improves overall survival of GBM patients compared to chemotherapy alone. This effect is probably due to transient normalization of tumor vasculature, resulting in enhanced delivery and efficacy of cytotoxic agents (9;10).

In addition to supplying tumor cells with oxygen and nutrients, endothelial cells are believed to form a niche-type entity in GBM. Evidence so far shows that endothelial cells indeed closely interact with brain CSCs and maintain them in a stem-like state (11). Vice versa, GBM CSCs are able to recruit endothelial cells by secreting VEGF, stimulating the formation of their own niche (12). Moreover, two recent reports indicate that GBM CSCs can differentiate into cells that very closely resemble tumor-associated vascular endothelial cells (13;14), suggesting that GBM CSCs can differentiate into niche-type cells. Therefore endothelial cells play major role in tumor growth and it is thus necessary to obtain knowledge on how treatment changes vascular function and subsequently their interaction with CSCs. However, observations on radiosensitivity of endothelial

cells vary considerably. It has been reported that the main response of tumor endothelial cells to irradiation is massive apoptosis and that this is dependent on the acid sphingomyelinase pathway (15). For GBM CSCs this would implicate partial eradication of their supportive niche after irradiation, leaving them unprotected and potentially more susceptible to treatment. On the other hand, different reports state that endothelial cells, such as HUVECs, mainly undergo senescence when irradiated (16). Here we re-evaluated these claims, especially in the context of the tumor microvascular endothelial cells (tMVECs) and their potential role as a protective niche for CSCs during therapy. We previously developed a method to co-isolate CSCs and tMVECs from human GBM specimens, which enabled us to reconstruct the physiological environment of GBM cells (17). Our data show that, when co-culturing these cells, tMVECs are capable of stimulating growth and stemness of GBM cells despite radiation and TMZ treatments. This is enabled primarily by their extensive cell death resistance to both therapies. While TMZ treatment had no effect on these cells, their preferential response to irradiation is irreversible senescence. Senescent tMVECs can still support CSC growth, with the same capacity as non-senescent ones. Moreover, GBM cells have the ability to differentiate into cells that phenocopy tMVECs, at least in some aspects, most important being senescent state upon radiation and support of GBM growth. This could, at least partially, explain therapy-resistance and recurrence of GBM.

Results

CD133 positive fraction of GBM cells is enriched for CSCs

GBM CSCs were isolated from tumor material of GBM patients who underwent surgical resection. These cells can be propagated in culture as spheroids resulting in the expansion of $CD133^+$ CSCs (Figure 1a). Consistent with previously published data, the $CD133^+$ tumor cells had high clonogenic capacity (Figure 1b) (4). Furthermore, as shown before the $CD133^+$ GBM cells were tumorigenic and gave rise to invasive, scattered tumors upon injection, while $CD133^-$ cells did not (Figure 1c, Supplementary Figure 1a). This confirms that the $CD133^+$ fraction is enriched for GBM CSCs.

Irradiation combined with TMZ is standard therapy for GBM patients. We therefore first exposed our GBM cultures to these treatments in order to investigate their sensitivity. GBM spheroid cultures showed increased amount of cell death when irradiated with 1x5Gy, although the level of sensitivity varied between cultures (Figure 1d). The two lines shown, display the most extreme response to radiotherapy when looking at cell death. In G073 only a very limited amount of apoptosis is observed, while apoptosis was induced in a large fraction of the G408 cells. In supplementary figure 3 several other GBM spheroid cultures are shown with varying response to irradiation. In the following experiments we mainly focused on two independent spheroid cultures isolated from different patients (G408 and G073). Both these lines appeared to be resistant to the alkylating agent TMZ, while a third line G077 was extremely sensitive to TMZ (Supplementary Figure 1b).

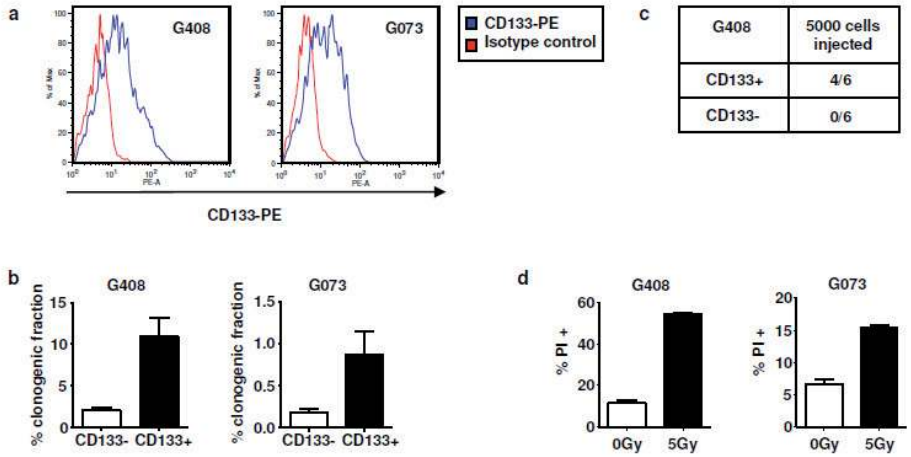

Figure 1 CD133 fraction is enriched for GBM CSCs. (a) Primary GBM cultures G408 and G073 show expression of CD133 marker when cultured under serum-deprived and growth factor enriched conditions. (b) A limiting dilution assay was performed on sorted $CD133^+$ and $CD133^-$ fraction of G408 and G073 cultures. The clonogenic potential of each fraction is depicted on the graphs and shows higher clonogenicity of $CD133^+$ population. A representative example of two independent experiments is shown. Error bars represent 95% confidence intervals. (c) Intracranial injection of G408 cells into nude mice; $5x10^3$ cells of either $CD133^+$ or $CD133^-$ G408 fraction were FACS sorted and injected. The number of successful tumor initiations out of six injections for each condition is shown. (d) Cell death of G408 and G073 upon treatment with 1x5Gy was measured five days after irradiation by PI exclusion. Error bars represent SD (*n*=3).

tMVECs support the growth of GBM CSCs despite irradiation and TMZ treatment

In addition to GBM CSCs we also co-isolated tMVECs from GBM specimens. These cells expressed endothelial markers CD31 and CD105 and demonstrated tube forming ability (Supplementary Figure 2a, b). Previously we showed that tMVECs support the expansion and stemness of GBM cells (17). Here, we investigated whether these stimulatory effects of tMVECs were preserved after irradiation or chemotherapy. As shown in Figure 2a, tMVECs induced expansion of GBM cells even after irradiation with 1x5Gy. The inhibition of proliferation upon irradiation in the absence of tMVECs differs between GBM lines (Figure 2a and Supplementary Figure 3a), but in all cases the tMVECs enhance proliferation. In other words, tMVECs protect GBM cells in part from the effects of irradiation. Moreover, we determined the CD133 expression of GBM cells after exposure to 1x5Gy in the absence or presence of tMVECs. Co-culture strongly increased the $CD133^+$ fraction in GBM cells, suggesting that tMVECs support stemness in CSC cultures. Importantly, this enhanced CD133-positivity was preserved after irradiation (Figure 2b, Supplementary Figure 3b). Thus, in addition to enhancing their expansion, tMVECs are able to provide factors that support CSCs to preserve their 'stemness', even upon irradiation.

The tMVEC-induced increase in GBM cell-numbers after irradiation could result from reduced cell death, increased proliferation or a combination of both. The dilution of CFSE, measured four days after the beginning of the experiment, demonstrated that GBM cells had higher proliferation rates

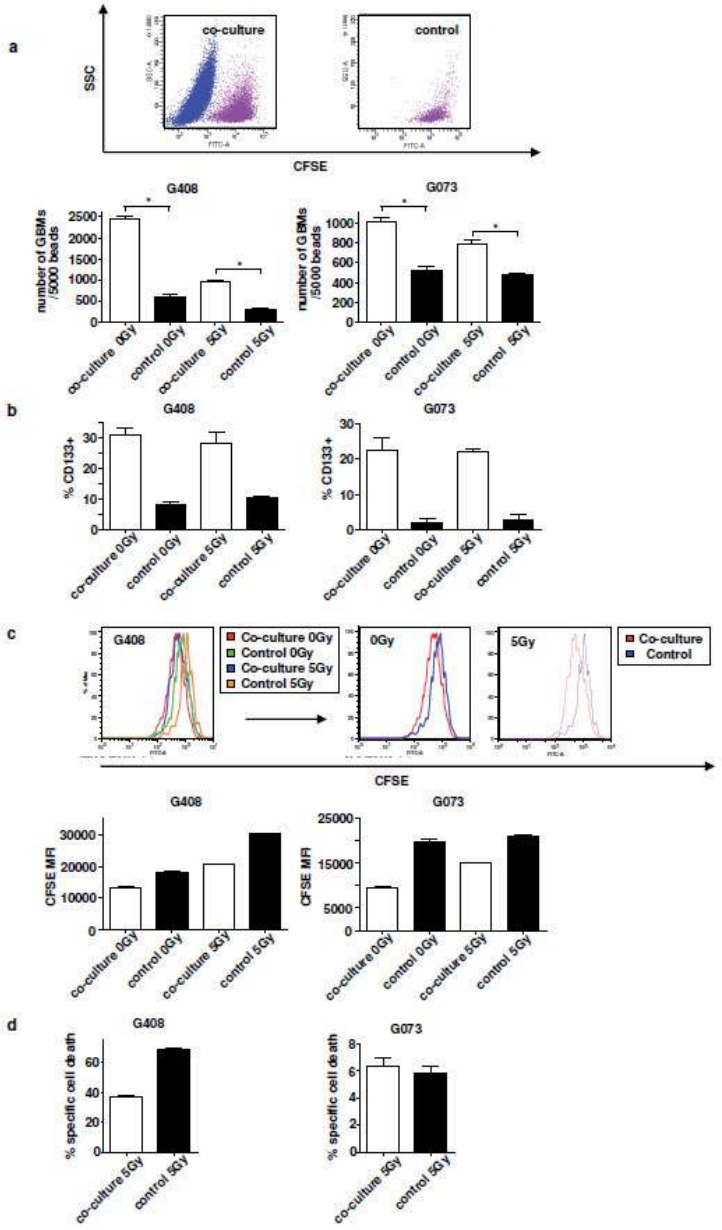

Figure 2 tMVECs support growth and stemness of GBM CSCs despite irradiation treatment. (a) FACS profiles show an example of co-culture and control; GBM cells were CFSE-labeled and thus distinguishable from tMVECs. Numbers of G408 and G073 were measured in control samples and co-culture with tMVECs, untreated or treated with 1x5Gy, by using calibrated beads. One representative example of five independent experiments is shown. Significance was tested with ANOVA and Tukey's post-test. Significant differences with $p<0.05$ in group comparisons are denoted by '*'. For clarity reasons, only 0Gy vs. 5Gy comparisons are shown. (b) Staining for CD133 was performed on co-culture and control samples, untreated or irradiated (5Gy). Percentages of $CD133^+$ G408 and G073 under different conditions are depicted on the graphs (n=3). (c) CFSE dilution was used to assess the proliferation of G408 and G073 when cultured with either tMVECs or alone, either with or without irradiation (5Gy); the graphs depict Mean Fluorescence Intensity (MFI) of the CFSE signal of GBM-cells under different conditions. One representative example of five independent experiments is shown. (d) Percentages of irradiation-induced cell death of GBM-cells in co-culture and control were measured by PI exclusion and calculated as follows: 100×(% experimental cell death − % spontaneous cell death)/(100 − % spontaneous cell death). Error bars represent SD.

in co-culture as compared to control samples (lower MFI means higher proliferation). Furthermore, when co-cultured with tMVECs, GBM cells recovered much faster from the irradiation treatment and re-entered the cell cycle (Figure 2c, Supplementary Figure 3c). Moreover, the amount of irradiation-induced cell death of GBM cells was in most cases lower in

co-culture as compared to control-irradiated cells (Figure 2d, Supplementary Figure 3d). The protective effect of tMVECs varied between GBM lines. Recently, GBM subtypes that differ in the presence of signalling-pathway alterations as well as in their response to therapy have been identified (18). The protective and proliferation-enhancing effect of tMVECs on GBMs is mediated by soluble and cell-bound factors (17). It is thus likely that the dependence on certain signalling pathways and presence of receptors on different GBM subtypes determines the effects of their interaction with tMVECs.

We next tested whether tMVECs can protect GBM cells from treatment with the chemotherapeutic agent TMZ. The TMZ-sensitive GBM line G077 showed a significantly higher cell number under TMZ-treatment when co-cultured with tMVECs as compared to the control, indicating that TMZ-sensitive CSCs are protected by tMVECs from chemotherapy as well (Supplementary Figure 3e). Moreover, under combined TMZ and radiation treatment, tMVECs also exert protective effects on these GBM cells (Supplementary Figure 3e). The underlying mechanism is unknown, but it has been reported that response of GBM patients to TMZ treatment largely depends on whether *MGMT* gene is silenced or not (19). Thus, it can be speculated that tMVECs might regulate *MGMT* levels in tumor cells or simply enhance the repair machinery necessary to deal with the damage induced by TMZ. Combined our data demonstrate that tMVECs not only increase the basal proliferation level of GBM cells, but provide additional protective effects from radio- and chemotherapy.

Endothelial cells undergo senescence after irradiation

As the effects of co-culture on GBM CSCs were still evident after treatment, we decided to investigate the response of tMVECs to these treatments. Cells were exposed to 1x5Gy or 1x15Gy gamma-irradiation and the amount of cell death was determined, with HUVECs serving as control. PI exclusion revealed a very low amount of cell death after irradiation in two separate tMVEC lines, E030 and E023, while HUVECs showed higher cell death rates under these conditions (Figure 3a, Supplementary Figure 4a). Even after high dose radiation with 1x15Gy we detected only around 5% of cell death in our tMVEC cultures, indicating that apoptosis is not a major response and that the vast majority of cells survived the treatment. This was consistent with other cell death measurements such as DNA fragmentation by Nicoletti assay, YO-PRO and Annexin V staining, which consistently showed low death rates (Supplementary Figure 4b and data not shown). Moreover, we exposed tMVECs to different doses of TMZ. PI exclusion showed that after TMZ treatment no cell death could be detected (Supplementary Figure 4c). Analysis of the cell cycle distribution also revealed no change in cell cycle profile after the treatment with this alkylating agent (Supplementary Figure 4c). Thus, we conclude that tMVECs are highly resistant to TMZ, in addition to irradiation.

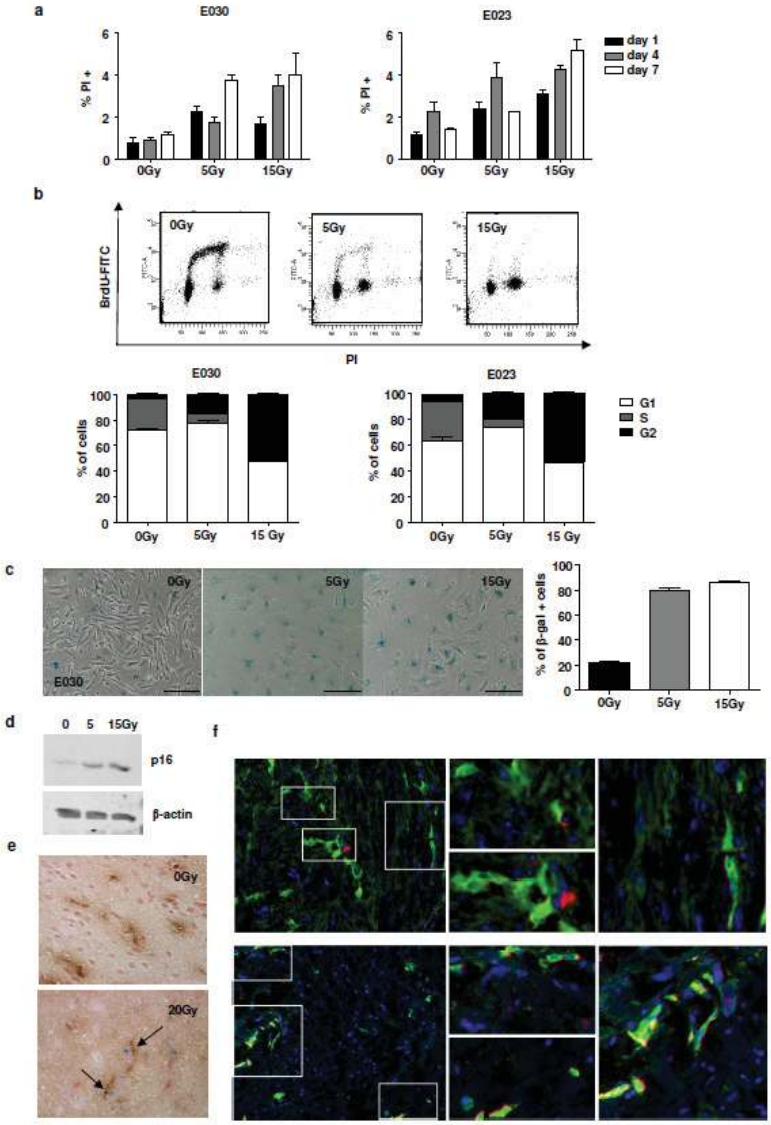

Figure 3 Irradiation induces senescence in tMVECs. (a) Graphs present the percentages of PI^+ cells day one/four/seven after 1x5Gy or 1x15Gy in two tMVEC cultures E030 and E023. Error bars represent SD (*n*=3). (b) FACS profiles show cell cycle distribution of tMVECs one week after irradiation treatment, measured by BrdU incorporation. Graphs show quantified cell cycle distribution of E030 and E023 after the treatment. Error bars represent SD (*n*=3). (c) β-gal assay was performed on E030 one week after 1x5Gy or 1x15Gy of irradiation. Senescent cells are evident by blue β-gal staining. Scoring of the blue cells revealed approximately 90% of senescent cells after irradiation in E030 culture. Scale bars 20 m. (d) Western blot demonstrates an increase in p16 levels in E030 after irradiation. (e) *In vivo* detection of senescent tMVECs. CD31 (dark brown) and β-gal (blue) co-staining on mice brains that were either irradiated (lower) or not (upper) with 20Gy. Nuclei were counterstained with nuclear red. Errors point the co-localisation of endothelial marker CD31 and β-gal staining. (f) Biopsy of GBM patient irradiated with 60Gy was co-stained for CD105 (green) and β-gal (red), nuclei (blue). Higher magnification of the boxed areas indicates senescent tMVECs (CD105 and β-gal co-localizing). Of note green represents tMVECs, red β-gal. Several endothelial cells show clear red areas or co-staining in yellow. For details see Materials and Methods and Supplementary Figure 4f.

Importantly, the DNA analysis revealed that the tMVECs appeared to undergo G_2 arrest after irradiation (Supplementary Figure 4b). To further determine the cell cycle distribution of tMVECs before and after treatment, we performed a BrdU incorporation assay. The results show that irradiation decreased the amount of proliferating cells in a dose-dependent manner, indeed mainly due to G_2 arrest (Figure 3b, Supplementary Figure 4a). Even a week after irradiation, cells remained growth arrested and did not resume proliferation (Figure 3b, Supplementary Figure 4a). Furthermore, we noticed a dramatic change in the light-scatter properties of the surviving tMVECs after irradiation (Supplementary Figure 4d). Senescence is known to be an irreversible cell cycle arrest, associated with morphological changes of the cells, where the cells get significantly larger, show flatten shape and express senescence-associated β-galactosidase. To determine if senescence was the preferential response of tMVECs to irradiation, we performed a β -gal assay. This assay confirmed a significant increase in the amount of senescent cells after treatment (Figure 3c, Supplementary Figure 4e). Accordingly, irradiated tMVECs also displayed increased levels of the CDK inhibitor p16, whose elevated expression was associated with senescence (Figure 3d) (17;20).

In an endeavor to validate if senescent endothelial cells can also be detected upon irradiation *in vivo*, we examined brains of nude mice that were exposed to 20Gy of irradiation and compared them to non-irradiated ones (Figure 3e). Co-staining for the senescence marker β-gal and the endothelial marker CD31 revealed that senescent endothelial cells can exclusively be detected in irradiated brains. None of the endothelial cells were senescent in the non-irradiated brains, indicating that senescence is a consequence of the radiation treatment. Moreover, we examined post-mortem biopsies of a GBM patient who displayed tumor recurrence after having received treatment with surgery and subsequent radiotherapy (60Gy). As this effectively represents an irradiated tumor these post-mortem samples were analyzed for the presence of senescent tMVECs. We clearly detected tMVECs in these tumor samples and the majority showed a co-staining for β-gal pointing to senescence (Figure 3f, Supplementary Figure 4f). These results strongly suggest that the irradiation response of (tumor) endothelial cells observed *in vitro* occurs in the physiological conditions as well where these cells could very well play the same role in tumor growth and tumor resistance as demonstrated *in vitro*.

Senescent endothelial cells preserve their capability to support GBM CSCs

Our results demonstrated that tMVECs become senescent when irradiated and that irradiation does not affect their supportive role to GBM cells. To further investigate the functionality of senescent tMVECs in relation to non-senescent ones, tMVECs were irradiated with a single dose of 15Gy one week prior to co-culture with GBM cells in order to allow them to become senescent. Intriguingly, senescent tMVECs are not only capable of sustaining the growth of GBM cells, but

this effect is comparable to co-culture with non-senescent tMVECs (Figure 4a). Furthermore, analysis of CD133 expression demonstrated a higher percentage of CD133$^+$ GBM cells in co-culture with both non-senescent and senescent tMVECs as compared to control, showing that tMVECs drive expansion of GBM cells and selectively support the CSC fraction even after they have become senescent (Figure 4b).

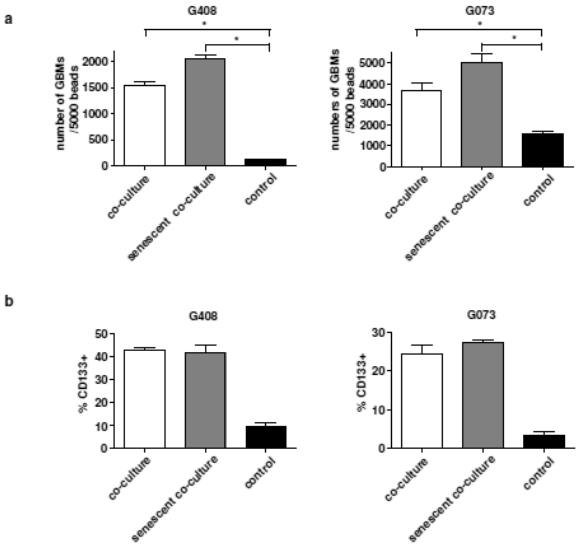

Figure 4 Senescent tMVECs support growth and stemness of GBM-cells. (a) GBM cultures G408 and G073 were co-cultured with non-senescent or senescent tMVEC (pre-irradiated with 1x15Gy one week before start of the co-culture) for four days before the measurement. Experimental set-up is same as in Figure 2. Graphs show the numbers of G408 and G073 under indicated conditions. A representative example of four independent experiments is shown; Significance was tested with ANOVA and Tukey's post-test. Significant differences with $p<0.05$ in group comparisons are denoted by '*'. For clarity reasons, only co-culture vs. control comparisons are shown. (b) Graphs show the percentages of CD133$^+$ G408 and G073 in control and co-culture with either senescent or non-senescent tMVECs. (n=3). Error bars represent SD.

GBM can differentiate into cells that mimic tMVECs in their radiation response and support of GBM expansion

It has been reported recently that GBM cells have the ability to differentiate into endothelial-like cells (13;14). This suggested that GBM cells could effectively generate their own niche by differentiating into an endothelial-like phenotype that would support the CSC fraction in the tumor. To test whether this is indeed the case, we allowed our GBM cultures to differentiate under conditions described to favor the endothelial-like lineage. The resulting cells, which we termed endothelial-like GBM (E-GBM) to reflect this phenotypical change, indeed resemble, at least in some aspects, endothelial cells. In a tube-formation assay E-GBMs had the ability to form vessel-like structures, similar to tMVECs (Supplementary Figure 2 and 5). To determine whether the E-GBMs show a similar radiation-response as tMVECs, we exposed them to gamma-irradiation. Strikingly, the results show minimal cell death of E-GBMs, in contrast to the response observed

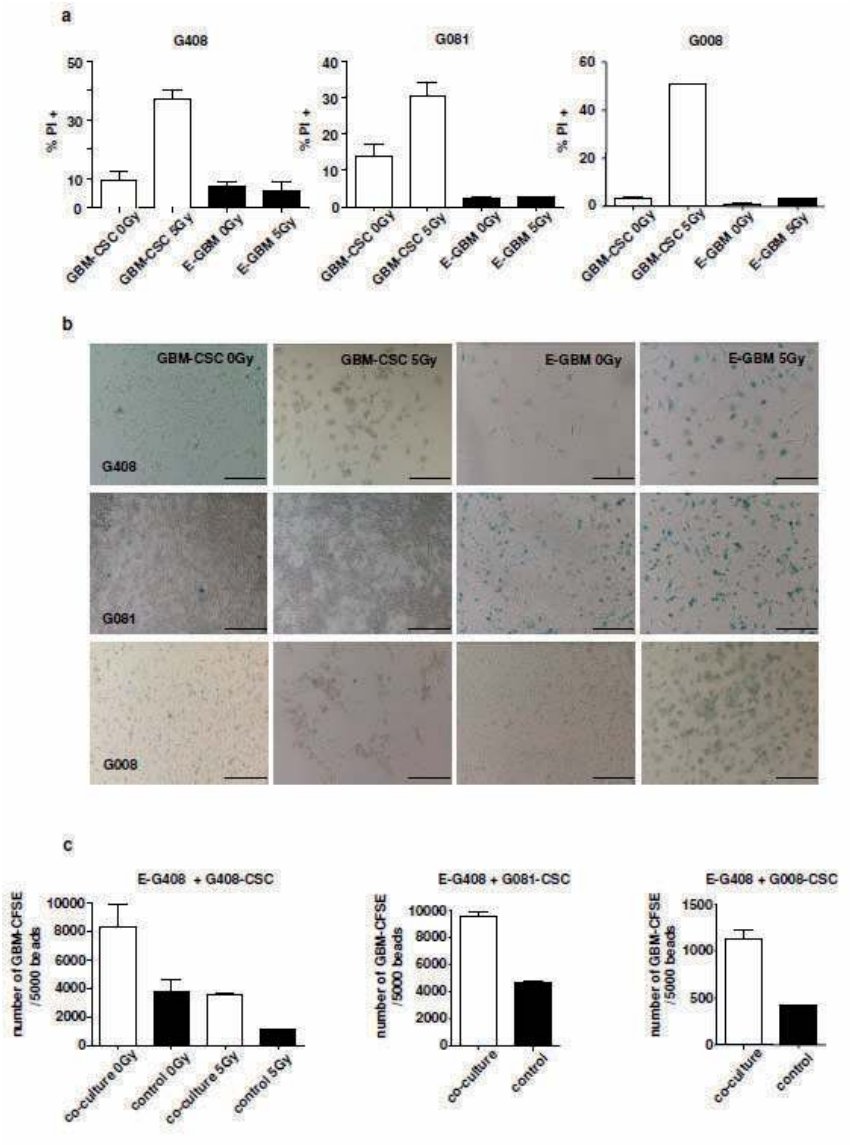

Figure 5 GBM that differentiate into endothelial-like E-GBMs become radiation-resistant and support the expansion of GBM-CSCs. (a) G408, G081 and G008 were either cultured in endothelial differentiation conditions (E-GBM) or maintained under CSC conditions (GBM-CSC) for five days, and subsequently were exposed to 1x5Gy. Cell death was measured by PI exclusion. Graphs show percentages of PI^+ cells five days after irradiation treatment. Error bars represent SD (n=3). (b) Treatment with γ-irradiation preferentially induces senescence in E-GBMs while the parental GBM-CSC's response is cell death. β-gal assay was performed on G408, G081 and G008 under conditions as described in 5a. Senescent cells are stained blue. Scale bars 20μm. (c) E-G408 were labeled with CFSE and co-cultured with G408, G081 and G008 GBM-CSCs; the numbers of $CFSE^+$ GBM-CSCs were measured using calibrated beads after four days of co-culturing. One representative example of two independent experiments is shown. Error bars represent SD.

with the undifferentiated parental GBM-CSC cultures (Figure 5a). This effect was evident even in the initially highly radiosensitive G408 cells that reverted to complete resistance to this treatment upon E-GBM differentiation (Figure 5a). Accordingly, the preferred response of E-GBMs to irradiation rather appeared to be senescence (Figures 5b). It is interesting to note that senescence seems to be a default response for these E-GBMs and in some cases is already observed in a significant fraction of the non-irradiated cells (E-G081). This is in line with previous observations showing that GBM-associated endothelial cells undergo senescence (21). The observed differences in basal senescence in the different isolates of E-GBM may reflect different GBM subtypes (18). However, the resistance to radiation and the induction of senescence is a common feature for all E-GBMs tested. Most strikingly, co-culture of E-GBMs, both non-irradiated and irradiated, led to a significant increase in the number of GBM-CSCs, suggesting that E-GBMs are also capable of supporting the growth of GBM-CSCs comparable to tMVECs (Figure 5c). Importantly, this was observed for various GBM cultures. Combined our data therefore point to a general tumor-supportive role for both tMVECs and E-GBMs that is sustained after irradiation.

Discussion

There is a growing body of literature concerning the effects of irradiation and TMZ on GBM cells. However, these data are mainly derived from *in vitro* studies using GBM cell lines. In addition, recent insights suggested an important role of the tumor microenvironment in tumor maintenance and progression, tumor vasculature in particular, in the case of GBM (11). The majority of brain tumor vasculature is structurally and functionally different from the vessels in healthy tissue as it is disorganized, tortuous, dilated and often displaying dead-end structures (22). These seemingly dysfunctional blood vessels still co-localize with tumor cells, the CSC fraction in particular, and form a niche for these cells. Published data demonstrate that tumor microvasculature plays an essential role in sustaining GBM CSCs, regulating their self-renewal and promoting their tumorigenicity (11). However, little is known about the consequences of treatment on these endothelial cells. The ability to isolate these cells from primary tumor material gives us the unique opportunity to study the effects of various treatments on isolated GBM CSC cultures, alone as well as in the context of their perivascular niche. Ionizing radiation is mostly contributing to survival of GBM patients (~7 months), next to surgery (~5 months) and chemotherapy (~2 months). The effects of ionizing radiation on angiogenesis in both, tumors and healthy tissues, have long been a matter of considerable debate and still remain largely elusive. At the cellular level, apoptosis of endothelial cells is believed to be the main biological process underlying irradiation-induced endothelial dysfunction, and this is thought to be dependent on the acid sphingomyelinase pathway (15). Our data, however, show that the endothelial cells are highly resistant to radiation treatment and that their main response to radiation is irreversible cell cycle arrest, senescence (Figure 3, Supplementary Figure 4). Our results are in agreement with the

observations of Garccia-Barros *et al*. who reported low cell death rates of endothelial cells at doses of irradiation up to 15Gy, and strong increase in apoptotic cells at higher doses (15). Here we extend these observations by showing that the majority of the surviving endothelial cells undergo senescence instead of cell death. Accordingly, HUVECs exposed to gamma-irradiation are also prone to become senescent (16). Importantly, senescent endothelial cells can be exclusively detected in mice brains upon irradiation treatment, while none of these cells were found in non-irradiated brains (Figure 3e), strongly suggesting senescent state of these cells to be the result of treatment itself. In addition, senescent tMVECs can also be detected in irradiated GBM samples (Figure 3f). This is consistent with previous reports stating that glioma-associated endothelial cells exhibit characteristics of cellular senescence, particularly in central parts of the tumor (21). More importantly, these senescent tumor endothelial cells seem to be more resistant to cytotoxic drugs and produce even more growth factors as compared to normal vasculature in the brain (21). Senescent cells, even though terminally arrested, are still metabolically active and able to secrete different growth factors, cytokines, immune modulators and enzymes all of which can alter tissue microenvironment and as such could potentially create a tumor microenvironment that harbors and supports cancer cells (23-25). Accordingly, senescent fibroblasts have already been shown to sustain growth of epithelial tumor cells and furthermore promote their tumorigenicity (26;27). Here we show that senescent endothelial cells are fully capable of supporting the expansion of GBM cells while maintaining the CSC fraction, with the same capacity as non-senescent tMVECs (Figure 4). Moreover, this supportive effect is still evident after irradiation treatment (Figure 2, Supplementary Figure 3). Even though GBM cells will undergo cell death upon irradiation and show reduced proliferation, tMVEC provide support to overcome this irradiation response. Importantly, it has been reported before that CD133+ GBM are more resistant to cell death induction by irradiation. In our *in vitro* experiments we do not observe a selective increase in the number of CD133+ cells upon irradiation, arguing against resistance of these cells. However, this experiment runs over a 5 day period, during which CSC divide and may yield new CD133- cells, potentially re-establishing the original ratio between CD133+ and CD133- cells. Using this set-up it is therefore difficult to conclude whether CSC are more resistant to irradiation treatment.

TMVEC also provide protection of GBM cells against TMZ treatment, as well as against an even more cytotoxic combination of gamma-irradiation with chemotherapy (Supplementary Figure 3e). Furthermore, we show that GBM cells can differentiate into cells that mimic some aspects of the tumor endothelial phenotype (E-GBM) as they become radioresistant upon differentiation and preferentially enter senescence. This is comparable to genuine tMVECs and in contrast to the radiosensitive parental GBM cells (Figures 5a and b). More importantly, E-GBMs share with tMVECs the capability to support the survival and expansion of GBM-CSCs after gamma-irradiation, the first-line treatment for GBM. These results suggest a striking scenario in which the tumor cells could potentially provide themselves with an environmental niche that allows them to survive and

even proliferate during and after treatment with gamma-irradiation and alkylating agents. Such a protective niche could contribute to the observed tumor relapse after an initial clinical response. Disrupting the interaction between tumor and its vascular niche would negate the protective effects for tumor cells and potentially sensitize them to treatment with DNA-damaging agents. The molecules that mediate this interaction are thus attractive therapeutic targets that could help to develop novel strategies to fight this disease.

Materials and methods

Isolation of tMVECs and CSCs

GBM and tMVECs were essentially isolated as described (Borovski *et al.*, 2009). In short, GBM specimens were cut into small pieces and digested in 1mg/ml Liberase-1 (Roche) for 10' at room temperature (RT). The cell suspension was passed through a 70μm cell strainer (BD). The flow-through containing the GBM cells was washed in CSC medium and cultured as described below. The tMVECs contained in the filter residue were further digested in 0.05U/ml Collagenase/Dispase (Roche) for 60' at 37°C, constantly agitated, and furthermore filtered through a 40μm cell strainer (BD) to remove undigested tissue components. The flow-through containing the tMVECs was washed in IMDM with 10%FCS and cultured as described below. Patient specimens were obtained according to established and approved protocols.

Cell culture

GBM CSCs were cultured in advanced DMEM/F12 medium (Invitrogen) supplemented with 2mM glutamine, 0.3% glucose, N2 supplement (Invitrogen), 100μM β-Mercaptoethanol, Trace-Elements B and C (VWR), 5mM HEPES, 2μg/ml heparin, lipid mixture (Sigma), 25μg/ml insulin, 50ng/ml h-bFGF and 20ng/ml h-EGF (Peprotech) in ultra-low attachment flasks (Corning). This will further be referred as CSC medium. Growth factors were supplemented twice weekly and spheroids were dissociated weekly with Accutase (Sigma). tMVECs and HUVECs (Promocell) were cultured in Endothelial Cell Growth Medium MV2 (Promocell) on gelatine-coated plates (0.2% gelatine, 2 hours 37°). In order to differentiate GBM cells into endothelial-like phenotype, cells were plated on gelatine-coated plate or growth factor reduced matrigel (BD) in the Endothelial Cell Growth Medium and incubated for five days.

Intracranial cell transplantation into nude mice

GBM cultures were stained for CD133 as described below, sorted for 10% of the highest $CD133^+$ and 10% of the $CD133^-$ and resuspended in 3μl PBS containing 5×10^3 cells. Aliquots were injected into the frontal cortex of five- to eight-week-old female nude mice following inhalation of general anesthesia. All animal experiments were approved by the local animal-welfare committee.

Mouse brain fixation

Mice brains were immediately removed from sacrificed mice and fixed in 4% formaldehyde. After fixation, samples were dehydrated by ethanol steps and embedded in paraffin. Brains were sectioned at 6μm thickness and stained for Ki67 as described below.

Senescence-associated β-galactosidase (SA-β-gal) assay

Cells were fixed in 0.2% glutaraldehyde for 5' at RT, washed with PBS, and incubated overnight at 37 °C in a phosphate buffer pH6 containing 5mM $K_3Fe(CN)_6$, 5mM $K_4Fe(CN)_6$, 2mM $MgCl_2$, 150mM NaCl and 1mg/ml X-gal (Fermentas). Cultures were assessed for SA-β-gal content using light microscopy.

Tube formation assay

Growth factor reduced matrigel (BD) was thawed on ice, 500μl per well was added in 24-well plate and incubated at 37°C for 30' to allow matrigel to solidify. tMVECs and GBM cultures were resuspended in endothelial culture medium, added onto solidified matrigel and incubated overnight at 37°C. Next day tubular structures were examined using light microscopy.

Limiting dilution assay (LDA)

Cells were deposited by FACS sorting into ultra-low adhesion 96-well plates (Corning) containing CSC medium. Different lines were plated in different dilutions depending on their clonogenicity, from complete saturation (all wells contained spheres) to complete dilution (none of the wells contained spheres). Plates were scored after two weeks. Medium was refreshed every three days. Frequency of clonogenic cells was calculated using ELDA software: http://bioinf.wehi.edu.au/software/elda/index.html

Co-cultures and measuring absolute cell numbers

tMVEC were grown in 12-well plates in Endothelial Cell Growth Medium until confluence. GBM CSCs were dissociated into single cell suspension and labelled with CFSE (0.5μM CFSE in PBS for 10' at 37°C, Molecular probes) to be distinguishable from tMVECs. $5x10^3$ GBM CSCs were added to each well containing growth-factor free CSC medium, either with or without tMVECs. Next day cells were irradiated with 1x5Gy gamma-irradiation using Cs^{137} source. Dosage-rate was approximately 0.8Gy/minute. TMZ (Sigma) was diluted in DMSO, added same day as cells were irradiated (10, 50 or 100μM TMZ) and refreshed two days later. Three days after the irradiation, samples were measured. Determination of absolute cell numbers: samples were resuspended in 200μl of FACS-buffer (2% BSA/0.01% Na-azide in PBS) containing 1μg/ml of propidium iodide (PI), added to Trucount tubes (BD) containing calibrated beads and cell numbers were determined by FACS, measuring each sample per same number of beads.

Immunocytochemistry

Staining for extracellular markers: Cells were resuspended in FACS buffer containing the antibody and incubated on ice for 30'. After washing with PBS, FACS buffer containing 1μg/ml of PI was added to exclude dead cells, and samples were measured by FACS. The antibodies used: CD133.1-APC (Miltenyi Biotec), CD31-PE (BD), CD105-PE (Invitrogen).

Ki67 staining: Brain sections were deparaffinised, antigens were retrieved by boiling in 10mM sodium citrate buffer pH6 for 10', followed by peroxide blocking (1% H_2O_2 in methanol for 15') and serum blocking, after which anti-human Ki67 antibody (Clone SP6, Thermoscientific) was added and incubated at 4°C overnight. For detection Powervision (Immunologic) and DAB solution (DAKO) were used, and slides were counterstained with haematoxylin.

BrdU staining: Cells were incubated with 10μM BrdU for 1 hour at 37°C and afterwards fixed in 80% ethanol. Staining included 4 steps: cells were incubated in 0.4mg/ml pepsin/0.1N HCl solution for 30', 2N HCl for 30', rat anti-BrdU antibody (Abcam) and anti-rat Alexa-Fluor 647 antibody (Invitrogen) for 1 hour each. First step was performed at RT, the following at 37°C. Antibodies were diluted in 0.1% Tween-20/PBS. Finally, samples were resuspended in FACS buffer containing 50μg/ml PI and measured by FACS.

Cell death measurement

PI exclusion was done by resuspending the samples in FACS buffer containing 1μg/ml PI and measuring by FACS. Nicoletti assay was performed by resuspending the samples in Nicoletti buffer (0.1% sodium citrate, pH7.4/0.1% TritonX-100) containing 50μg/ml PI and keeping them overnight at 4°C. DNA content was determined on FACS. Sub-G_0/G_1 was considered apoptotic; the cellular debris was excluded from the analysis. Specific cell death was calculated using formula: 100×(% experimental cell death − % spontaneous cell death)/(100 − % spontaneous cell death).

Western blot

Cells were lysed with TritonX-100 lyses buffer, and proteins were separated on a SDS/10% polyacrylamide gel and blotted onto transfer membrane (Immobilone-FL, Millipore). Blots were blocked for 1 hour at RT in Odyssey blocking buffer LI-COR (Westburg), diluted in PBS 1:1. Blots were incubated with 1μg/ml anti-p16 antibody (BD) in blocking buffer overnight at 4°C, in IRDye 680 anti-mouse (LI-COR Biosciences) for 1 hour at RT and detected using the Odyssey system.

In vivo detection of (senescent) endothelial cells

FVB/nude mice received a single local irradiation dose of 20 Gy on the right hemisphere of the brain applied as a 5 mm wide beam by -Image Guided Radiotherapy using the X-Rad 225Cx (Precision X-Ray Inc., North Branford, CT, USA). Non irradiated mice were used as a control. After 7 days, the mice were sacrificed.

Tumor specimen was collected after written informed consent, in accordance with the Declaration of Helsinki and after approval by the Academic Medical Center Institutional Review Board (EudraCT2007-005644-24/CCMO NL20411.018.07/NTR 1148).

The samples were frozen ion carbon dioxide and kept at -80°C until further processing.

Cryosections were stained for β-gal and CD31/CD105 as follows: fixation and β-gal staining was performed according to manufacturer's instructions (Millipore. KAA0022RF). Upon peroxide blocking (1%H_2O_2 in methanol 15' RT) and serum blocking, samples were incubated with anti-CD31 (BD, 555444) or CD105 (DAKO, M3527) for 2 hours at RT. Powervision anti-mouse-poly HRP (Immunologic) and DAB (DAKO) were used to detect endothelial cells. Nuclei were counterstained with nuclear red and haematoxylin.

Visualization of staining on GBM samples: Multispectral data sets from slides stained for CD105 and β-gal were acquired using a Nuance camera system (Caliper Life Science/CRiHopkinton, MA) from 420-720 nm at intervals of 20nm. After loading the DAB, β-gal and haematoxylin spectra obtained from single-staining slides, data sets were spectrally unmixed allowing for exclusive visualization of stained cells and conversion of colors. Original staining can be viewed in Supplementary Figure 4f and converted image in Figure 3f.

Conflict of Interest: The authors declare no conflict of interest.

Grant support: Jan Paul Medema is supported by a VICI grant (NWO) and a KWF grant (2009-4416); Martin R. Sprick was partially funded by an EMBO Long-Term Fellowship (ALTF 1063-2005).

Acknowledgments
The authors thank Jan-Jacob Sonke and Alessia Gasparini for setting up the irradiation machine for irradiating mice, Dr. E. Aronica for helping with preparation of GBM samples and Dr. Louis Vermeulen for helpful discussions and critical reading of the manuscript.

References

(1) Giese A, Bjerkvig R, Berens ME, Westphal M. Cost of migration: Invasion of malignant gliomas and implications for treatment. Journal of Clinical Oncology 2003 Apr 15;21(8):1624-36.

(2) Stupp R, Hegi ME, Mason WP, van den Bent MJ, Taphoorn MJB, Janzer RC, et al. Effects of radiotherapy with concomitant and adjuvant temozolomide versus radiotherapy alone on survival in glioblastoma in a randomised phase III study: 5-year analysis of the EORTC-NCIC trial. Lancet Oncology 2009 May;10(5):459-66.

(3) Clarke MF, Fuller M. Stem cells and cancer: Two faces of eve. Cell 2006 Mar 24;124(6):1111-5.

(4) Singh SK, Hawkins C, Clarke ID, Squire JA, Bayani J, Hide T, et al. Identification of human brain tumour initiating cells. Nature 2004 Nov 18;432(7015):396-401.

(5) Clarke MF, Dick JE, Dirks PB, Eaves CJ, Jamieson CH, Jones DL, et al. Cancer stem cells--perspectives on current status and future directions: AACR Workshop on cancer stem cells. Cancer Res 2006 Oct 1;66(19):9339-44.

(6) Bao SD, Wu QL, McLendon RE, Hao YL, Shi Q, Hjelmeland AB, et al. Glioma stem cells promote radioresistance by preferential activation of the DNA damage response. Nature 2006 Dec 7;444(7120):756-60.

(7) Bleau AM, Hambardzumyan D, Ozawa T, Fomchenko EI, Huse JT, Brennan CW, et al. PTEN/PI3K/Akt Pathway Regulates the Side Population Phenotype and ABCG2 Activity in Glioma Tumor Stem-like Cells. Cell Stem Cell 2009 Mar 6;4(3):226-35.

(8) Louis DN, Ohgaki H, Wiestler OD, Cavenee WK, Burger PC, Jouvet A, et al. The 2007 WHO classification of tumours of the central nervous system. Acta Neuropathologica 2007 Aug;114(2):97-109.

(9) Dickson PV, Hamner JB, Sims TL, Fraga CH, Ng CYC, Rajasekeran S, et al. Stem cell-like glioma cells promote tumor angiogenesis through vascular endothelial growth factor. Clinical Cancer Research 2007 Jul 1;13(13):3942-50.

(10) Verhoeff JJ, van TO, Claes A, Stalpers LJ, van Linde ME, Richel DJ, et al. Concerns about anti-angiogenic treatment in patients with glioblastoma multiforme. BMC Cancer 2009;9:444.

(11) Calabrese C, Poppleton H, Kocak M, Hogg TL, Fuller C, Hamner B, et al. A perivascular niche for brain tumor stem cells. Cancer Cell 2007 Jan;11(1):69-82.

(12) Bao SD, Wu QL, Sathornsumetee S, Hao YL, Li ZZ, Hjelmeland AB, et al. Stem cell-like glioma cells promote tumor angiogenesis through vascular endothelial growth factor. Cancer Research 2006 Aug 15;66(16):7843-8.

(13) Wang R, Chadalavada K, Wilshire J, Kowalik U, Hovinga KE, Geber A, et al. Glioblastoma stem-like cells give rise to tumour endothelium. Nature 2010 Dec 9;468(7325):829-U128.

(14) Ricci-Vitiani L, Pallini R, Biffoni M, Todaro M, Invernici G, Cenci T, et al. Tumour vascularization via endothelial differentiation of glioblastoma stem-like cells. Nature 2010 Dec 9;468(7325):824-U121.

(15) Garcia-Barros M, Paris F, Cordon-Cardo C, Lyden D, Rafii S, Haimovitz-Friedman A, et al. Tumor response to radiotherapy regulated by endothelial cell apoptosis. Science 2003 May 16;300(5622):1155-9.

(16) Igrashi K, Sakimoto I, Kataoka K, Ohta K, Miura M. Radiation-induced senescence-like phenotype in proliferating and plateau-phase vascular endothelial cells. Experimental Cell Research 2007 Sep 10;313(15):3326-36.

(17) Borovski T, Verhoeff JJC, ten Cate R, Cameron K, de Vries NA, van Tellingen O, et al. Tumor microvasculature supports proliferation and expansion of glioma-propagating cells. International Journal of Cancer 2009 Sep 1;125(5):1222-30.

(18) Verhaak RGW, Hoadley KA, Purdom E, Wang V, Qi Y, Wilkerson MD, et al. Integrated Genomic Analysis Identifies Clinically Relevant Subtypes of Glioblastoma Characterized by Abnormalities in PDGFRA, IDH1, EGFR, and NF1. Cancer Cell 2010 Jan 19;17(1):98-110.

(19) Hegi ME, Diserens A, Gorlia T, Hamou M, de Tribolet N, Weller M, et al. MGMT gene silencing and benefit from temozolomide in glioblastoma. New England Journal of Medicine 2005 Mar 10;352(10):997-1003.

(20) Romagosa C, Simonetti S, Lopez-Vicente L, Mazo A, Lleonart ME, Castellvi J, et al. p16(Ink4a) overexpression in cancer: a tumor suppressor gene associated with senescence and high-grade tumors. Oncogene 2011 May 5;30(18):2087-97.

(21) Charalambous C, Virrey J, Kardosh A, Jabbour MN, Qazi-Abdullah L, Pen L, et al. Glioma-associated endothelial cells show evidence of replicative senescence. Experimental Cell Research 2007 Apr 1;313(6):1192-202.

(22) Jain RK, di TE, Duda DG, Loeffler JS, Sorensen AG, Batchelor TT. Angiogenesis in brain tumours. Nat Rev Neurosci 2007 Aug;8(8):610-22.

(23) Coppe JP, Patil CK, Rodier F, Sun Y, Munoz DP, Goldstein J, et al. Senescence-Associated Secretory Phenotypes Reveal Cell-Nonautonomous Functions of Oncogenic RAS and the p53 Tumor Suppressor. Plos Biology 2008 Dec;6(12):2853-68.

(24) Rodier F, Coppe JP, Patil CK, Hoeijmakers WAM, Munoz DP, Raza SR, et al. Persistent DNA damage signalling triggers senescence-associated inflammatory cytokine secretion. Nature Cell Biology 2009 Aug;11(8):973-U142.

(25) Kuilman T, Peeper DS. Senescence-messaging secretome: SMS-ing cellular stress. Nature Reviews Cancer 2009 Feb;9(2):81-94.

(26) Krtolica A, Parrinello S, Lockett S, Desprez PY, Campisi J. Senescent fibroblasts promote epithelial cell growth and tumorigenesis: A link between cancer and aging. Proceedings of the National Academy of Sciences of the United States of America 2001 Oct 9;98(21):12072-7.

(27) Rodier F, Campisi J. Four faces of cellular senescence. Journal of Cell Biology 2011 Feb 21;192(4):547-56.

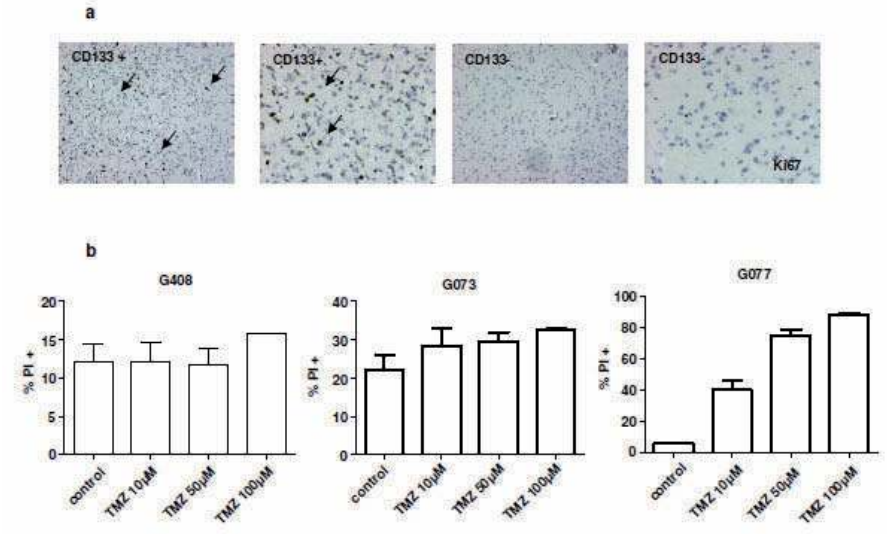

Supplementary Figure 1 (a) 5x10^3 cells of either CD133$^+$ or CD133$^-$ G408 fraction were FACS sorted and intracranial injection into nude mice was performed. Human-specific Ki67 staining was performed to identify scattered, invasive tumor cells (arrows). (b) The response of GBM cells to TMZ; G408, G073 and G077 were treated with 10µM, 50µM and 100µM TMZ respectively, and cell death was determined by PI exclusion. Percentages of PI$^+$ cells are depicted.

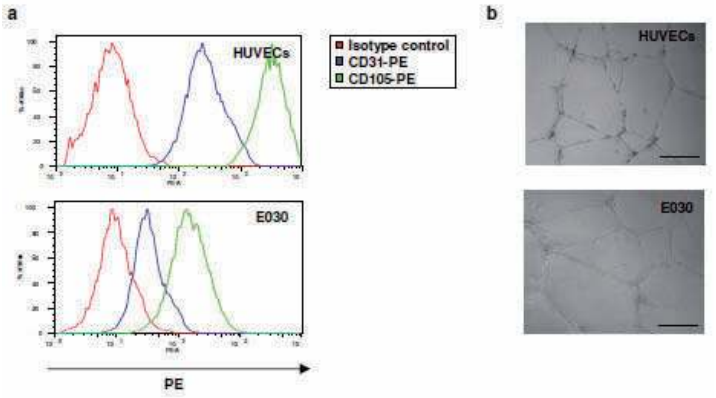

Supplementary Figure 2 (a) Staining for endothelial markers CD31 and CD105 demonstrated positivity in the tMVEC culture E030. HUVECs were used as a positive control. (b) Tube formation assay on E030 demonstrate a formation of tubular patterns, verifying that the tMVEC cultures contain functional endothelial cells. HUVECs were used as a positive control. Scale bars 20µm.

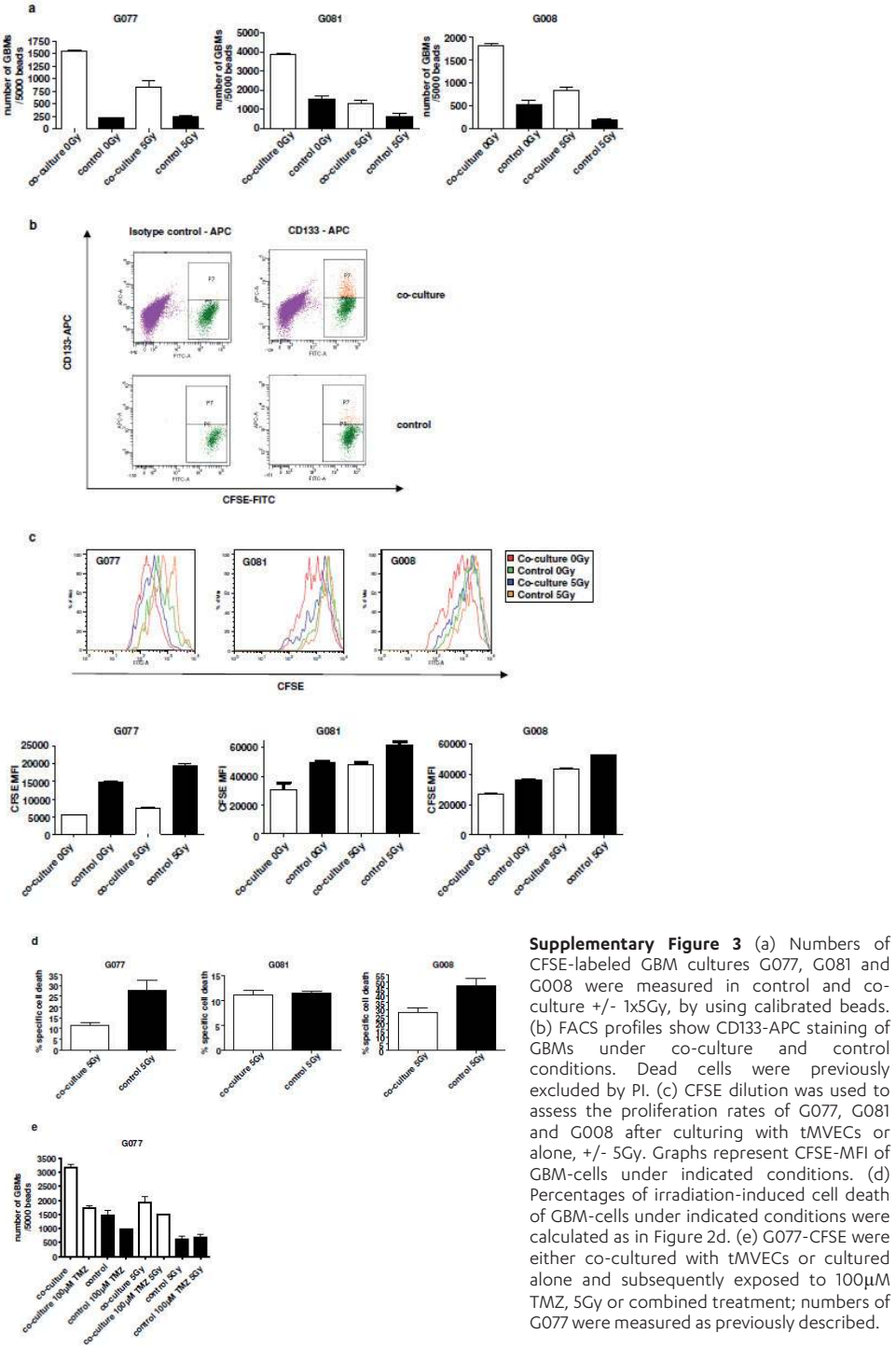

Supplementary Figure 3 (a) Numbers of CFSE-labeled GBM cultures G077, G081 and G008 were measured in control and co-culture +/- 1x5Gy, by using calibrated beads. (b) FACS profiles show CD133-APC staining of GBMs under co-culture and control conditions. Dead cells were previously excluded by PI. (c) CFSE dilution was used to assess the proliferation rates of G077, G081 and G008 after culturing with tMVECs or alone, +/- 5Gy. Graphs represent CFSE-MFI of GBM-cells under indicated conditions. (d) Percentages of irradiation-induced cell death of GBM-cells under indicated conditions were calculated as in Figure 2d. (e) G077-CFSE were either co-cultured with tMVECs or cultured alone and subsequently exposed to 100µM TMZ, 5Gy or combined treatment; numbers of G077 were measured as previously described.

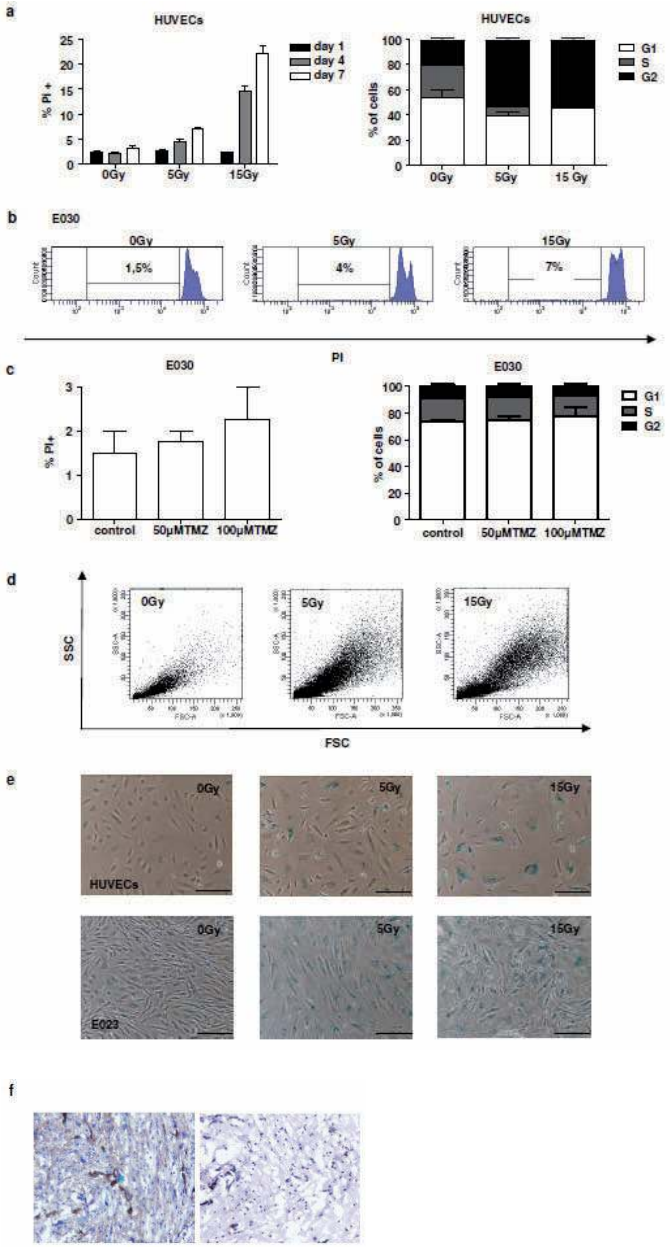

Supplementary Figure 4 (a) Graphs show percentages of PI⁺ HUVECs one/four/seven days after irradiation (left graph); cell cycle distribution was analyzed by BrdU incorporation one week after the treatment (right graph). (b) Nicoletti assay on E030 five days after irradiation, showing the percentage of DNA fragmentation and cell cycle distribution. (c) E030 were treated with 50µM or 100µM TMZ and cell death, measured by PI exclusion (left graph) together with BrdU cell cycle analysis (right graph) was conducted on day one/four/seven after the treatment; results from day seven are depicted on the figure; of note, there was no difference in results between the different days. (d) FACS profiles demonstrate change in light-scatter (SSC/FSC) profile of E030 after irradiation. (e) β-gal assay was conducted on E023 and HUVECs a week after irradiation; senescent cells are blue. Scale bars 20µm. (f) Biopsy of GBM patient irradiated with 60Gy was co-stained for CD105 (dark brown) and β-gal (light blue). Nuclei were counterstained with haematoxylin.

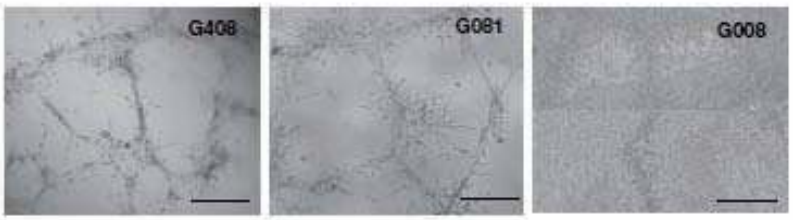

Supplementary Figure 5 G408, G081 and G008 GBM-cells demonstrate tube forming ability under endothelial differentiation conditions, comparable to tMVECs.

7

Tumor Microvascular Endothelial Cells Restore Stem-Like Features In Non-Stem Glioblastoma Cells

Tijana Borovski and Jan Paul Medema

Laboratory for Experimental Oncology and Radiobiology (LEXOR), Center for Experimental and Molecular Medicine (CEMM), Academic Medical Center (AMC), University of Amsterdam, Meibergdreef 15, 1105 AZ, Amsterdam, The Netherlands

Work in progress

Abstract

Glioblastoma multiforme (GBM) is a fast growing, primary malignant brain tumor with poor clinical outcome. GBM cancer stem cells (CSCs) have recently been identified as a significant factor in cancer maintenance and progression, as they have the exclusive ability to serially propagate tumors in xenograft models and furthermore contribute to therapy resistance and tumor angiogenesis unlike the rest of the tumor bulk. Within the tumor, the CSC fraction is mainly located in their vascular niche, essential for maintaining their undifferentiated state and self renewal. We now extend this knowledge to the role of tumor vasculature in regulating tumor cell plasticity. We show that tumor endothelial cells have the ability to promote a stem-like phenotype in the non-stem fraction, assessed by marker expression and increased neurosphere formation. This finding underscores the importance of developing therapeutics that will target the tumor microenvironment in addition to CSCs.

Introduction

Glioblastoma multiforme (GBM) is a nearly universally lethal, heterogeneous primary brain tumor. Florid angiogenesis and pseudopallisading necrosis are defining hallmarks of this cancer. The prognosis for this malignancy has remained poor despite the aggressive treatments, with the 5-year survival rate of 10% (1). The maximal surgical resection combined with the irradiation is the most efficient therapy for GBM. Nevertheless, these treatments are providing only palliation. Radiation has a limited efficiency due to the resistance and survival of small fraction of tumor cells, named cancer stem cells (CSCs) (1). They share numerous features with normal stem cells, such as expression of stem cell markers, self renewal capacity and long term proliferation, and the ability to differentiate into multiple lineages (neurons, astrocytes and oligodendrocytes). However, in contrast to normal stem cells, CSCs carry numerous mutations and chromosomal aberrations and can serially propagate tumors that phenotypically resemble the original malignancy. Being the clonogenic and tumorigenic fraction of tumor cells and the most therapy resistant, CSCs are believed to be the driving force of tumor regrowth after treatment (1, 2). Accordingly, GBMs almost inevitably recur after the treatment and frequently do so in a nodular pattern which suggests a clonal source of tumor regrowth, consistent with the CSC hypothesis.

Since CSCs have been implicated in tumor growth and its resistance to conventional treatments, recent research heavily focused on elucidating the molecular pathways and factors that regulate CSC maintenance and survival. One of the main sites of regulation are distinct areas inside a tumor termed CSC niche that extrinsically regulates this fraction of cells. Neural stem cells are located in a complex, vascular environment essential for their maintenance in an undifferentiated state, their self renewal and regulation of asymmetric divisions (3). GBM CSCs reside in a similar perivascular niche that orchestrates their cell fate decisions and consequently sustains the CSC pool (4). In addition to their maintenance, this interaction seems to provide a survival advantage for CSCs after treatment, thus creating a possibility for them to repopulate the tumor. CSCs are therefore highly dependent on their niche. They secrete the pro-angiogenic factor VEGF that stimulates endothelial cell growth and expansion of the surrounding vasculature (5). In turn, endothelial cells maintain CSCs by expressing Notch ligands and nitric oxide that subsequently activate the Notch signaling pathway (6, 7). Furthermore, this bidirectional communication is protecting both sides from various DNA-damaging insults such as irradiation (8, 9). Thus, when talking about the CSC niche, we are referring to a rather complex crosstalk between CSCs and tumor microvasculature with direct implications for the clinic.

Even though differentiation of cells was for decades considered to be the point of no return, recent evidence is suggesting the opposite and proposing a certain level of plasticity of this process. A turning point in the field was the work of Takahashi *et al*. who demonstrated that fully differentiated fibroblasts can be reprogrammed by defined factors, Oct3/4, Sox2, c-Myc and Klf4 into fully functional pluripotent stem cells (10, 11). Compared to normal, healthy tissues, tumor

cells are believed to have a much higher potential with respect to plasticity. GBM CSCs are one example of tumor cells with this capacity. Ricci-Vitiani *et al*. and Wang *et al*. recently demonstrated that GBM CSCs can differentiate into an endothelial-like phenotype, both *in vitro* and *in vivo*, and thus contribute to tumor angiogenesis (12, 13). This was done by identifying endothelial cells in GBM vasculature that carry tumor-specific chromosomal aberrations, suggesting that they originate from tumor cells. Importantly, this work strongly implies that, when critical microenvironmental components are lacking, CSCs are able to differentiate into required cell type by intrinsic lineage plasticity.

In light of current knowledge on the CSC niche, it can be hypothesized that CSC differentiation and de-differentiation can be influenced and directed by environmental cues. Recent data demonstrated this to be the case for some factors such as hypoxia. GBM CSCs are enriched in hypoxic regions, defined by low oxygen tension, and hypoxia-inducible factors (HIFs), HIF-2α in particular, are involved in their maintenance (14). Strikingly, HIF2α was able to convert differentiated GBM cells into a more stem-like phenotype, promoting cell growth and self renewal (15). Other external factors were also suggested to play a similar role. For example, acidic stress was also implicated in influencing the plasticity of GBM cells towards a CSC-like phenotype (16). We now extend these studies to the tumor microvasculature. Our results show that the perivascular GBM CSC niche is also capable of promoting stem-like features in a non-stem population, up-regulating the expression of CSC-related marker CD133 and increasing neurosphere forming capacity, thus adding an additional layer of complexity to the CSC microenvironmental interplay.

Results

Endothelial cells stimulate expression of CSC marker CD133 in negative population

GBM CSCs have been identified using several markers the most common being CD133. Tumor cells with an immature phenotype expressing the cell surface marker CD133 have been demonstrated by us and others to have the exclusive capacities to self-renew, differentiate and transplant the malignancy into nude mice (2) (Chapter 6). Thus, to address the question as to whether tumour microvascular endothelial cells (tMVECs) can induce stem-like features in non-stem GBM cells, we first focused on the expression of CD133. The main question we wanted to address is whether CD133, a marker for GBM CSCs, can be re-expressed by differentiated tumour cells under the influence of tMVECs.

Thus, we sorted CD133 positive and negative fractions from a GBM culture ($CD133^+$ and $CD133^-$), as shown in Figure 1a, and plated them either on top of tMVECs or in conditioned medium derived from tMVECs cultures, in addition to the control. GBM cells were CFSE labelled to be able to distinguish them from tMVECs. After three days of culture, samples were stained for CD133 in order to investigate if the expression of CD133 had changed in the presence of tMVECs. Our results

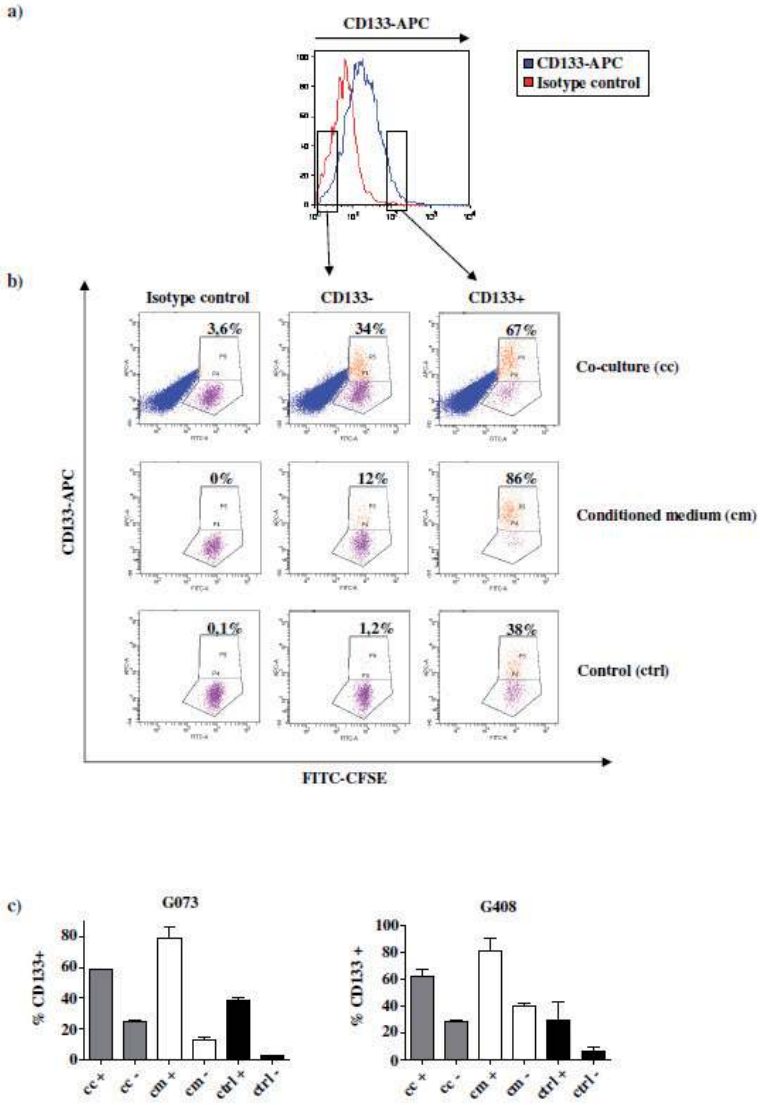

Figure 1. tMVECs can restore CD133 expression in the negative fraction of GBM cells a) GBM cells were stained for CD133 and sorted for 10% high expressing and negative fraction ($CD133^+$ and $CD133^-$). b) Immediately upon sorting, GBM cells were plated either on top of tMVEC monolayer for co-culture (cc), in tMVECs conditioned medium (cm) or as a control (ctrl). 72 hours later, CD133 staining was repeated. FACS profiles show representative staining. c) Quantification of CD133 positive fraction under indicated conditions is depicted in the graphs. + and – stand for initially sorted $CD133^+$ and $CD133^-$ fraction. Experiment was done for two different GBM cultures, G073 and G408.

show that, in addition to maintaining the initial $CD133^+$ CSC fraction, tMVECs were also able to significantly increase the frequency of $CD133^+$ cells in the initially negative population, suggesting the shift of non-stem GBM cells towards a stem-like phenotype (Figure 1b, c). This effect was

consistent for all the GBM cultures tested, demonstrating it to be a more general effect of tMVECs.

Endothelial cells promote self-renewal capacity in CD133 negative fraction

Self renewing ability is one of the main criteria for defining the CSC as such. To investigate whether the clonogenic capacity can also be reacquired under the influence of tMVECs, we examined the sphere forming ability of the $CD133^-$ fractions in the presence of tMVECs-derived factors (Figure 2). Cells were sorted as described previously. $CD133^+$ and $CD133^-$ fractions were plated for a limiting dilution assay and incubated for two weeks to allow sphere formation.

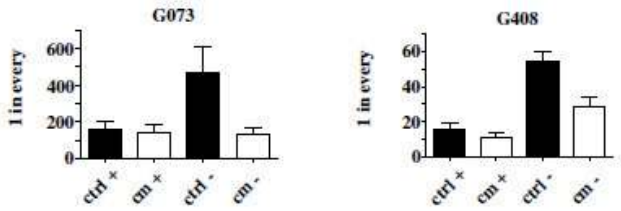

Figure 2. tMVECs can install self renewing capacity in poorly clonogenic GBM cells; A limiting dilution assay was performed on sorted $CD133^+$ and $CD133^-$ fraction of G073 and G408 cultures. Cells were cultured either in tMVECs conditioned medium (cm) or fresh CSC medium (ctrl). + and - refers to $CD133^+$ and $CD133^-$ fraction. The clonogenic potential of each fraction under indicated conditions is depicted on the graphs.

The $CD133^+$ fraction displayed, as expected, the highest clonogenicity regardless of the conditions, while $CD133^-$ cells had significant lower clonogenic capacity. Strikingly, the $CD133^-$ fraction demonstrated an increased clonogenic capacity when cultured in tMVEC conditioned medium (Figure 2). Thus, tMVECs seem to be able to convert differentiated GBM fraction to less differentiated state according to marker expression and acquisition of stem-like behaviour.

Materials and Methods

Cell culture

GBM CSCs and tMVECs were isolated from patient material as described previously (17). Cells were cultured under the following conditions, further referred to as CSC medium: Advanced DMEM/F12 medium (Invitrogen) supplemented with N2 supplement (Invitrogen), 2mM glutamine, 0,3% glucose, 100uM beta-Mercaptoethanol, Trace-Elements B and C (VWR), 5mM HEPES, 2ug/ml heparine, lipid mixture (Sigma) , 25ug/ml insulin, 50 ng/ml h-bFGF and 20ng/ml h-EGF (Peprotech) in ultra low attachment flasks (Corning). Growth factors were supplemented twice weekly and spheroids were dissociated weekly with Accutase (Sigma). tMVECS were cultured in Endothelial Cell Medium MV2 (Promocell) on gelatine-coated plates (Greiner Bio-One).

Immuno-fluorescence and co-culture/conditioned medium experiments

CSC cultures were dissociated using accutase and filtered through 40μm pore size cell strainer to get single cell suspension. They were incubated with CD133.1-APC (Miltenyi Biotec) antibody for 25 minutes and sorted for 10% of the highest CD133 expressing fraction and CD133 negative fraction ($CD133^+$ and $CD133^-$). Dead cells were excluded with propidium iodide. Immediately after sorting, GBM cells were labeled with CFSE (0.5μM CFSE in PBS for 10 minutes at 37°C, Molecular probes), to be distinguishable from tMVECs, and plated either on top of tMVEC monolayer, in tMVECs conditioned medium (conditioned for 24h) or in a control medium. In all these conditions, we used CSC medium without the addition of bFGF or EGF. Three days later, cells were harvested and CD133 staining was again performed and analyzed by Flow cytometry.

Clonogenic assays

Positive and negative fractions of CD133.1-APC labeled GBM cells were FACS deposited for limiting dilution assay. Cells were plated in low-attachment 96-wells plates (Corning) at ascending clonal densities, from complete saturation to complete dilution, and incubated either in a fresh CSC medium or in a CSC medium previously incubated with tMVECs for 24h. Fresh medium was added every three days. Plates were scored two weeks later. Clonogenicity was determined using Extreme Limiting Dilution Analysis (ELDA) software: http://bioinf.wehi.edu.au/software/elda/index.html

Discussion

For the last few decades, major effort has been invested into development of more efficient treatment for GBM. Nevertheless, despite all novel therapeutics, there is a very limited increase in the lifespan of patients. The refractory nature of the tumor still provides a challenge for the treatment and this disease to date remains incurable. The recurrence of GBM has mainly been attributed to the small fraction of CSCs able to survive the treatment and subsequently repopulate the tumor (1). The maintenance of this fraction, however, is primarily enabled by their supportive microvascular environment (4). The cues from the niche are critical for the CSC self renewal and survival.

Increasing data are suggesting that cells, tumor cells in particular, possess a certain level of plasticity and can revert from a differentiated state into a less differentiated phenotype. It remains a matter of debate if this ability of cells is regulated intrinsically or by microenvironmental cues. Gupta *et al*. recently proposed that, in contrast to normal stem cells that require their niche for this kind of regulation, cancer cells can stochastically enter a stem-like phenotype due to their genetic changes alone (18). Although ability of tumor cells to revert to a less differentiated state could be, at least in part, an intrinsic feature, recent data demonstrate however this process to be

significantly influenced and supported by the microenvironment. For example, in colon cancer the microenvironment was shown to be critical for this step. HGF secreted by surrounding myofibroblasts was the key factor in restoring a CSC phenotype in non-stem tumor cells, demonstrated both *in vitro* and *in vivo* (19). Even in the previously mentioned paper by Gupta *et al.* some experiments suggest that the microenvironment is not a completely irrelevant factor in this process. More specifically, when testing for tumor seeding ability, the cancer stem cell fraction was successful in initiating new tumors, however the differentiated tumor cells were also capable of inducing tumors provided so-called carrier cells were co-injected (18). Even though carrier cells alone did not have tumorigenic potential, they could potentially provide a preferable surrounding and factors necessary for differentiated tumor cells to revert to cancer stem-like cells.

Here we demonstrate that tumor microvascular endothelial cells can play a similar role in GBM, namely regulate cell differentiation and plasticity by restoring the stem-like phenotype in differentiated fraction of GBM cells, resulting in the enrichment of CSC pool. What are the clinical implications of this finding? Considering all the current knowledge on CSC therapy resistance, a lot of effort is being invested into development of CSC targeted therapies. Our results suggest, however, that targeting only CSCs might be insufficient due to their complex cross-talk with the microvasculature. Under the influence of their niche, differentiated tumor cells could potentially re-acquire stem cell features and re-establish the CSC pool to maintain tumor cell homeostasis. Thus finding a way to target the CSCs through treatment modalities designed to intersect the effects of the tumor surrounding might be essential for development of effective therapies.

Reference List

(1) Bao SD, Wu QL, McLendon RE, Hao YL, Shi Q, Hjelmeland AB, et al. Glioma stem cells promote radioresistance by preferential activation of the DNA damage response. Nature 2006;444:756-60.

(2) Singh SK, Hawkins C, Clarke ID, Squire JA, Bayani J, Hide T, et al. Identification of human brain tumour initiating cells. Nature 2004;432:396-401.

(3) Shen Q, Goderie SK, Jin L, Karanth N, Sun Y, Abramova N, et al. Endothelial cells stimulate self-renewal and expand neurogenesis of neural stem cells. Science 2004;304:1338-40.

(4) Calabrese C, Poppleton H, Kocak M, Hogg TL, Fuller C, Hamner B, et al. A perivascular niche for brain tumor stem cells. Cancer Cell 2007;11:69-82.

(5) Bao SD, Wu QL, Sathornsumetee S, Hao YL, Li ZZ, Hjelmeland AB, et al. Stem cell-like glioma cells promote tumor angiogenesis through vascular endothelial growth factor. Cancer Research 2006;66:7843-8.

(6) Charles N, Ozawa T, Squatrito M, Bleau AM, Brennan CW, Hambardzumyan D, et al. Perivascular Nitric Oxide Activates Notch Signaling and Promotes Stem-like Character in PDGF-Induced Glioma Cells. Cell Stem Cell 2010;6:141-52.

(7) Zhu TS, Costello MA, Talsma CE, Flack CG, Crowley JG, Hamm LL, et al. Endothelial Cells Create a Stem Cell Niche in Glioblastoma by Providing NOTCH Ligands That Nurture Self-Renewal of Cancer Stem-Like Cells. Cancer Research 2011;71:6061-72.

(8) Brown CK, Khodarev NN, Yu JQ, Moo-Young T, Labay E, Darga TE, et al. Glioblastoma cells block radiation-induced programmed cell death of endothelial cells. Febs Letters 2004;565:167-70.

(9) Hovinga KE, Shimizu F, Wang R, Panagiotakos G, van der Heijden M, Moayedpardazi H, et al. Inhibition of Notch Signaling in Glioblastoma Targets Cancer Stem Cells via an Endothelial Cell Intermediate. Stem Cells 2010;28:1019-29.

(10) Takahashi K, Yamanaka S. Induction of pluripotent stem cells from mouse embryonic and adult fibroblast cultures by defined factors. Cell 2006;126:663-76.

(11) Takahashi K, Tanabe K, Ohnuki M, Narita M, Ichisaka T, Tomoda K, et al. Induction of pluripotent stem cells from adult human fibroblasts by defined factors. Cell 2007;131:861-72.

(12) Ricci-Vitiani L, Pallini R, Biffoni M, Todaro M, Invernici G, Cenci T, et al. Tumour vascularization via endothelial differentiation of glioblastoma stem-like cells. Nature 2010;468:824-U121.

(13) Wang R, Chadalavada K, Wilshire J, Kowalik U, Hovinga KE, Geber A, et al. Glioblastoma stem-like cells give rise to tumour endothelium. Nature 2010;468:829-U128.

(14) Li Z, Bao S, Wu Q, Wang H, Eyler C, Sathornsumetee S, et al. Hypoxia-Inducible Factors Regulate Tumorigenic Capacity of Glioma Stem Cells. Cancer Cell 2009;15:501-13.

(15) Heddleston JM, Li ZZ, McLendon RE, Hjelmeland AB, Rich JN. The hypoxic microenvironment maintains glioblastoma stem cells and promotes reprogramming towards a cancer stem cell phenotype. Cell Cycle 2009;8:3274-84.

(16) Hjelmeland AB, Wu Q, Heddleston JM, Choudhary GS, MacSwords J, Lathia JD, et al. Acidic stress promotes a glioma stem cell phenotype. Cell Death and Differentiation 2011;18:829-40.

(17) Borovski T, Verhoeff JJC, ten Cate R, Cameron K, de Vries NA, van Tellingen O, et al. Tumor microvasculature supports proliferation and expansion of glioma-propagating cells. International Journal of Cancer 2009;125:1222-30.

(18) Gupta PB, Fillmore CM, Jiang GZ, Shapira SD, Tao K, Kuperwasser C, et al. Stochastic State Transitions Give Rise to Phenotypic Equilibrium in Populations of Cancer Cells. Cell 2011;146:633-44.

(19) Vermeulen L, Melo FDSE, van der Heijden M, Cameron K, de Jong JH, Borovski T, et al. Wnt activity defines colon cancer stem cells and is regulated by the microenvironment. Nature Cell Biology 2010;12:468-U121.

8

Chromatin Mobility Is Increased At Sites of DNA Double-Strand Breaks

P.M. Krawczyk[1], T. Borovski[2*], J. Stap[1*], A. Cijsouw[3], R. ten Cate[2], J.P. Medema[2], R. Kanaar[4,5], N.A.P. Franken[2], J.A. Aten[1]

1 van Leeuwenhoek Centre for Advanced Microscopy-AMC, Department of Cell Biology & Histology, 2 Laboratory for Experimental Oncology and Radiobiology, Center for Experimental and Molecular Medicine and Department of Radiotherapy, Academic Medical Center, University of Amsterdam, Meibergdreef 15, 1105 AZ, Amsterdam, The Netherlands , 3 Department of Functional Genomics, Center for Neurogenomics and Cognitive Research, Vrije Universiteit Amsterdam, De Boelelaan 1087, 1081 HV, Amsterdam, The Netherlands, 4 Department of Cell Biology & Genetics, Cancer Genomics Center, 5 Department of Radiation Oncology, Erasmus Medical Center, PO Box 2040, 3000 CA, Rotterdam, The Netherlands

* These authors contributed equally to this work

JCS, accepted for publication December 2011

Abstract

DNA double-strand breaks (DSBs) can efficiently kill cancer cells, but they can also produce unwanted chromosome rearrangements (CRs) when DNA ends from different DSBs are erroneously joined. Movement of DSB-containing chromatin domains might facilitate these DSB interactions and promote formation of CRs. We, therefore, analyzed the mobility of DSB-containing chromatin domains in living mammalian cells and compared it to the mobility of non-damaged chromatin on a time-scale relevant for DSB repair. We found that DSB-containing chromatin domains are significantly more mobile than intact chromatin and capable of roaming a more than 2-fold larger area of the cell nucleus. Moreover, this increased DSB mobility, but not mobility of undamaged chromatin, can be reduced by agents that affect higher-order chromatin organization.

Introduction

Most anticancer therapies induce multiple DSBs to kill cancer cells but concurrent induction of DSBs in non-tumor cells can result in CRs that may be a source of new, therapy-related tumors in treated patients (Allan & Travis, 2005; Stephens *et al.*, 2011). DSBs represent the most challenging type of DNA damage (Suzuki *et al.*, 2003). A failure to rejoin DSBs leads to cell death, whereas joining of DNA ends originating from different DSBs results in structural chromosome rearrangements (CRs). The mechanisms that control CR formation are a subject of ongoing debate. One of the favored theories postulates interactions between separately generated DSBs followed by incorrect joining of DSB ends. Accordingly, DSB proximity and movement would be factors that are crucial to the process.

The cellular response to DSBs starts with a complex signaling cascade leading to alterations in organization and composition of large mega-base chromatin domains surrounding the breaks (Murr *et al.*, 2006; Rogakou *et al.*, 1999; Ziv *et al.*, 2006; van Attikum & Gasser, 2005). Such a large-scale reorganization could affect chromatin mobility. Experiments with yeast and mammalian cells all indicate that DSB-containing chromatin domains (referred to as ionizing-radiation induced foci, or IRIF) are mobile in the micrometer range (Aten *et al.*, 2004; Kruhlak *et al.*, 2006; Soutoglou *et al.*, 2007).

Accurate description of the behavior of unrepaired DSBs in the cell nucleus, and of their mobility in particular, is of key importance in understanding how DSB interactions may be initiated. If DSB motility does play a role in CR formation, the ability to manipulate their movement might reduce dangerous side-effects of anti-cancer therapy. To obtain detailed insight in the nature of DSB movement, we analyzed the mobility of IRIF in living mammalian cells and compared it to the mobility of non-damaged chromatin domains, telomeres and centromeres. We also investigated the involvement of various chromatin and repair-related processes in DSB movement with the aim to reduce DSB mobility.

Results and discussion

Visualization of chromatin domains

Undamaged chromatin domains in U2OS cells, roughly 1 Mb in size, were visualized by incorporation of the fluorescent nucleotide analogue Cy3-dUTP (Figure 1a) (Pliss *et al.*, 2009). The mobility of fluorescently labeled, capped telomeres was measured in U2OS cells transiently transfected with a TRF1-dsRED expression construct (Figure 1b) and the mobility of centromeres in U2OS cells stably expressing the centromeric factor CENPB-GFP (Figure 1c) (Shelby *et al.*, 1996). To analyze the mobility of DSB-containing chromatin we studied IRIF in -irradiated U2OS cells

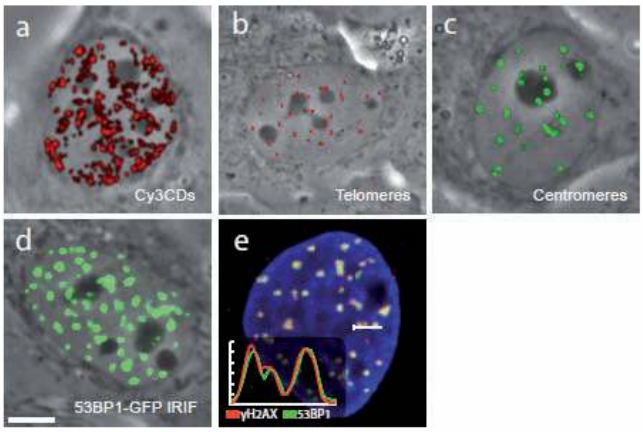

Figure 1. Visualization of intact and DSB-containing chromatin domains in U2OS cells. (a), intact chromatin domains labeled with Cy3-dUTP (red). (b), cells with telomeres labeled by TRF1-mCherry construct (red). (c), cells with centromeres labeled by CENP-B-GFP construct (green). (d), cells expressing 53BP1-GFP (green), exposed to 5Gy of -radiation, and fixed 30 min later. (e), cells treated as in (d), additionally stained for H2AX (red). Inset shows intensity profile of a single confocal scan measured along the white bar. Scale bar – 5μm

expressing 53BP1-GFP fusion protein (Figure 1d) (Bekker-Jensen *et al.*, 2005). 53BP1-GFP forms IRIF that co-localize with H2AX in nuclei of irradiated cells (Figure 1e).

Functionally distinct chromatin domains have diverse motilities

To illustrate movement of chromatin domains, we first plotted 2D trajectories of 100 randomly selected domains as emerging from the same origin in the XY plane (Figure 2a). Our analysis revealed that IRIF are significantly more mobile than Cy3-labeled chromatin domains (Cy3CDs) and centromeres (Figure 2). At the end of the 60 min observation period the roaming range of the IRIF, expressed as mean square displacement (MSD), had increased 1.7-fold relative to the Cy3CD MSD and the nuclear area roamed by the DSB was 2.2-fold higher (the nuclear area is proportional to $(MSD)^{3/2}$). The average stepsize (S) covered by the IRIF during 2 min intervals was approximately 20% larger than S of Cy3CDs (Figure 2). IRIF mobility measured in normal human fibroblasts was also higher than the mobility of Cy3CDs, indicating that increased IRIF mobility is a general phenomenon, rather than a cell-line specific effect (Supplementary figure 1c). We analyzed the mobility of foci marking DSBs induced by the topoisomerase II inhibitor etoposide (Osheroff, 1989). Etoposide, a frequently used anti-cancer drug, promotes the formation of CRs that can lead to specific types of leukemia. Etoposide-induced foci showed 2.2- and 3.2-fold increases in MSD and the nuclear area roamed, as compared to Cy3CDs (Supplementary Figure 1). The etoposide induced foci disappeared faster than IRIF signals and could be followed for 40 min only. A more detailed analysis showed that local damage did not globally influence chromatin mobility, as a

dose of 10 Gy of radiation did not enhance the mobility of Cy3CDs (Supplementary figure 2). Centromeres displayed a mobility similar to that of Cy3CDs. Telomeres, on the other hand, were as mobile as IRIF. Previous observations also indicated relatively high mobility of telomeres (Molenaar *et al.*, 2003; de Vos *et al.*, 2009), which might stem from the fact that ends of chromosomes are attached to the bulk of chromatin by 1 chromatin fiber only, in contrast to other chromatin domains. It should be noted that the mobility of telomeres in U2OS cells might be altered by activity of the ALT telomere maintenance pathway, hallmarked by telomeric -H2AX or 53BP1 foci (Cesare *et al.*, 2009). Although we cannot completely exclude the possibility, we did not observe the classical signs of telomere dysfunction in the cell line used for our study. Another strong indication that telomere mobility measured in our study is not affected by their ALT-state comes from the study of De Vos *et al.*, who reported nearly identical mobility of telomeres in ECV-304, a non-ALT cell line, (derivative of the human bladder carcinoma, de Vos *et al.*, 2009).

Interestingly, most MSD curves of the analyzed chromatin domains did not reach plateau within 60 min, likely indicating that the full range of local movement of the domains is not reached within this time period. Alternatively, this might be explained by the long time-scale drift of large chromosome territories (Zink *et al.*, 1998).

Some of the chromatin domains analyzed here differ in size, with IRIF and centromeres being ≈1 μm in diameter, telomeres and Cy3CDs roughly half that size, which might influence direct comparison in two ways. First, the domain size might influence the calculation of its position. However, to calculate domain positions we used the intensity-based center of gravity, a parameter insensitive to object size. Second, the domain mobility is likely to be influenced by its size due to physical constraints imposed by chromatin organization. However, our results indicate that in the case of IRIF other factors play more significant role. Accordingly, data in figure 2 show that while IRIF display mobility similar to telomeres which are much smaller, the mobility of IRIF is larger than that of Cy3CDs.

Results of our analysis contrast with conclusions drawn by Kruhlak et al (2006). In their experiments the mobility of chromatin pre-sensitized by Hoechst and damaged by laser UV light was similar to that of intact chromatin, when measured over a 20 min period. This comparison was based on analysis of the dynamics of relatively large chromatin regions. Random movements of individual DSBs within these regions could have partly canceled out, resulting in a lower overall mobility compared to the mobility of the individual IRIF analyzed in our experiments. An alternative explanation could be that the mobility of DSBs varies depending on the type of treatment used to induce DNA damage. Our observation that DSBs produced by the topoisomerase II inhibitor etoposide are significantly more mobile than DSBs induced by ionizing radiation demonstrates that this is indeed possible. Kruhlak *et al.* (2006) also published data on

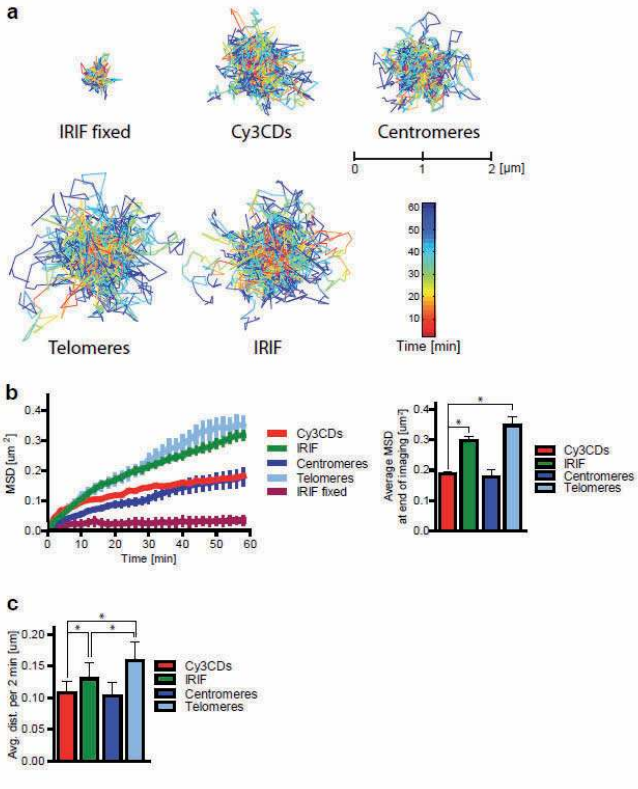

Figure 2. Mobility of the DSB-containing and intact chromatin domains. (a), 100 randomly selected trajectories, depicting movement of the indicated type of chromatin domains during 60 min, were plotted as originating from the same point on the 2D plane. The color of the segments of the trajectories represents time after the start of imaging. (b), MSD of the indicated types of chromatin domains. Bar graph shows MSD of the respective domains averaged over the last 3 time points. (c), average distance covered by the indicated type of chromatin domains per 2 min interval. Asterisks indicate statistical significance with $p < 0.05$, assessed using the student t-test. Error bars represent SEM. At least 30 cells and at least 5 foci per cell were analyzed per data series.

mobility of 53BP1-GFP IRIF in U2OS cells. The mobility of 53BP1-GFP IRIF reported in this study was higher than measured here (MSD of 0.9 m^2 after 50 min, compared to approximately 0.3 m^2) but absence of corresponding data on mobility of non-damaged chromatin in their study hampers direct comparison with our results and conclusions.

To exclude the possibility that the observed effects are caused by fluorescence imaging conditions, we tested the toxicity of the illumination regimes. Neither fluorescence imaging nor irradiation induced significant cytotoxicity during the observation period, as confirmed by prolonged time-lapse, phase-contrast observation of illuminated and/or irradiated cells (Supplementary materials and methods).

IRIF motility depends on chromatin organization and varies with cell cycle phase

A wealth of data indicates that the presence of DSBs leads to local chromatin relaxation, possibly to admit repair factors to the damaged DNA, e.g. (Falk *et al.*, 2007; Ziv *et al.*, 2006). It is tempting to speculate that low-density chromatin would be more mobile than condensed chromatin. Chromatin relaxation might then provide a straightforward, elegant, explanation for the increased mobility of IRIF. In our experiments de-condensed euchromatic Cy3CDs in desynchronized cells

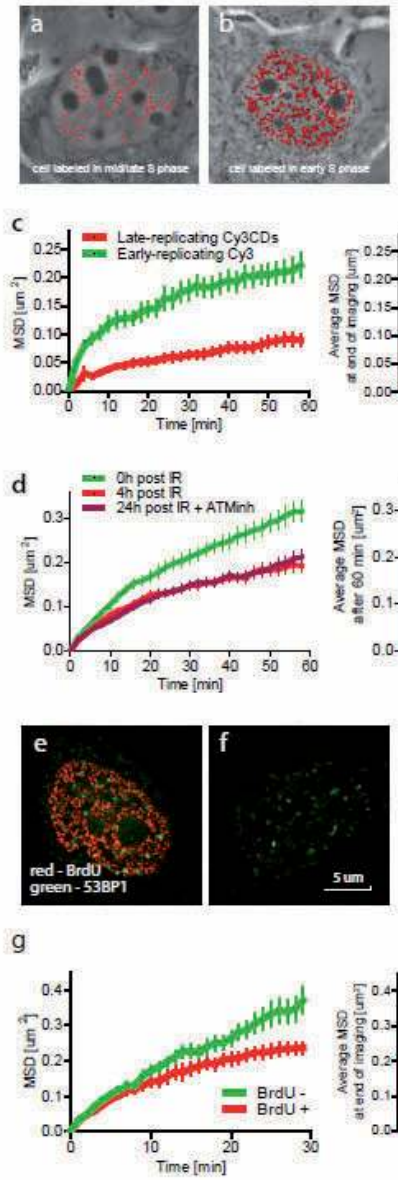

displaying early-S phase labeling patterns (Figure 3b) were more mobile than the condensed heterochromatic Cy3CDs in cells displaying mid/late-S phase patterns (Figure 3a, c). This is in agreement with previously published results (Pliss *et al.*, 2009). The affirmation that relaxation increases the mobility of non-damaged chromatin motivated us to investigate the effect of chromatin condensation on IRIF movement.

In order to test the influence of chromatin organization on the mobility of DSBs, we focused on a small fraction of persistent IRIF that could be traced up to 4h after irradiation and on IRIF persisting 24h after irradiation in cells incubated with ATM inhibitor Ku55933, as these lasting DSBs are frequently associated with heterochromatic regions (Goodarzi *et al.*, 2008). Our results show that heterochromatin-associated persistent IRIF were, indeed, significantly less mobile (≈40%) compared to randomly distributed IRIF imaged early after irradiation (Figure 3d), in agreement with the hypothesis that chromatin relaxation is one of the factors leading to enhanced IRIF mobility.

In addition to the epi-genetically determined differences between eu- and hetero-chromatin, nuclear chromatin undergoes

Figure 3. Mobility of eu- versus heterochromatin domains and cell cycle effect. (a, b), Cy3CDs in cells labeled in mid/late (a) or early (b) S-phase and fixed 48 h later. (c), MSD of Cy3CDs in cells labeled in mid/late or early S-phase. Cells were analyzed 48h post labeling. (d), MSD of IRIF imaged immediately after irradiation (green), of persistent IRIF imaged 4 h after exposing cells to -radiation (red) and of IRIF 24h after irradiation in cells incubated in the presence of ATM inhibitor Ku55933 (purple). Bar graph shows MSD averaged over last 3 time points. Asterisks indicate statistical significance with $p < 0.05$, assessed using the student t-test. Error bars represent SEM. At least 30 cells were analyzed per data series. (e-g), Cells expressing 53BP1-GFP were irradiated, imaged for 60 min and then incubated for 5 min in the presence of BrdU to label cells undergoing DNA replication. (e) BrdU pattern of cells in S-phase undergoing DNA replication. (f), No BrdU incorporation in $G_1/G_0/G_2$ cells. (g), MSD of IRIF in BrdU-positive (replicating) cells (red) and BrdU-negative (non-replicating) cells (green). Bar graph shows MSD averaged over last 3 time points. Asterisk indicates statistical significance with $p < 0.05$, assessed using the student t-test. Error bars represent SEM. At least 30 cells and at least 5 foci per cell were analyzed per data series.

dramatic changes during cell cycle progression (Chuang & Belmont, 2007). We therefore examined the cell cycle dependence of IRIF mobility. In these experiments we incubated cells with thymidine analog BrdU, immediately after imaging. This allowed us to discriminate between BrdU-negative G_1/G_2 nuclei (Figure 3f) and BrdU-positive S-phase nuclei (Figure 3e). Our results show that IRIF move significantly (≈35%) less in S-phase nuclei (Figure 3g), which might be surprising in view of the replication-related unwinding and de-condensation of chromatin.

The outcome of the latter experiment indicated that chromatin relaxation or de-condensation is not the only factor affecting IRIF mobility. We, therefore, concluded that other types of changes in the organization or composition of chromatin might also influence IRIF mobility. Of special interest to us were changes in chromatin organization or composition that can be induced on demand.

Changes in IRIF mobility after treatments that affect chromatin organization and composition

Recently published data indicate that 53BP1, a protein involved in local modification of chromatin in response to DSBs, promotes interactions between DSBs during V(D)J recombination (Difilippantonio *et al.*, 2008). Moreover, the motility of uncapped telomeres, which physiologically resemble one-ended DSBs and recruit DSB repair proteins, is decreased after 53BP1 knock-down (Dimitrova *et al.*, 2008). Taken together, these results suggest that 53BP1 might influence the mobility of DSBs as well. To examine this possibility we measured the mobility of IRIF in MDC1-GFP expressing U2OS cells transfected with siRNA targeted against 53BP1. Even though 53BP1 was effectively down-regulated, we observed no reduction of IRIF mobility in these cells as compared to cells transfected with scrambled siRNA (Figure 4a), suggesting that the mobility of IRIF is regulated by mechanisms independent of 53BP1. Neither did we observe a change in IRIF mobility when we inhibited Tip60, a protein also implicated in chromatin remodeling at DSB sites (Sun *et al.*, 2006) (Figure 4a). Even though neither siRNA approach nor chemical inhibition can fully suppress protein activity and we cannot completely exclude involvement of 53BP1 or Tip60 in increased mobility of IRIF, our results did not provide any indication that inhibition of these early repair-related factors can reduce IRIF mobility.

As chromatin remodeling requires metabolic energy, we examined the effect of ATP depletion on IRIF mobility. We found that a combination of the ATP synthesis inhibitors 2-deoxyglucose and sodium azide significantly (34%) decreased the MSD of IRIF (Figure 4b). When we, subsequently, explored the impact of transcription, a process strongly associated with chromatin remodeling, we detected only a moderate effect on IRIF movement. Treatment with the transcription inhibitor 5,6-dichloro-1 -D-ribofuranosyl benzimidazole (DRB) did reduce IRIF mobility but the change was not statistically significant (Figure 4c).

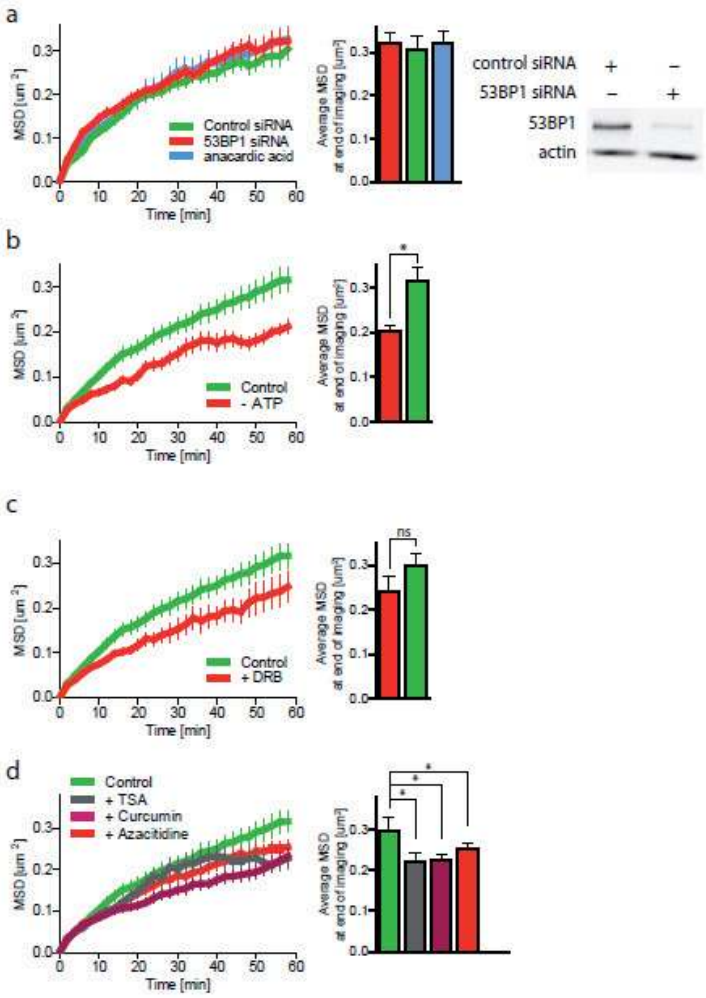

Figure 4. Influence of DSB-related and global chromatin modifications on IRIF mobility. (a), Left panel - MSD of MDC1-GFP IRIF in U2OS cells transfected with scrambled or anti-53BP1 siRNA or incubated for 24h with Tip60 inhibitor anacardic acid. Bar graph shows MSD of IRIF averaged over last 3 time points. Right panel – detection of 53BP1 by western blotting in cells transfected with scrambled siRNA (left lane) or siRNA targeting 53BP1 (right lane). (b), MSD of IRIF in cells exposed to 5 Gy of -rays, incubated for 30 min in the presence or the absence of ATP synthesis inhibitors 2-deoxyglucose and sodium azide and imaged for 60 min, without refreshing the medium. Bar graph – as in (a). (c), MSD of IRIF in cells incubated for 4h in the presence or the absence of transcription inhibitor DRB, irradiated as in (a) and imaged for 60 min. Bar graph – as in (a). (d), MSD of IRIF in cells irradiated and imaged after incubation for 24 h with 150nM histone deacetylase inhibitor TSA, 48h with 0.75 uM non-methylable cytidine analogue 5-azacytidine or 1h with 1uM histone acetyltransferase inhibitor curcumin. Bar graph shows MSD of IRIF under respective conditions, averaged over last 3 time points. Asterisks indicate statistical significance with $p < 0.05$, assessed using the student t-test. Error bars represent SEM. At least 30 cells and at least 5 foci per cell were analyzed per data series.

Several studies indicate that ATP supply and transcription influence movement of non-damaged chromatin (Dundr *et al.*, 2007; Heun *et al.*, 2001; Levi *et al.*, 2005; Marshall *et al.*, 1997; Mearini & Fackelmayer, 2006). Likewise, our results indicate that energy-dependent chromatin remodeling processes could contribute to IRIF movement.

The above experiments did not reveal whether chromatin organization by itself has the capacity to affect IRIF mobility. To examine this question we focused on treatments that modify the organization of chromatin, without directly interfering with DNA repair or transcription. In these studies we used agents that, among other activities, affect the organization of chromatin at a global level by inhibiting DNA methylation, or histone acetylation/de-acetylation. When we applied 5-azacytidine, an inhibitor of DNA methylation, or trichostatin A, an inhibitor of histone

deacetylation (Supplementary figure 3) and curcumin, a histone acetyltransferase inhibitor (Yoshida *et al.*, 1995), we found that all these chromatin modifying treatments induced a significant reduction in IRIF mobility (Figure 4d). The curcumin treatment, in particular, reduced the IRIF MSD to a level that was only 20% higher than the MSD of non-damaged Cy3CDs. This effect appeared to be limited to damaged chromatin, as curcumin treatment did not change the mobility of Cy3CDs (Supplementary Figure 2). Importantly, treatment of cells with TSA, curcumin or 5-azacytidine did not disturb cell cycle progression as measured by BrdU incorporation assay, nor did we detect significant changes in repair, according to the kinetics of -H2AX IRIF disassembly after irradiation (Supplementary figure 3). Together, these experiments demonstrate that the modes of IRIF- and Cy3CD-movement are different and, moreover, that IRIF mobility can be reduced on request.

An important consequence of chromatin mobility is the fusion of IRIF (Aten *et al.*, 2004) which brings in close proximity unrepaired DNA ends from initially distant DSBs and might thereby increase in the chance of chromosome rearrangement induction. We indeed observed occasional fusions of multiple IRIF (Figure 5), although whether the actual rejoining of open DNA ends takes place within fused IRIF cannot be confirmed. In order to investigate whether changes in IRIF mobility affect IRIF fusion rate, we measured the frequencies of IRIF fusions in cells treated with curcumin, which modifies IRIF mobility. Importantly, IRIF fusion frequencies were indeed decreased in cells treated with curcumin, likely due to decreased IRIF mobility.

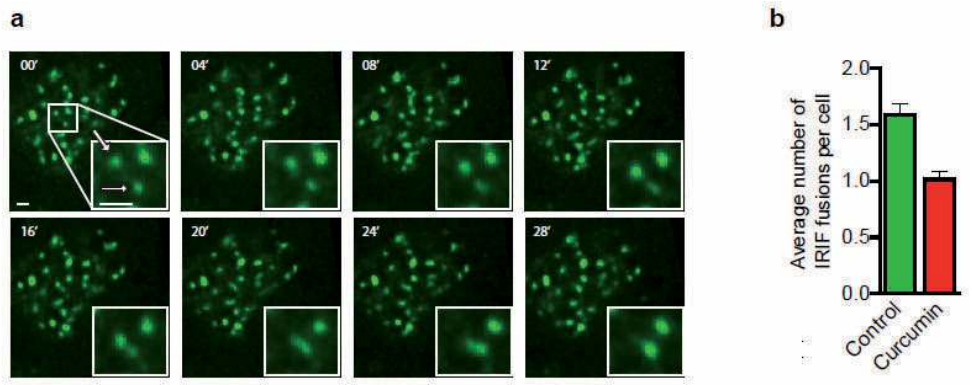

Figure 5. Fusion of multiple IRIF. (a) Multiple IRIF occasionally fuse. Image gallery shows fusion of 2 IRIF initially spaced by approximately 2 µm. Scale bar – 2 µm. (b) IRIF fusion frequency is decreased in U2OS cells incubated in the presence of curcumin. Time-lapse movies of 53BP1-GFP IRIF in control cells and in cells incubated with curcumin, exposed to 5 Gy of -radiation were scored 'blindly' by 2 observers. Graph represents average number of observed IRIF fusions per cell. Error bars represent range of frequencies obtained by the 2 observers. At least 100 cells were scored per data point.

Conclusions

Our results demonstrate that the presence of DSBs locally increases the motility of chromatin, resulting in a 2- to 3-fold larger nuclear area roamed by the DSBs as compared to intact chromatin and that the increase depends, to some extent, on the agent used to induce DSBs. Moreover, IRIF mobility can be reduced by exogenous agents that affect higher-order chromatin organization. Factors that reduce IRIF mobility may not affect the mobility of undamaged chromatin or uncapped telomeres, or vice-versa, indicating that IRIF movement involves additional and/or different mechanisms.

The movement of DSBs may, at first sight, appear to be of little consequence as their range is less than a micrometer. However, their non-directional walk can cover an area in the cell nucleus of about 1 μm^3, which is a highly relevant size in the context of cancer treatment. Each treatment in a fractionated therapy produces about 100 DSBs per cell, even in healthy tissues directly surrounding the malignancy. Considering that the volume of a typical mammalian cell nucleus is about 250 μm^3, a single treatment can thus result in multiple accidental DSB interactions leading to CR. Fusions between IRIF have been earlier reported in cells exposed to alpha particles (Aten *et al.*, 2004) and X-rays (Falk *et al.*, 2007). Thus the 2.2- and 3.2-fold increases in nuclear area roamed by DSBs induced by ionizing radiation and etoposide, as compared to non-damaged chromatin, should increase DSB interaction probabilities. Furthermore, it is feasible that the reverse process, a reduction of DSB mobility, might decrease IRIF fusion frequency and reduce DSB interactions.

Materials and methods

To measure the mobility of the various labeled chromatin domains, we captured 3D time-lapse movies of cells at 2 min intervals for 60 min and corrected the individual images for shift and rotation of cell nuclei during the imaging. Movements of chromatin domains were interpreted as a restrained random walk. We determined the average distance (S) covered by the domains during the 2 min intervals between images and the mean squared displacement (MSD) in the 3D images, as a function of time (Krawczyk *et al.*, 2008). To compare the range of movement of chromatin domains we used the average of the last 3 MSD values. Cells that displayed extensive morphing of their nuclei during the imaging period were excluded from the analysis.

Reference list

Allan, J.M. and Travis, L.B. (2005). Mechanisms of therapy-related carcinogenesis. *Nat. Rev. Cancer*. 5, 943-955.

Aten, J., Stap, J., Krawczyk, P., van Oven, C., Hoebe, R., Essers, J. and Kanaar, R. (2004). Dynamics of DNA double-strand breaks revealed by clustering of damaged chromosome domains. *Science*. 303, 92-95.

Bekker-Jensen, S., Lukas, C., Melander, F., Bartek, J. and Lukas, J. (2005). Dynamic assembly and sustained retention of 53BP1 at the sites of DNA damage are controlled by Mdc1/NFBD1. *J. Cell Biol*. 170, 201-211.

Cesare, A.J., Kaul, Z., Cohen, S.B., Napier, C.E., Pickett, H.A., Neumann, A.A. and Reddel, R.R. (2009). Spontaneous occurrence of telomeric DNA damage response in the absence of chromosome fusions. *Nat. Struct. Mol. Biol.* 16, 1244-1251.

Chuang, C. and Belmont, A.S. (2007). Moving chromatin within the interphase nucleus-controlled transitions?. *Semin. Cell Dev. Biol*. 18, 698-706.

Difilippantonio, S., Gapud, E., Wong, N., Huang, C., Mahowald, G., Chen, H.T., Kruhlak, M.J., Callen, E., Livak, F., Nussenzweig, M.C. et al. (2008). 53BP1 facilitates long-range DNA end-joining during V(D)J recombination. *Nature*. 456, 529-533.

Dimitrova, N., Chen, Y.M., Spector, D.L. and de Lange, T. (2008). 53BP1 promotes non-homologous end joining of telomeres by increasing chromatin mobility. *Nature*. 456, 524-528.

Dundr, M., Ospina, J.K., Sung, M., John, S., Upender, M., Ried, T., Hager, G.L. and Matera, A.G. (2007). Actin-dependent intranuclear repositioning of an active gene locus in vivo. *J. Cell Biol*. 179, 1095-1103.

Falk, M., Lukasova, E., Gabrielova, B., Ondrej, V. and Kozubek, S. (2007). Chromatin dynamics during DSB repair. *Biochim. Biophys. Acta*. 1773, 1534-1545.

Goodarzi, A.A., Noon, A.T., Deckbar, D., Ziv, Y., Shiloh, Y., Löbrich, M. and Jeggo, P.A. (2008). ATM signaling facilitates repair of DNA double-strand breaks associated with heterochromatin. *Mol. Cell*. 31, 167-177.

Heun, P., Laroche, T., Shimada, K., Furrer, P. and Gasser, S.M. (2001). Chromosome dynamics in the yeast interphase nucleus. *Science*. 294, 2181-2186.

Krawczyk, P.M., Stap, J., Hoebe, R.A., van Oven, C.H., Kanaar, R. and Aten, J.A. (2008). Analysis of the mobility of DNA double-strand break-containing chromosome domains in living Mammalian cells. *Meth Mol Biol*. 463, 309-320.

Kruhlak, M., Celeste, A., Dellaire, G., Fernandez-Capetillo, O., Muller, W., McNally, J., Bazett-Jones, D. and Nussenzweig, A. (2006). Changes in chromatin structure and mobility in living cells at sites of DNA double-strand breaks. *J. Cell Biol*. 172, 823-834.

Levi, V., Ruan, Q., Plutz, M., Belmont, A. and Gratton, E. (2005). Chromatin dynamics in interphase cells revealed by tracking in a two-photon excitation microscope. *Biophys. J*. 89, 4275-4285.

Marshall, W.F., Straight, A., Marko, J.F., Swedlow, J., Dernburg, A., Belmont, A., Murray, A.W., Agard, D.A. and Sedat, J.W. (1997). Interphase chromosomes undergo constrained diffusional motion in living cells. *Curr. Biol*. 7, 930-939.

Mearini, G. and Fackelmayer, F.O. (2006). Local chromatin mobility is independent of transcriptional activity. *Cell Cycle*. 5, 1989-1995.

Molenaar, C., Wiesmeijer, K., Verwoerd, N.P., Khazen, S., Eils, R., Tanke, H.J. and Dirks, R.W. (2003). Visualizing telomere dynamics in living mammalian cells using PNA probes. *EMBO J*. 22, 6631-6641.

Murr, R., Loizou, J.I., Yang, Y.G., Cuenin, C., Li, H., Wang, Z.Q. and Herceg, Z. (2006). Histone acetylation by Trrap-Tip60 modulates loading of repair proteins and repair of DNA double-strand breaks. *Nat. Cell Biol*. 8, 91-99.

Osheroff, N. (1989). Effect of antineoplastic agents on the DNA cleavage/religation reaction of eukaryotic topoisomerase II: inhibition of DNA religation by etoposide. *Biochemistry*. 28, 6157-6160.

Pliss, A., Malyavantham, K., Bhattacharya, S., Zeitz, M. and Berezney, R. (2009). Chromatin dynamics is correlated with replication timing. *Chromosoma*. 118, 459-470.

Rogakou, E., Boon, C., Redon, C. and Bonner, W. (1999). Megabase chromatin domains involved in DNA double-strand breaks in vivo. *J. Cell Biol*. 146, 905-916.

Shelby, R.D., Hahn, K.M. and Sullivan, K.F. (1996). Dynamic elastic behavior of alpha-satellite DNA domains visualized in situ in living human cells. *J. Cell Biol.* 135, 545-557.

Soutoglou, E., Dorn, J.F., Sengupta, K., Jasin, M., Nussenzweig, A., Ried, T., Danuser, G. and Misteli, T. (2007). Positional stability of single double-strand breaks in mammalian cells. *Nat. Cell Biol.* 9, 675-682.

Stephens, P.J., Greenman, C.D., Fu, B., Yang, F., Bignell, G.R., Mudie, L.J., Pleasance, E.D., Lau, K.W., Beare, D., Stebbings, L.A. et al. (2011). Massive genomic rearrangement acquired in a single catastrophic event during cancer development. *Cell*. 144, 27-40.

Sun, Y., Jiang, X., Chen, S. and Price, B.D. (2006). Inhibition of histone acetyltransferase activity by anacardic acid sensitizes tumor cells to ionizing radiation. *FEBS Lett*. 580, 4353-4356.

Suzuki, K., Ojima, M., Kodama, S. and Watanabe, M. (2003). Radiation-induced DNA damage and delayed induced genomic instability. *Oncogene*. 22, 6988-6993.

Yoshida, M., Horinouchi, S. and Beppu, T. (1995). Trichostatin A and trapoxin: novel chemical probes for the role of histone acetylation in chromatin structure and function. *BioEssays*. 17, 423-430.

Zink, D., Cremer, T., Saffrich, R., Fischer, R., Trendelenburg, M.F., Ansorge, W. and Stelzer, E.H. (1998). Structure and dynamics of human interphase chromosome territories in vivo. *Human Genet*. 102, 241-251.

Ziv, Y., Bielopolski, D., Galanty, Y., Lukas, C., Taya, Y., Schultz, D.C., Lukas, J., Bekker-Jensen, S., Bartek, J. and Shiloh, Y. (2006). Chromatin relaxation in response to DNA double-strand breaks is modulated by a novel ATM-and KAP-1 dependent pathway. *Nat. Cell Biol.* 8, 870-876.

de Vos, W.H., Hoebe, R.A., Joss, G.H., Haffmans, W., Baatout, S., Van Oostveldt, P. and Manders, E.M.M. (2009). Controlled light exposure microscopy reveals dynamic telomere microterritories throughout the cell cycle. *Cytometry A*. 75, 428-439.

van Attikum, H. and Gasser, S.M. (2005). The histone code at DNA breaks: a guide to repair? *Nat. Rev. Mol. Cell Biol.* 6, 757-765.

Supplementary materials and methods

Cell culture and treatments

U2OS cells were cultured in DMEM (Gibco) supplemented with 10% FCS, 200mM L-glutamine (Gibco) and pen/strep (Gibco) in 10% CO_2. For Cy3-dUTP labeling, confluent cell cultures grown on coverslips were scratch-loaded in the presence of 50 μM Cy3-dUTP (Sigma-Aldrich) in PBS (Gibco). For BrdU labeling, cells were incubated for 5 min in the presence of 10 μM BrdU (Sigma-Aldrich). The following inhibitor concentrations were used (unless stated otherwise): trichostatin A (TSA, Sigma-Aldrich) – 150nM, 5-azacytidine (5-AzaC, Sigma-Aldrich) - 0.75 μM, 5,6-dichloro-1β-D-ribofuranosyl benzimidazole (DRB, Sigma-Aldrich) - 100 μM, anacardic acid (AA, Sigma-Aldrich) - 100nM, curcumin (Sigma-Aldrich) – 1uM. Cells were irradiated with a ^{137}Cs source at a dose rate of 0.6 Gy/min for a total dose of 5 or 8 Gy or treated with 15 μg/ml etoposide (Sigma-Aldrich) for 15 min.

siRNA and western blotting

Cells were transfected with scrambled siRNA or siRNA against targeting 53BP1 (Dharmacon) using lipofectamine 2000 (Invitrogen) using standard manufacturer protocols. Western blot analysis and imaging of siRNA transfected cells was performed 48h post-transfection. Cells were lysed in a buffer containing 2% SDS, 10% glycerol, 60 mM Tris-HCl pH 6.8, 50 mM DTT, protease and phosphatase inhibitors and 0.02% bromophenol blue. After fractionation by SDS-PAGE, proteins were transferred to a nitrocellulose membrane and probed with the relevant antibodies.

Time-lapse microscopy and image processing

Cells were imaged with a Leica IRBE (Leica Microsystems) inverted wide field microscope, 63x oil objective, at 37°C in an atmosphere of 10% CO_2. Z-stacks of 5 images, 300 nm apart along the z-axis, were taken at 2 min intervals. 3D images were then reconstructed using Huygens Professional (Scientific Volume Imaging). Semi-automated 3D image registration and object tracking was performed as described previously (Krawczyk *et al*, *Meth Mol Biol* , 2008).

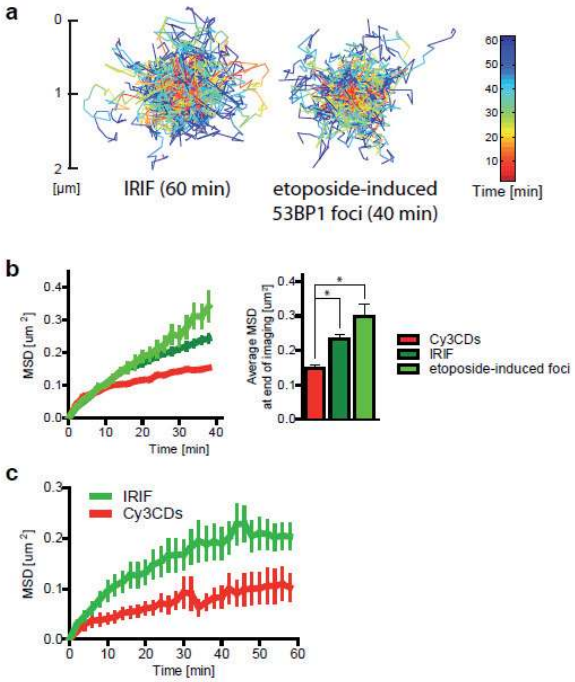

Supplementary figure 1. Mobility of chromatin domains containing DSBs induced by Topoisomerase inhibitor etoposide (in U2OS cells) and by -radiation (in normal human fibroblasts). (a), 100 randomly selected trajectories, depicting movement of the ionizing irradiation and etoposide induced DSBs in U2OS cells were plotted as originating from the same point on the 2D plane. The color of the segments of the trajectories represents time after the start of imaging. (b), MSD of the indicated types of chromatin domains. Bar graph shows MSD of the respective domains averaged over last 3 time points. Asterisks indicate statistical significance with $p < 0.05$, assessed using the student t-test. Error bars represent SEM. At least 30 cells and at least 150 foci were analyzed per data series. (c) MSD of the indicated types of chromatin domains in normal human fibroblasts. Error bars represent SEM. At least 10 cells and at least 5 foci per cell were analyzed per data series.

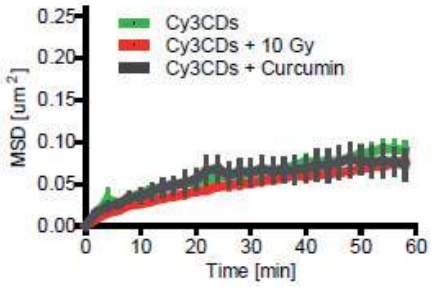

Supplementary figure 2. Mobility of Cy3CDs in U2OS cells is not altered by irradiation or curcumin treatment. MSD of Cy3CDs in cells exposed to 0 or 10 Gy of -radiation or to 1uM curcumin. Error bars represent SEM. At least 20 cells and at least 5 foci per cell were analyzed per data series.

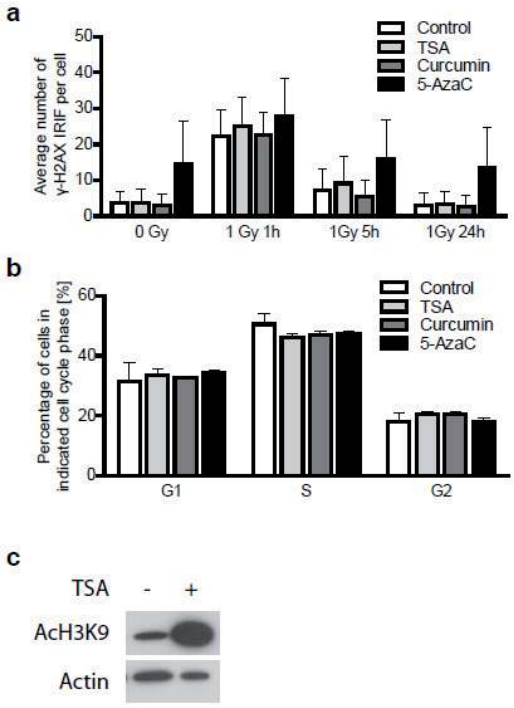

Supplementary figure 3. -H2AX IRIF frequencies and cell cycle distribution in cells treated with TSA, curcumin and 5-azacitidine. (a) U2OS cells expressing 53BP1-GFP were incubated in the presence of the indicated inhibitor, exposed to 1Gy of -radiation, fixed 1, 5 or 24 h after irradiation and stained using antibodies against histone -H2AX. Bars indicate average number of -H2AX IRIF per cell. At least 100 cells were scored per data point. Error bars indicate standard deviation. (b) U2OS cells expressing 53BP1-GFP were incubated in the presence of the indicated inhibitors, as described in the supplementary materials and methods section, then incubated in the presence of BrdU and fixed. Standard cell cycle distribution analysis was then performed by FACS analysis of cells stained using antibodies against BrdU. Graph represents average percentage of cells in the indicated cell cycle phase, obtained from duplicate samples per data point. Error bars indicate range of values obtained from 2 duplicates. (c) TSA treatment increases histone acetylation. Detection of acetylated histone H3 K9 (upper panel) in cells incubated in standard medium (left lane) or in medium supplemented with 150nM TSA for 24h (right lane). Sample loading is controlled by probing for actin (lower panel). Panels show a representative experiment

9 Summary and General Discussion

Summary and General Discussion

Introduction: Glioblastoma Multiforme and Cancer Stem Cells

Glioblastoma multiforme (GBM) is by far the most malignant brain tumor. The abundant migration of glial-like cancer cells away from primary tumor mass, infiltrating into the surrounding healthy tissue is one of the main histo-pathological features of GBMs. It is also one of the main difficulties when dealing with this disease. The infiltrating part of the tumor is considered to play a key role in inevitable tumor recurrence that follows surgical resection. Subsequently, patients with a malignant glioma have a very poor prognosis and only approximately 10% of the newly diagnosed survive more then 5 years despite multimodality treatment that comprises of surgery, radiation and temozolomide (TMZ) chemotherapy (1).

An additional difficulty in therapeutic management of GBM is its therapy resistance due to invariable survival of a small fraction of tumor cells when either radiotherapy or chemotherapy is applied. This resistant population of cells was, according to recent reports, characterized as the cancer stem cell (CSC) fraction due to their similarities with normal stem cells, namely self renewal and multi-lineage differentiation capacity. The main criteria, however, for defining CSCs is their ability to give rise to tumors that phenocopy an original malignancy after serial transplantation in a xenograft model, demonstrating that newly generated tumors contain a fraction of functionally multipotent, stem-like cells capable to self-renew (2). Increasing amount of evidence is demonstrating that one single CSC is able to reconstitute the whole tumor phenotype (3, 4). Accordingly, it can be anticipated that their escape from therapy could consequently result in tumor regrowth. Therefore, it is not surprising that CSCs are currently considered to be the underlying reason of tumor recurrence. This is in part attributed to their highly efficient DNA-damage repair mechanisms and cell-cycle check points as well as the activation of anti-apoptotic pathways that all together result in CSCs being extremely therapy resistant (5).

Recently an additional layer of complexity has been added to the CSC biology and the existence of small, (epi)genetically identical fraction of CSCs has been challenged. One of the first clues was provided by Quintana *et al*. who showed that as much as one in four melanoma cells has tumorigenic potential and that furthermore tumorigenicity of cells in xenograft model is highly dependent on the level of immunodeficiency of the host (4). More importantly, xenografts obtained from the same patient specimen were heterogeneous and differed from one another. This raised a doubt of whether tumors contain few (epi)genetically distinct populations of stem-like cells. In order to address this matter, namely whether a single, uniform population of CSCs is responsible for the tumor phenotype or if several distinct CSC clones co-exist in the tumor, we analyzed the GBM CSC fraction in more detail (**Chapter 3**). To do so, we investigated the

differentiation potential of single-cell derived CSC lineages. In case of the single, multipotent population of CSCs, single-cell cloning of the culture would yield clones with the same differentiation pattern as the parental one. Our results, however, demonstrated unexpected variety in that respect with a broad range of differentiation patterns that varied from one clone to the other. Since all the clones were kept under the same culturing conditions and demonstrated a stable phenotype in our cultures, these results suggest that the original tumor contained several CSC driven clones that differ in their differentiation abilities, possibly due to their diverse genetic or epigenetic background. How could that be explained? It can be speculated that due to various selective pressures in different tumor areas, clones that initially arose from the same cell acquired different mutations that could influence their differentiation program but also better survival and higher invasiveness. Notably, invasive morphology of tumors is a direct consequence of their hierarchical organization and is driven by CSCs themselves, invasive clones more in particular (**Chapter 4**).

In the light of the development of novel anti-cancer treatments, these findings certainly need to be considered. There is a tendency to develop treatments that would drive tumors towards differentiation, directing it thus towards the cell type most sensitive to therapy. If different CSC fractions are present within a malignancy that also display different differentiation dynamics, this kind of approach might be insufficient, as different CSC clones could respond differently to this or any other treatment for that matter. Thus, targeting more than one population of CSCs would probably be a more promising strategy with the main focus on identifying the most dominant, resistant, invasive clones and accordingly determinants that sustain them. In that respect, the tumor microenvironment has been proposed to play a key role.

Tumor Microenvironment

The tumor microenvironment has been, in numerous instances, demonstrated to be a major determinant of tumor maintenance and progression. For GBM in particular, this role has been assigned to the endothelial cells comprising the tumor vasculature (**Chapter 2**). In analogy to neural stem cells (NSCs), microvascular endothelial cells have been reported to form a GBM CSC niche, directing cell fate decisions and expanding the CSC pool (6, 7) (**Chapter 5**). One of the mediators of the CSC-vasculature interaction was reported to be nitric oxid produced by endothelial cells that maintains the CSC fraction by triggering the Notch pathway (8). The existence of a vascular niche seems to be essential for GBM CSCs to such an extent that these cells themselves are promoting the formation of new blood vessels and furthermore are protecting them from various insults (9-11). GBM CSCs are not only secreting considerable amounts of vascular endothelial growth factor (VEGF) that triggers and directs neovascularisation, but are themselves capable to differentiate into an endothelial-like phenotype and as a consequence generate their own niche (9, 12, 13). In addition, hypoxic regions have also been reported to form

a GBM CSC niche (14) (**Chapter 2**). HIF2α is considered to be the key mediator of hypoxia mediated effects in GBM, maintaining the CSC pool by an additional mechanism. Even though one might intuitively think that the tumor vasculature on one hand and hypoxic regions on the other represent unrelated niche-entities, this does not necessarily have to be the case. In addition to being highly vascularized, GBMs are also characterized by an abundantly dysfunctional vasculature. In addition, as introduced previously, GBM cells themselves can also differentiate into cells that mirror an endothelial phenotype. However, these cells often build structures that end up being vascular mimicry rather than functional vessels. This implies that tumor cells benefit from endothelial (-like) cells surrounding them, but not necessarily real vasculature. Thus, hypoxic regions and non-functional blood vessels could very well co-localize within the tumor and synergistically support CSCs. From a clinical point-of-view it is essential to break the niche-mediated support of CSCs so that the tumorigenic core of the tumor can be targeted effectively.

Therapy resistance

In addition to maintaining the CSC fraction, the tumor microenvironment has also been implicated in its therapy resistance. For example, angiogenesis inhibition by bevacizumab, a VEGF-neutralizing antibody, by itself decreased the CSC pool and consequently inhibited tumor growth (6). It also increased the susceptibility of CSCs to cytotoxic agents (15). Moreover, inhibition of Notch signaling is reported to enable cross-talk between CSCs and their surrounding niche and significantly increases efficacy of radiotherapy on these cells (16). Therefore, learning more about the role of the tumor microvasculature in GBM therapy resistance appears essential, when considering novel therapeutic approaches.

Current data on radiotherapy response of tumor endothelial cells are incomplete and controversial. While some reports claim these cells to be highly sensitive to the treatment and undergoing apoptosis, others suggest the opposite (17, 18). To address this question in more detail, we recently evaluated the response of tumor microvascular endothelial cells (tMVECs) to conventional treatments, with special emphasis on radiation, being the pivotal treatment for GBM patients, and further analyzed how this influences their interaction with CSCs (**Chapter 6**). Our data show that, when co-culturing tMVECs and CSCs, tMVECs are able to stimulate growth and stemness of GBM cells despite the treatment, due to their extreme therapy resistance. Their preferential response to irradiation is permanent cell cycle arrest, senescence. Intriguingly, senescent tMVECs support the CSC growth with the same efficacy as non-senescent ones. Moreover, GBM CSCs themselves, upon differentiating into an endothelial-like phenotype, subsequently respond by adopting a senescent state when exposed to radiation and obtain the role of the CSC niche in supporting the expansion of tumor cells (Figure 1).

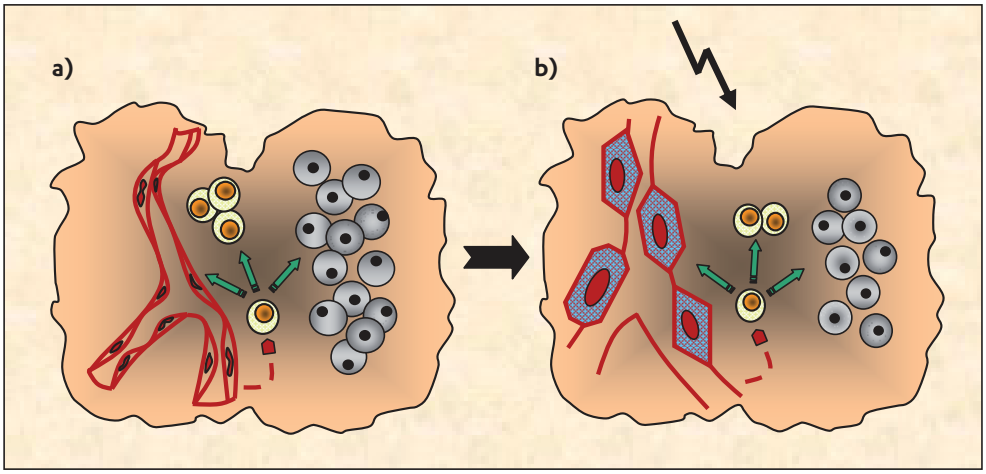

Figure 1. a) GBM CSCs (yellow) reside close to tMVECs (red) that form their niche and maintain them in stem-like state (red arrow). CSCs on one hand self renew and give rise to new CSCs, and on the other hand differentiate into tumor cells (gray) as well as tMVECs (green arrows). b) Due to their therapy resistance, upon irradiation tMVECs do not die but undergo senescence (blue) and continue to support CSC pool (red arrow). CSCs that differentiate into endothelial-like phenotype acquire the same response to irradiation.

These results propose a discouraging scenario where the tumor cells themselves are able to generate their own environmental niche. This allows them to survive and further expand after treatment with gamma-irradiation and alkylating agents. Such a niche could contribute to the tumor relapse commonly observed after an initial clinical response. Crucially, in addition to sustaining the existing fraction of CSCs, tMVECs seem to be able to reprogram differentiated tumor cells and convert them back from a non-stem- into a more stem-like phenotype (**Chapter 7**). Thus, the end result of modulating plasticity of tumor cells is the enrichment of a tumorigenic, therapy resistant and invasive fraction of cells. Therefore, interfering with and disrupting the interaction between tumor cells and their vascular niche would potentially sensitize them to treatment. The molecules that mediate this interaction are attractive therapeutic targets that could help to develop novel strategies to fight this disease. However, the genetic diversity of these tumors should be taken into account when dealing with this matter. Even though GBMs in general share the main hallmarks, each individual tumor has a unique pattern of genetic alterations. This creates a considerable obstacle for the development of universal treatments for this disease. Four different subtypes of GBM have been described, with different sets of mutations underlying their pathogenesis (19). It is likely that the genetic variation of GBM also impinges on the interaction with the vascular niche. This complex interplay is a finely tuned system, and so far various signaling pathways, secreted and membrane bound molecules have been reported to be the mediators. Below the main suspects are reviewed.

Potential candidates that enable CSC-niche cross-talk

Notch pathway

The Notch pathway is a highly conserved pathway that mainly works *in trans*. Activation therefore needs direct cell-to-cell contact. Upon ligand-receptor interaction between two neighboring cells, γ-secretase proteolytically cleaves the receptor, which releases the Notch intracellular domain (NICD). This part of the protein translocates into the nucleus and subsequently activates the transcription of downstream targets such as Hes and Hey that further modulate cell fate. So far four NOTCH receptors (NOTCH 1-4), five ligands (Jagged 1-2, Delta-like ligand (DLL) 1,3,4) and numerous effector molecules (Hes 1-6, Hey 1,2,L) have been identified. The complexity of the pathway allows for cell-type specific signal outputs, which are still poorly understood. However, in general signal-sending cells are usually the ones undergoing differentiation or being differentiated whereas signal-receiving cells remain in an undifferentiated state. This is referred to as so-called 'lateral specification'.

The Notch pathway was reported to be one of the key mediators of cross-talk between the CSCs and their vascular microenvironment, similar to the neural stem cell niche (7, 8, 16). This signaling pathway has a dual role: it directs angiogenesis and regulates stem cell maintenance, emphasizing the tight bond between these two processes. Within the CSC niche, endothelial cells express the Notch ligands DLL4 and JAG1 that bind to the NOTCH1 receptor on the membrane of GBM CSCs and activate this pathway in CSCs (20). Furthermore, endothelial cells produce nitric oxide, a short range molecule that also stimulates CSCs and indirectly triggers Notch signaling in this fraction through the NO/cGMP/PKG pathway (8). Inhibiting this pathway by the γ-secretase inhibitor DAPT leads to reduction of the CSC fraction as a consequence of the initial loss of endothelial cells preceding this event, due to Notch blockade. Combination of radiation and Notch inhibition had a profound therapeutic effect and dramatically reduced the growth of both endothelial and tumor cells as compared to radiation treatment alone *in vitro* (16).

Tumor angiogenesis is essential for GBM growth and metastasis and is regulated by various pro-angiogenic factors and signaling pathways, the most important being VEGF. Thus, it is not surprising that anti-VEGF treatment has already been approved for clinical trials and is demonstrating a certain clinical benefit for the patients, although these studies are still ongoing. However, resistance to or escape from this kind of treatment evolves in many cases and tumor growth and angiogenesis are able to proceed despite potent VEGF blockade. Furthermore, an increase in metastatic incidence upon this treatment has been reported, creating room for novel, improved therapies (21). Targeting the microvascular CSC niche by Notch inhibition might be an alternative approach for treatment of GBM. From a clinical perspective, Notch inhibition should affect two main targets: the CSC pool as well as angiogenesis. Data so far are strongly suggesting

an enhanced therapeutic effect of radiation in the absence of Notch signaling, thereby creating support for pursuing this research path further.

DLL4-mediated Notch signaling is essential for embryonic vascular development and haplo-insufficiency leads to embryonic lethality caused by severe vascular defects (22). In adults, DLL4 is largely enrolled in tumor angiogenesis and even speculated to be expressed on tumor vasculature at considerably higher levels compared to normal, healthy blood vessels (23). It is a critical negative regulator of (tumor) angiogenesis, acting to restrain excessive VEGF-induced vascular sprouting (24, 25). Thus, there is a feed back loop between VEGF and DLL4/Notch signaling and the blockade of VEGF results in decreased expression of DLL4 on tumor vasculature. Even though both anti-DLL4 and anti-VEGF therapy inhibit tumor growth in mouse models, these treatments had the opposite effects on tumor vasculature. While anti-VEGF therapy reduced vascular density, anti-DLL4 treatment resulted in an abundant increase of non-productive tumor vascularisation accompanied by enhanced sprouting and branching (24, 25). Despite the increase in vascular density, these were poorly perfused vessels and were not part of a functional vascular network. Thus it seems that tumors, despite their abnormal vasculature, nevertheless require a balanced hierarchy of well-organized, functional blood vessels, at least up to a certain degree.

What would be the advantage of targeting DLL4? The main concern regarding the general inhibition of Notch signaling are its potential serious side affects as this pathway regulates the postnatal stem cell compartment in many tissues. γ-secretase inhibitors that non-selectively block all Notch activities have already been shown to cause unwanted side-effects in rodents by disrupting intestinal homeostasis. The advantage of targeting DLL4 specifically lies in its more restricted expression in the postnatal vascular system, especially tumor vasculature. Importantly, DLL4 blocking antibodies efficiently reduced the growth of tumors that were resistant to anti-VEGF treatment. The treatment inhibited productive angiogenesis and reduced the CSC fraction. Whereas chemotherapy alone, despite tumor shrinkage, resulted in an increased fraction of CSCs, this treatment combined with anti-DLL4 had the opposite effect. A recent report even suggested that DLL4 mediated Notch signaling could be one of the exact underlying causes of tumor resistance to anti-VEGF treatment using bevacizumab (26). Even though the efficacy of anti-DLL4 has yet to be proven in clinical studies, and the concerns regarding its potential side effects need to be considered, data so far are strongly suggesting its therapeutic potential (27) .

Integrins

Integrins are cell surface receptors responsible for communication of cells with extra cellular matrix (ECM) protein components as well as cell-to-cell adhesion. They are heterodimeric, transmembrane proteins consisting of α and β subunits, and so far 16 α and 8 β subunits occurring in 21 different combinations have been described (28). In addition to their key roles in regulating cell adhesion and subsequently mediating tumor migration and invasion, their role in

angiogenesis has also been established (29). Therefore, as GBM is a highly infiltrative and vascularized malignancy, targeting integrins might be an interesting option to pursue. There is an analogy between normal- and cancer- stem cells. Adult NSC are located in the subventricular zone (SVZ) and the hippocampal dentate gyrus in the unique vascular niche that regulates their asymmetric division and maintains their stemness (30). In addition to Notch signaling, integrins have been reported to mediate this interaction (7, 31, 32). More specifically, laminin is expressed abundantly by endothelial cells in the SVZ, and the laminin receptor $\alpha6\beta1$ integrin on NSCs plays a critical role in their adhesion to vascular endothelial cells and regulation of their proliferation. Accordingly, blocking of $\alpha6\beta1$ integrin detaches NSC from their niche, alters their position and has differentiation inducing effects. In analogy, integrin $\alpha6\beta1$ was suggested to be a functional marker of GBM CSCs as well (33). Its expression overlaps with CD133, a well recognized GBM CSC marker, and furthermore is located in close proximity of CD31 positive endothelial cells. Blocking or knockdown of integrin resulted in a compromised CSC phenotype, it reduced their proliferation, and more importantly, their tumorigenic potential. Taken together, these data underscore integrin signaling in GBM as a possible therapeutic target. However, targeting integrins should be done with caution considering diverse roles they play in the process of tumorigenesis. For example, $\alpha_v\beta8$ integrin has a dual role as a negative regulator of GBM angiogenesis and a mediator of tumor invasion (34, 35). Targeting $\alpha_v\beta8$ integrin considerably reduced infiltration capacity of astrocytomas and resulted in localized lesions, however these tumors were significantly larger then the non-treated ones. This was partially due to increased vascularization, in agreement treated mice had significantly shorter lifespan as compared to control and the overall result of targeting $\alpha_v\beta8$ integrin was a pro-tumorigenic effect (34). On the other hand, blocking integrin $\alpha_v\beta3$ mainly had anti-tumorigenic effect in preclinical models (22). Cilengitide, a specific $\alpha_v\beta3$ inhibitor, combined with radiation more then doubled a median survival time of mice when compared to radiation alone, significantly reduced migration and invasion of tumor cells in preclinical models and is currently in a phase I/II clinical trial. Thus, targeting the right integrins could be a potential therapeutic option.

PI3K pathway

Another pathway that has been implicated in the cross-talk between the CSC compartment and its endothelial microenvironment is the PI3K signaling pathway (36). PI3 kinases are activated by a broad range of tyrosine kinase receptors to produce phosphatidulinositol-3,4,5-trisphosphate (PIP_3). This molecule couples PI3 kinase to its downstream effectors, like AKT (also known as PKB) that signals to promote cell growth and proliferation, and suppress apoptosis. This is enabled by the numerous substrates of AKT. One of the key targets is GSK3 that plays a role in preventing the progression through the cell cycle. AKT phosphorylates and subsequently inactivates GSK3 thus

driving cell into proliferation. PI3K and AKT also target mTOR, a protein kinase involved in protein synthesis and cells growth in response to available nutrients and growth factors. PTEN, on the other hand antagonizes PI3K signaling and is frequently mutated in tumors including GBM. This pathway is also involved in the regulation of migration and invasion, mainly by Rho family members Cdc42, Rac and Rho. These small GTPases dynamically remodel the actin cytoskeleton leading to formation of filopodia, lamellipodia and stress fibers. In addition to conferring growth advantage of tumor cells by increasing their survival and migration, PI3K/AKT pathway has also been implicated in tumor angiogenesis.

In meduloblastoma, Hambardzumyan *et al*. suggested this pathway to be crucial for the interaction between medulloblastoma CSCs and their perivascular niche (36). Furthermore, the absence of PI3K signaling seems to have clinical implications, as the inhibition of AKT phosphorylation significantly sensitized tumor cells in the perivascular niche to apoptosis (36). Accordingly, abundant data is suggesting that the PI3K pathway could play the same role in GBM. AKT signaling has been seriously implicated in the formation and growth of high-grade gliomas (37, 38). Both *EGFR* amplification and *PTEN* deletion, frequent mutations in GBM, are well-known alterations that activate the AKT pathway and are furthermore a specific distinction of grade IV gliomas, as compared to lower-grade lesions (39). Several other receptors present on tumor cells have also been implicated in activation of Pi3K, IGF-1 receptor for example (40). GBM subtypes characterized by loss of PTEN and enhanced PI3K signaling are associated with poor outcome (41). Importantly, this pathway seems to be involved in the maintenance of the GBM CSC fraction. Loss of the tumor suppressor PTEN and subsequent activation of PI3K/AKT signaling leads to an increase in the so-called side population in GBM (42). The side population, defined by FACS analysis, is a result of the ABCG-2-mediated efflux of Hoechst dye and is a surrogate marker for the CSC fraction. Furthermore, PI3K/AKT signaling directly regulates the activity of ABCG-2 drug transporters, thus making CSCs more resistant to chemotherapy (42). In addition, the activation of this pathway plays a role in radioresistance of glioma (43).

Even though the inhibition of PI3K signaling appears to have therapeutic potential, complexity of the PI3K pathway and its regulation by tumor cell itself or by signals received from its microenvironment has to be considered in order to target it properly. mTOR inhibitors are currently being tested and even though they have proven to be highly cytostatic in many preclinical studies, they failed to show the same effect in clinical trials (44-46). It has been proposed, however, that selective inhibition of mTOR could result in PI3K activation by an ill-defined feedback loop, demonstrating that mTOR inhibition alone is not sufficient to shut down this pathway (47). In that respect, a highly promising molecule seems to be PI-103, a selective dual PI3K/mTOR inhibitor that showed unique activity against genetically different GBM lines (48). PI-103 was already efficient at nanomolar concentrations, non-toxic and demonstrated tremendous efficacy in reducing the growth of malignant glioma in xenograft models regardless of their PTEN,

p53 and EGFR status. A clinical trial is yet to be performed, and in the meantime these results might provide cues to why PI3K inhibitors currently being tested are failing.

Conclusions

In conclusion, the tumor microenvironment needs to be taken into account when studying GBM. tMVECs play a critical role in GBM CSC maintenance on one hand, and display excessive therapy resistance on the other that likely contributes crucially to the treatment resistance of the tumor itself. How the tumor vasculature is exactly sustaining the CSC fraction and whether this holds true for all the CSCs in the tumor is yet to be determined. Current data are suggesting a close contact between CSCs and endothelial cells to be necessary, including direct cell-to-cell contact, short range molecules or most likely a combination of both, depending on the GBM subtype. This triggers different survival pathways in the CSCs, that still need to be identified more in detail, and allows them to escape the therapy. Directly targeting vasculature so far did not yield too encouraging data, as consequences of the treatment, such as increase in metastasis, overweighed the initial positive effect of therapy on tumor shrinkage. As tMVECs display strong resistance to conventional treatments, a way to potentially bypass the CSC niche could be the detachment of CSCs from it by interference with signals, which could have pro-differentiation effect and make them more susceptible for the treatment. Thus, understanding this interaction more in detail seems to be almost a prerequisite for more successful treatment of GBM.

Reference List

(1) Stupp R, Hegi ME, Mason WP, van den Bent MJ, Taphoorn MJB, Janzer RC, et al. Effects of radiotherapy with concomitant and adjuvant temozolomide versus radiotherapy alone on survival in glioblastoma in a randomised phase III study: 5-year analysis of the EORTC-NCIC trial. Lancet Oncology 2009;10:459-66.

(2) Clarke MF, Dick JE, Dirks PB, Eaves CJ, Jamieson CH, Jones DL, et al. Cancer stem cells--perspectives on current status and future directions: AACR Workshop on cancer stem cells. Cancer Res 2006;66:9339-44.

(3) Vermeulen L, Melo FDSE, van der Heijden M, Cameron K, de Jong JH, Borovski T, et al. Wnt activity defines colon cancer stem cells and is regulated by the microenvironment. Nature Cell Biology 2010;12:468-U121.

(4) Quintana E, Shackleton M, Sabel MS, Fullen DR, Johnson TM, Morrison SJ. Efficient tumour formation by single human melanoma cells. Nature 2008;456:593-U33.

(5) Bao SD, Wu QL, McLendon RE, Hao YL, Shi Q, Hjelmeland AB, et al. Glioma stem cells promote radioresistance by preferential activation of the DNA damage response. Nature 2006;444:756-60.

(6) Calabrese C, Poppleton H, Kocak M, Hogg TL, Fuller C, Hamner B, et al. A perivascular niche for brain tumor stem cells. Cancer Cell 2007;11:69-82.

(7) Shen Q, Goderie SK, Jin L, Karanth N, Sun Y, Abramova N, et al. Endothelial cells stimulate self-renewal and expand neurogenesis of neural stem cells. Science 2004;304:1338-40.

(8) Charles N, Ozawa T, Squatrito M, Bleau AM, Brennan CW, Hambardzumyan D, et al. Perivascular Nitric Oxide Activates Notch Signaling and Promotes Stem-like Character in PDGF-Induced Glioma Cells. Cell Stem Cell 2010;6:141-52.

(9) Bao SD, Wu QL, Sathornsumetee S, Hao YL, Li ZZ, Hjelmeland AB, et al. Stem cell-like glioma cells promote tumor angiogenesis through vascular endothelial growth factor. Cancer Research 2006;66:7843-8.

(10) Brown CK, Khodarev NN, Yu JQ, Moo-Young T, Labay E, Darga TE, et al. Glioblastoma cells block radiation-induced programmed cell death of endothelial cells. Febs Letters 2004;565:167-70.

(11) Ezhilarasan R, Mohanam I, Govindarajan K, Mohanam S. Glioma cells suppress hypoxia-induced endothelial cell apoptosis and promote the angiogenic process. International Journal of Oncology 2007;30:701-7.

(12) Ricci-Vitiani L, Pallini R, Biffoni M, Todaro M, Invernici G, Cenci T, et al. Tumour vascularization via endothelial differentiation of glioblastoma stem-like cells. Nature 2010;468:824-U121.

(13) Wang R, Chadalavada K, Wilshire J, Kowalik U, Hovinga KE, Geber A, et al. Glioblastoma stem-like cells give rise to tumour endothelium. Nature 2010;468:829-U128.

(14) Li Z, Bao S, Wu Q, Wang H, Eyler C, Sathornsumetee S, et al. Hypoxia-Inducible Factors Regulate Tumorigenic Capacity of Glioma Stem Cells. Cancer Cell 2009;15:501-13.

(15) Folkins C, Man S, Xu P, Shaked Y, Hicklin DJ, Kerbel RS. Anticancer therapies combining antiangiogenic and tumor cell cytotoxic effects reduce the tumor stem-like cell fraction in glioma xenograft tumors. Cancer Research 2007;67:3560-4.

(16) Hovinga KE, Shimizu F, Wang R, Panagiotakos G, van der Heijden M, Moayedpardazi H, et al. Inhibition of Notch Signaling in Glioblastoma Targets Cancer Stem Cells via an Endothelial Cell Intermediate. Stem Cells 2010;28:1019-29.

(17) Garcia-Barros M, Paris F, Cordon-Cardo C, Lyden D, Rafii S, Haimovitz-Friedman A, et al. Tumor response to radiotherapy regulated by endothelial cell apoptosis. Science 2003;300:1155-9.

(18) Igrashi K, Sakimoto I, Kataoka K, Ohta K, Miura M. Radiation-induced senescence-like phenotype in proliferating and plateau-phase vascular endothelial cells. Experimental Cell Research 2007;313:3326-36.

(19) Verhaak RGW, Hoadley KA, Purdom E, Wang V, Qi Y, Wilkerson MD, et al. Integrated Genomic Analysis Identifies Clinically Relevant Subtypes of Glioblastoma Characterized by Abnormalities in PDGFRA, IDH1, EGFR, and NF1. Cancer Cell 2010;17:98-110.

(20) Zhu T, Costello MA, Talsma CE, Flack CG, Crowley JG, Hamm LL, et al. Endothelial cells create a stem cell niche in glioblastoma by providing Notch ligands that nurture self-renewal of cancer stem-like cells. Cancer Res 2011.

(21) Paez-Ribes M, Allen E, Hudock J, Takeda T, Okuyama H, Vinals F, et al. Antiangiogenic Therapy Elicits Malignant Progression of Tumors to Increased Local Invasion and Distant Metastasis. Cancer Cell 2009;15:220-31.

(22) Gale NW, Dominguez MG, Noguera I, Pan L, Hughes V, Valenzuela DM, et al. Haploinsufficiency of delta-like 4 ligand results in embryonic lethality due to major defects in arterial and vascular development. Proceedings of the National Academy of Sciences of the United States of America 2004;101:15949-54.

(23) Patel NS, Li JL, Generali D, Poulsom R, Cranston DW, Harris AL. Up-regulation of delta-like 4 ligand in human tumor vasculature and the role of basal expression in endothelial cell function. Cancer Research 2005;65:8690-7.

(24) Noguera-Troise I, Daly C, Papadopoulos NJ, Coetzee S, Boland P, Gale NW, et al. Blockade of Dll4 inhibits tumour growth by promoting non-productive angiogenesis. Nature 2006;444:1032-7.

(25) Ridgway J, Zhang G, Wu Y, Stawicki S, Liang WC, Chanthery Y, et al. Inhibition of Dll4 signalling inhibits tumour growth by deregulating angiogenesis. Nature 2006;444:1083-7.

(26) Li JL, Sainson RC, Oon CE, Turley H, Leek R, Sheldon H, et al. DLL4-Notch signaling mediates tumor resistance to anti-VEGF therapy in vivo. Cancer Res 2011.

(27) Yan MH, Callahan CA, Beyer JC, Allamneni KP, Zhang G, Ridgway JB, et al. Chronic DLL4 blockade induces vascular neoplasms. Nature 2010;463:E6-E7.

(28) Chothia C, Jones EY. The molecular structure of cell adhesion molecules. Annual Review of Biochemistry 1997;66:823-62.

(29) Desgrosellier JS, Cheresh DA. Integrins in cancer: biological implications and therapeutic opportunities. Nature Reviews Cancer 2010;10:9-22.

(30) Knoblich JA. Mechanisms of asymmetric stem cell division. Cell 2008;132:583-97.

(31) Kokovay E, Goderie S, Wang Y, Lotz S, Lin G, Sun Y, et al. Adult SVZ Lineage Cells Home to and Leave the Vascular Niche via Differential Responses to SDF1/CXCR4 Signaling. Cell Stem Cell 2010;7:163-73.

(32) Shen Q, Wang Y, Kokovay E, Lin G, Chuang SM, Goderie SK, et al. Adult SVZ stem cells lie in a vascular niche: A quantitative analysis of niche cell-cell interactions. Cell Stem Cell 2008;3:289-300.

(33) Lathia JD, Gallagher J, Heddleston JM, Wang JL, Eyler CE, MacSwords J, et al. Integrin Alpha 6 Regulates Glioblastoma Stem Cells. Cell Stem Cell 2010;6:421-32.

(34) Tchaicha JH, Reyes SB, Shin J, Hossain MG, Lang FF, McCarty JH. Glioblastoma angiogenesis and tumor cell invasiveness are differentially regulated by {beta}8 integrin. Cancer Res 2011.

(35) Chatterjee S, Matsumura A, Schradermeier J, Gillespie GY. Human malignant glioma therapy using anti-alpha(v)beta3 integrin agents. J Neurooncol 2000;46:135-44.

(36) Hambardzumyan D, Becher OJ, Rosenblum MK, Pandolfi PP, Manova-Todorova K, Holland EC. PI3K pathway regulates survival of cancer stem cells residing in the perivascular niche following radiation in medulloblastoma in vivo. Genes & Development 2008;22:436-48.

(37) Knobbe CB, Merlo A, Reifenberger G. Pten signaling in gliomas. Neuro-Oncology 2002;4:196-211.

(38) Sonoda Y, Ozawa T, Aldape KD, Deen DF, Berger MS, Pieper RO. Akt pathway activation converts anaplastic astrocytoma to glioblastoma multiforme in a human astrocyte model of glioma. Cancer Research 2001;61:6674-8.

(39) Stiles B, Gilman V, Khanzenzon N, Lesche R, Li A, Qiao R, et al. Essential role of AKT-1/protein kinase B alpha in PTEN-controlled tumorigenesis. Molecular and Cellular Biology 2002;22:3842-51.

(40) Soroceanu L, Kharbanda S, Chen R, Soriano RH, Aldape K, Misra A, et al. Identification of IGF2 signaling through phosphoinositide-3-kinase regulatory subunit 3 as a growth-promoting axis in glioblastoma. Proc Natl Acad Sci U S A 2007;104:3466-71.

(41) Chakravarti A, Zhai G, Suzuki Y, Sarkesh S, Black PM, Muzikansky A, et al. The prognostic significance of phosphatidylinositol 3-kinase pathway activation in human gliomas. Journal of Clinical Oncology 2004;22:1926-33.

(42) Bleau AM, Hambardzumyan D, Ozawa T, Fomchenko EI, Huse JT, Brennan CW, et al. PTEN/PI3K/Akt Pathway Regulates the Side Population Phenotype and ABCG2 Activity in Glioma Tumor Stem-like Cells. Cell Stem Cell 2009;4:226-35.

(43) Schlegel J, Durchschlag G, Piontek G, Grosu AL. Activation of the phosphatidylinositol-3 '-kinase/protein kinase B-dependent antiapoptotic pathway plays an important role in the development of radioresistance of human glioma cells. Cell Signaling, Transcription, and Translation As Therapeutic Targets 2002;973:224-7.

(44) Easton JB, Houghton PJ. Therapeutic potential of target of rapamycin inhibitors. Expert Opinion on Therapeutic Targets 2004;8:551-64.

(45) Takeuchi H, Kondo Y, Fujiwara K, Kanzawa T, Aoki H, Mills GB, et al. Synergistic augmentation of rapamycin-induced autophagy in malignant glioma cells by phosphatidylinositol 3-kinase/protein kinase B inhibitors. Cancer Research 2005;65:3336-46.

(46) Margolin K, Longmate J, Baratta T, Synold T, Christensen S, Weber J, et al. CCI-779 in metastatic melanoma - A phase II trial of the California Cancer Consortium. Cancer 2005;104:1045-8.

(47) Hay N. The Akt-mTOR tango and its relevance to cancer. Cancer Cell 2005;8:179-83.

(48) Fan QW, Knight ZA, Goldenberg DD, Yu W, Mostov KE, Stokoe D, et al. A dual PI3 kinase/mTOR inhibitor reveals emergent efficacy in glioma. Cancer Cell 2006;9:341-9.

Nederlandse samenvatting

Introductie: Glioblastoma Multiforme en kankerstamcellen

Glioblastoma Multiforme (GBM) is de meest voorkomende en meest agressieve kwaadaardige tumor die ontstaat in de hersenen. Het GBM ontstaat uit de gliacellen, de steuncellen rond de zenuwcellen. Het kwaadaardige karakter van GBM wordt onder andere verklaard door de massale verspreiding van kankercellen uit de primaire tumor die infiltreren in de omliggende gezonde hersenen. Tumorinfiltratie is een van de belangrijke oorzaken waarom deze ziekte zo moeilijk te behandelen is en de tumor weer verder groeit na chirurgie. Patiënten met een maligne glioom hebben een slechte prognose; slechts 10% van de patiënten met een GBM overleeft meer dan 5 jaar ondanks gecombineerde behandelingen met chirurgie, radiotherapie en chemotherapie in de vorm van temozolomide (TMZ) (1).

Een extra moeilijkheid in de behandeling van GBM is de resistentie van een klein aantal tumorcellen tegen radiotherapie of chemotherapie. Deze populatie van resistente tumorcellen wordt, volgens recente literatuur, gekarakteriseerd als de kankerstamcel-fractie. Dit komt omdat veel karakteristieken van deze fractie cellen overeenkomen met eigenschappen van normale stamcellen: ze kunnen zichzelf vermenigvuldigen en ze kunnen zich differentiëren. Differentiëren wil zeggen dat de stamcellen kunnen uitrijpen van een primitieve tumorcel tot een meer ontwikkelde tumor met gliale kenmerken. Het belangrijkste criterium echter om kankerstamcellen te definiëren is de eigenschap tot een nieuwe tumor uit te groeien, tot een tumor die alle uiterlijke kenmerken heeft de oorspronkelijke tumor (fenotypisch kopie), ook nog nadat tumorcellen herhaaldelijk worden getransplantateerd in muizen (xenograft model). Dit laat zien dat de nieuw gegenereerde tumoren een fractie van functionele multipotente stamcellen bevatten, die in staat zijn zichzelf te vernieuwen (2). Extra bewijs vormen studies die laten zien dat één enkele kankerstamcel in staat is tot een nieuwe tumor met het oorspronkelijke fenotype uit te groeien (3,4). Verondersteld mag worden dat de kankerstamcellen die ontsnappen aan de behandeling, verantwoordelijk zijn voor hergroei van de tumor. Zeer efficiënte DNA herstelmechanismen en celcyclus 'checkpoints', evenals activering van anti-apoptose mechanismen zorgen ervoor dat kankerstamcellen extreem resistent zijn tegen behandeling (5).

Onlangs is een extra moeilijkheid toegevoegd aan de kankerstamcel biologie namelijk het bestaan van een kleine (epi)genetische fractie van cellen identiek aan kankerstamcellen. Er is aangetoond dat een op de vier melanoomcellen de potentie heeft om tumoren te vormen, en dat de mate waarin ze tumoren kunnen vormen in het xenograft model in hoge mate afhankelijk is van het immuunsysteem van de gastheer (4). Nog belangrijker was dat xenograftcellen die verkregen waren van de tumor van een eenzelfde patiënt zeer heterogeen zijn.

Er ontstond twijfel of tumoren wel verschillende populaties van die (epi)genetische, stamcelachtige cellen bevatten. Om te onderzoeken of een uniforme populatie van kankerstamcellen verantwoordelijk is voor het tumor fenotype of dat er verscheidene kanker stam cel klonen in een tumor huizen hebben we GBM kankerstamcellen geanalyseerd (Hoofdstuk 3).

Hiervoor hebben we van één enkele cel afgeleide kankerstamcel lijnen de potentie tot differentiatie bepaald. In geval van een enkele multipotente populatie van kankerstamcellen vormt een enkele cel klonen met eenzelfde differentiatiepatroon als de parentale stamcel. Onze resultaten toonden een onverwacht brede variatie van differentiatie patronen die varieerden van kloon tot kloon. Omdat alle klonen onder gelijke kweekcondities werden gehouden suggereren deze resultaten dat de oorspronkelijke tumor verschillende kankerstamcellen bevat met verschillende differentiatie patronen, wat we toeschrijven aan een andere epigenetische achtergrond. Dit kan weer verklaard worden door een variatie in selectie druk in verschillende delen van de tumor. Klonen die in eerste instantie uit eenzelfde cel zijn ontstaan hebben verschillende mutaties verkregen die van invloed zijn op hun differentiatie programma maar ook op een betere celoverleving en op het invasie gedrag.

Het invasieve gedrag van tumoren is een direct gevolg van de wijze waarop celdifferentiatie hiërarchisch is georganiseerd, wat wordt gestuurd door de kankerstamcellen zelf (Hoofdstuk 4).

Bij de ontwikkeling van nieuwe antikanker behandelingen zal met deze bevindingen zeker rekening moeten worden gehouden. Er is een tendens om middelen te ontwikkelen die tumoren laten differentiëren en dus de cellen gevoeliger maken voor behandeling. In geval dat er verschillende fracties van kankerstamcellen in een tumor aanwezig zijn met een verschillende dynamiek moeten daarvoor dus ook geschikte middelen voor ontwikkeld worden. De meest belovende behandeling is die behandeling, die verschillende fracties van kankerstamcellen tegelijkertijd aanvalt. De behandeling moet daarbij effectief zijn tegen dominante en resistente klonen. Er wordt gedacht dat het micromilieu rond de tumor hierbij een belangrijke rol speelt.

Tumor Micro-milieu

Het Tumor Micro-milieu speelt een belangrijke rol in de groei en ontwikkeling van de tumor. Voor het GBM vervullen endotheelcellen van de tumorvaten deze rol (Hoofdstuk 2). Naar analogie aan neurale stamcellen (NSCs), vormen microvasculaire endotheelcellen een niche rond de GBM kankerstamcellen. Deze niche bevordert de proliferatie en verspreiding van de kankerstamcellen (6,7) (Hoofdstuk 5). Eén van de mediatoren van de kankerstamcellen is stikstof oxide dat geproduceerd wordt door endotheelcellen die de fractie van kankerstamcellen in stand houden door het 'notch' mechanisme aan te zwengelen (8).

Het bestaan van een vasculaire niche lijkt essentieel voor GBM kankerstamcellen omdat deze cellen zelf de vorming van nieuwe bloedvaten stimuleren en zichzelf beschermen tegen beschadigingen (9-11). GBM kanker stamcellen produceren niet alleen aanzienlijke hoeveelheden VEGF dat de groei van tumorvaten (neovascularisatie) stimuleert. Maar de tumorstamcellen zijn ook in staat te differentiëren in endotheelachtige cellen waarmee ze hun eigen niche vormen (9,12,13). Daarbij worden gebieden met hypoxie, waarvan bekend is dat die resistentie bevorderen,

ook genoemd als GBM kankerstamcel niche (14) (Hoofdstuk 2). De hypoxie geïnduceerde factor 2-alfa (Hif-2α) vormt een sleutelrol hierbij door gebrek aan zuurstof veroorzaakte effecten.
Ofschoon men intuïtief zou denken dat tumor vasculatuur en hypoxie twee ongerelateerde niche eigenschappen zijn, is dit niet zondermeer het geval. Hoewel een GBM rijk is aan bloedvaten, blijkt dat deze vaten zwak zijn en slecht functioneren.
Bovendien, zoals zojuist vermeld, kunnen GBM cellen zelf differentiëren in endotheelachtige cellen. Echter, deze tumorcellen vormen structuren die uiterlijk meer lijken op bloedvaten dan dat ze het werkelijk zijn. Dit betekent dat tumorcellen wel een endotheelachtige structuur maar niet noodzakelijkerwijs echte goed functionerende bloedvaten nodig hebben. Dus in een tumor kunnen hypoxische gebieden en functionele bloedvaten heel goed tegelijkertijd aanwezig zijn en de kankerstamcellen ondersteunen.
Hoe dan ook zal een toekomstige behandeling van het GBM niet alleen bestaan uit directe behandeling van de tumorstamcellen, maar ook uit gerichte verstoring van de ondersteunende niche voor de kankerstamcellen!

Behandelingsresistentie

Behalve dat de kankerstamcel-populatie bijdraagt in het in stand houden van de tumor speelt deze celpopulatie ook een belangrijke rol in de resistentie tegen behandeling.
Er zijn echter wel nieuwe ontwikkelingen in de behandelingen. Behandeling met de angiogenese remmer bevacizumab verkleinde de kankerstamcel populatie en remde daarmee de tumorgroei (6). Ook vergrootte dit middel de gevoeligheid van kankerstamcellen voor andere cytotoxische agentia (15). Bovendien wordt door remming van de moleculaire 'Notch' route, het contact tussen kankerstamcellen en de niche verstoord, waardoor het effect van bestraling op deze cellen toeneemt (16). Het is daarom van belang om meer over de microvasculatuur van GBM te weten voor de ontwikkeling van nieuwe behandelingen.
De huidige gegevens over de effecten van straling op endotheelcellen zijn onvolledig en tegenstrijdig. In verscheidene artikelen werd gerapporteerd dat de endotheelcellen heel gevoelig zijn voor radiotherapie en door apoptose bezwijken. Maar er zijn even zo vele artikelen waarin het tegengesteld beweerd wordt (17, 18). Om duidelijkheid over deze kwestie te verkrijgen hebben we het effect van conventionele behandelingen op tumor microvasculaire endotheelcellen (tMVECs) onderzocht. De nadruk lag daarbij op de stralingsbehandeling omdat dit de meest effectieve behandeling is voor GBM en we onderzochten daarbij de interactie van kankerstamcellen met tMVECs (Hoofdstuk 6). Wij vonden dat, wanneer tMVECs samen groeien met kankerstamcellen, de tMVECs de groei van GBM kankerstamcellen cellen stimuleren en zorgen voor het behoud van de stamceleigenschappen, zelfs als de tMVECs behandeld waren met bestraling of chemotherapie. Door de behandeling gaan tMVECs weliswaar in een permanente cel cyclus arrest of senescentie. Maar de senescente tMVECs onderhouden de groei van de kankerstamcel groei

met dezelfde efficiëntie als niet senescente tMVECs. Bovendien kunnen GBM kankerstamcellen zelf ook differentiëren in een endotheelachtig fenotype en vervolgens na bestraling in senescentie gaan om de rol van de kankerstamcel niche in te nemen en de uitbreiding van tumorcellen te ondersteunen.

Deze resultaten laten een gewiekst scenario zien, waarbij tumorcellen in staat zijn hun eigen omgevende niche te creëren. Dit geeft ze de mogelijkheid te overleven en uit te breiden zelfs na bestraling of chemotherapie. Een dergelijke niche kan heel goed bijdragen aan het opnieuw uitgroeien van de tumor na een initiële goede klinische respons. Behalve in hun bijdrage om de kankerstamcel populatie te onderhouden, zijn tMVECs in staat gedifferentieerde tumorcellen te reprogrammeren en te laten terugkeren tot een stamcelachtig fenotype (Hoofdstuk 7). Het eindresultaat van deze geprogrammeerde plasticiteit leidt tot een toename van een tumorigene behandelingsresistente en agressievere celpopulatie. Het verstoren en ontmantelen van de interactie tussen tumorcellen en hun vasculaire niche zou de tumor daarom gevoeliger kunnen maken voor behandeling. De moleculen die deze interactie onderhouden vormen aantrekkelijke therapeutische aangrijpingspunten om nieuwe doelgerichte geneesmiddelen te ontwikkelen en deze ziekte effectief te lijf te gaan. Daarbij mogen we de genetische diversiteit van deze tumoren niet uit het oog verliezen: ofschoon de verschillende GBMs gelijke uiterlijke kenmerken hebben, heeft elke afzonderlijke tumor een min of meer uniek genetisch patroon. Dit geeft een extra moeilijkheid om een specifieke behandeling te ontwikkelen. Vier verschillende GBM-subtypes zijn beschreven gekenmerkt door typische clusters van genetische mutaties (19). Het ligt voor de hand dat de genetische variaties van GBM ook effect heeft op de interactie binnen de vasculaire niche.

Het ingewikkelde samenspel tussen kankerstamcellen en niche is een zorgvuldig geregeld systeem waarvan inmiddels verschillende signaal transductie wegen bekend zijn met kenmerkende moleculen die worden uitgescheiden of aan de celmembraan vastzitten.

Conclusies

Om het biologisch gedrag en de therapieresistentie van het GBM te kunnen begrijpen, is een beter inzicht in het micro-milieu van de tumor noodzakelijk. De vasculaire endotheelcellen die door de tumor zelf worden gemaakt, de tMVECS, spelen een belangrijke rol bij de levensvatbaarheid van kankerstamcellen in een GBM. Bovendien zijn deze tMVECS zelf weinig gevoelig voor bestraling en chemotherapie en daardoor dragen zij bij aan de resistentie voor de behandeling van de tumor. Het is nog niet precies bekend hoe het tumorendotheel de kankerstamcellen ondersteunt en of het voor alle kankerstamcellen in dezelfde tumor geldt. De huidige data suggereren dat endotheelcellen en kankerstamcellen elkaar hard nodig hebben. Zij maken daarbij gebruik maken van direct cel-cel contact en van uitwisseling van moleculen, afhankelijk van het GBM-subtype. Hoe de kankerstamcellen vervolgens overleven ondanks behandeling is nog niet precies bekend. De resultaten van studies waarbij het endotheel van de

tumorbloedvaten direct werd aangepakt met zogenaamde angiogeneseremmers vielen tot nu toe tegen. Het lijkt erop dat deze middelen de verspreiding van de tumor in de hersenen juist bevorderen, en daarmee het succes van verschrompeling van de primaire tumor teniet doen. Omdat het endotheel in de bloedvaten zo resistent is tegen de conventionele antikanker-behandelingen, zou het misschien beter werken als de kankerstamcellen worden losgemaakt uit de endotheliale niche rondom de kankerstamcel. Dit kan stamcellen ertoe dwingen om zich te differentiëren waardoor ze gevoeliger worden voor bestraling en chemotherapie. Daarom is het van essentieel belang om de interactie tussen de kankerstamcellen en hun niche nog beter te begrijpen om een patiënt met een GBM definitief te kunnen genezen.

Reference List

(1) Stupp R, Hegi ME, Mason WP, van den Bent MJ, Taphoorn MJB, Janzer RC, et al. Effects of radiotherapy with concomitant and adjuvant temozolomide versus radiotherapy alone on survival in glioblastoma in a randomised phase III study: 5-year analysis of the EORTC-NCIC trial. Lancet Oncology 2009;10:459-66.

(2) Clarke MF, Dick JE, Dirks PB, Eaves CJ, Jamieson CH, Jones DL, et al. Cancer stem cells--perspectives on current status and future directions: AACR Workshop on cancer stem cells. Cancer Res 2006;66:9339-44.

(3) Vermeulen L, Melo FDSE, van der Heijden M, Cameron K, de Jong JH, Borovski T, et al. Wnt activity defines colon cancer stem cells and is regulated by the microenvironment. Nature Cell Biology 2010;12:468-U121.

(4) Quintana E, Shackleton M, Sabel MS, Fullen DR, Johnson TM, Morrison SJ. Efficient tumour formation by single human melanoma cells. Nature 2008;456:593-U33.

(5) Bao SD, Wu QL, McLendon RE, Hao YL, Shi Q, Hjelmeland AB, et al. Glioma stem cells promote radioresistance by preferential activation of the DNA damage response. Nature 2006;444:756-60.

(6) Calabrese C, Poppleton H, Kocak M, Hogg TL, Fuller C, Hamner B, et al. A perivascular niche for brain tumor stem cells. Cancer Cell 2007;11:69-82.

(7) Shen Q, Goderie SK, Jin L, Karanth N, Sun Y, Abramova N, et al. Endothelial cells stimulate self-renewal and expand neurogenesis of neural stem cells. Science 2004;304:1338-40.

(8) Charles N, Ozawa T, Squatrito M, Bleau AM, Brennan CW, Hambardzumyan D, et al. Perivascular Nitric Oxide Activates Notch Signaling and Promotes Stem-like Character in PDGF-Induced Glioma Cells. Cell Stem Cell 2010;6:141-52.

(9) Bao SD, Wu QL, Sathornsumetee S, Hao YL, Li ZZ, Hjelmeland AB, et al. Stem cell-like glioma cells promote tumor angiogenesis through vascular endothelial growth factor. Cancer Research 2006;66:7843-8.

(10) Brown CK, Khodarev NN, Yu JQ, Moo-Young T, Labay E, Darga TE, et al. Glioblastoma cells block radiation-induced programmed cell death of endothelial cells. Febs Letters 2004;565:167-70.

(11) Ezhilarasan R, Mohanam I, Govindarajan K, Mohanam S. Glioma cells suppress hypoxia-induced endothelial cell apoptosis and promote the angiogenic process. International Journal of Oncology 2007;30:701-7.

(12) Ricci-Vitiani L, Pallini R, Biffoni M, Todaro M, Invernici G, Cenci T, et al. Tumour vascularization via endothelial differentiation of glioblastoma stem-like cells. Nature 2010;468:824-U121.

(13) Wang R, Chadalavada K, Wilshire J, Kowalik U, Hovinga KE, Geber A, et al. Glioblastoma stem-like cells give rise to tumour endothelium. Nature 2010;468:829-U128.

(14) Li Z, Bao S, Wu Q, Wang H, Eyler C, Sathornsumetee S, et al. Hypoxia-Inducible Factors Regulate Tumorigenic Capacity of Glioma Stem Cells. Cancer Cell 2009;15:501-13.

(15) Folkins C, Man S, Xu P, Shaked Y, Hicklin DJ, Kerbel RS. Anticancer therapies combining antiangiogenic and tumor cell cytotoxic effects reduce the tumor stem-like cell fraction in glioma xenograft tumors. Cancer Research 2007;67:3560-4.

(16) Hovinga KE, Shimizu F, Wang R, Panagiotakos G, van der Heijden M, Moayedpardazi H, et al. Inhibition of Notch Signaling in Glioblastoma Targets Cancer Stem Cells via an Endothelial Cell Intermediate. Stem Cells 2010;28:1019-29.

(17) Garcia-Barros M, Paris F, Cordon-Cardo C, Lyden D, Rafii S, Haimovitz-Friedman A, et al. Tumor response to radiotherapy regulated by endothelial cell apoptosis. Science 2003;300:1155-9.

(18) Igrashi K, Sakimoto I, Kataoka K, Ohta K, Miura M. Radiation-induced senescence-like phenotype in proliferating and plateau-phase vascular endothelial cells. Experimental Cell Research 2007;313:3326-36.

(19) Verhaak RGW, Hoadley KA, Purdom E, Wang V, Qi Y, Wilkerson MD, et al. Integrated Genomic Analysis Identifies Clinically Relevant Subtypes of Glioblastoma Characterized by Abnormalities in PDGFRA, IDH1, EGFR, and NF1. Cancer Cell 2010;17:98-110.

LIST OF PUBLICATIONS

T.Borovski, P.Beke, O. van Tellingen, H.M.Rodermond, J.J.Verhoeff, V.Lascano, J.B.Daalhuisen, J.P.Medema* and M.R.Sprick*, *Therapy resistant tumor microvascular endothelial cells contribute to treatment failure in glioblastoma multiforme,* Oncogene, Accepted March 2012, *shared senior authorship

P.M.Krawczyk, **T.Borovski**, J.Stap, A.Cijsouw, R. ten Cate, J.P.Medema, R.Kanaar, N.A.P.Franken, J.Aten, *Chromatin mobility is increased at sites of DNA double-strand breaks,* Journal of Cell Science, Accepted December 2011

T.Borovski, F. De Sousa E Melo, L.Vermeulen, J.P.Medema, *Cancer stem cell niche – the place to be*, Cancer Research, 2011

L.Vermeulen*, F. De Sousa E Melo*, M. van der Heijden, K.Cameron, J.H. de Jong, **T.Borovski,** J.B.Tuynman, M.Todaro, C.Merz, H.Rodermond, M.R.Sprick, K.Kemper, D.J.Richel, G.Stassi, J.P.Medema, *Wnt Activity defines colon cancer stem cells and is regulated by the microenvironment,* Nature Cell Biology, 2010 *shared first authorship

A.Sottoriva, J.J.Verhoeff, **T.Borovski**, S.K.McWeeney, L.Naumov, J.P.Medema, P.M.Sloot, L.Vermeulen, *Cancer stem cell tumour model reveals invasive morphology and increased phenotypical heterogeneity,* Cancer Research, 2010

T.Borovski, J.J.Verhoeff, R. ten Cate, K.Cameron, N.A. de Vries, O. van Tellingen, D.J.Richel, W.R. van Furth, J.P.Medema*, M.R.Sprick*, *Tumour vasculature supports proliferation and expansion of glioma-propagating cells,* International Journal of Cancer, 2009 *shared senior authorship

T.Borovski, L.Vermeulen, M.R.Sprick, J.P.Medema, *One renegade cancer stem cell?,* Cell Cycle, 2009

ACKNOWLEDGEMENTS

Hereby I would like to thank everyone who stood by me for the last five years and made a completion of this thesis possible.

First of all, I want to thank Jan Paul for all the guidance and unconditional support. Thank you for stepping in even when you didn't have to. It has been a great privilege to be part of your team and to have you as a boss. Also, I want to thank you for dealing with my Serbian temperament with such patience and tolerance. This experience will surely come handy in handling future PhDs!

Martin and Klaas, my co-promoters, I want to thank both of you for the guidance you've provided and everything you've taught me.

I would also like to thank the committee members for agreeing to evaluate this thesis, for their thoughtful readings and comments, and for their participation in the defense.

LEXOR group, to all the previous and current members, I want to thank you for this amazing and unforgettable journey over the years. Our lab has established the reputation of being international conglomerate (and proud of it!), and this mixed with Dutch culture makes it truly a unique environment. We have learned so much about each other and from each other, changing and growing as people accordingly. Thus I honestly hope that next LEXOR generations will also cherish this experience and keep this spirit alive in the years to come.

Needless to say, some people have to be mentioned individually. Ladies first, Melania, Valeria and Catarina, girls you are the greatest, thank you for being such devoted friends! The combination of charm, honesty and kindness that you constantly irradiate is priceless, don't ever change that. And Franziska, the one and only, I am so happy that I've met you. You and I have been the perfect match since the day one. Felipe and Louis, I am not sure whether I'm more impressed with your brilliant minds or your personalities, you guys are one of the kind. And Marco, please stay in charge of the good atmosphere, LEXOR would not be half as fun without the laughter you are injecting on daily bases.

I want to thank the "Cell biology" group: Jacob, Jan, Przemek and also Tony. It was an honor and a challenge to be the only female in the team, but you guys would be so bored otherwise! Thank you for the collaboration and all the scientific input. Tony and Przemek, thank you for being who you are, I hope that our beer-supported friendship will never end!

Also I would like to thank the whole CEMM department, all the M3 and L3 people who supported me scientifically and/or as being my friends, all the collaborators who helped me deal with science that eventually lead to this book

Most of all, I want to thank my family for being my rock, all this is for you...

There Is A Light That Never Goes Out...

T.